Technische Universität München

II. Medizinische Klinik und Poliklinik
Klinikum rechts der Isar

Next-generation genetically engineered mouse models to study PI3K/3-phosphoinositide-dependent protein kinase 1 (Pdk1) signaling in pancreatic cancer

Nina Schönhuber

Vollständiger Abdruck der von der Fakultät für Medizin der Technischen Universität München zur Erlangung des akademischen Grades eines

Doktors der Naturwissenschaften

genehmigten Dissertation.

Vorsitzender: Univ.-Prof. Dr. Roland M. Schmid
Prüfer der Dissertation: 1. apl. Prof. Dr. Dieter K.M. Saur
2. Univ.-Prof. Angelika Schnieke, PhD
3. Univ.-Prof. Dr. Oliver Krämer, Johannes-Gutenberg-Universität Mainz

Die Dissertation wurde am 17.02.2015 bei der Technischen Universität München eingereicht und durch die Fakultät für Medizin am 16.09.2015 angenommen.

Table of contents

List of tables

List of figures

Abbreviations

°C	degree Celsius
4-OHT	4-hydroxytamoxifen
ADM	acinar-to-ductal metaplasia
AFL	atypical flat lesion
AKT	protein kinase B
APS	ammonium persulfate
bp	base pairs
BrdU	5-bromo-2'-deoxyuridine
BSA	bovine serum albumin
CDK	Cyclin-dependent kinase
cDNA	complementary desoxyribonucleic acid
CK19	cytokeratin 19
cm	centimeter
D-MEM	Dulbecco's modified eagle medium
DMSO	dimethylsulfoxide
DNA	desoxyribonucleic acid
DTA	diphtheria toxin A
EGF	epidermal growth factor
EGFP	enhanced green fluorescent protein
EGFR	epidermal growth factor receptor
ER	estrogen receptor
Erk	extracellular signal-regulated kinase
ES	embryonic stem
EtBr	ethidium bromide
EtOH	ethanol
FCS	fetal calf serum
FGF	fibroblast growth factor
FSF	frt-stop-frt
GEMM	genetically engineered mouse model
h	hours
HBSS	Hanks' balanced salt solution
H&E	hematoxylin and eosin
i.p.	intraperitoneal
IPMN	intraductal papillary mucinous neoplasm

kb	kilo base pairs
LBD	ligand-binding domain
LIF	leukemia inhibitory factor
LOH	loss of heterozygosity
LSL	loxP-stop-loxP
M	mol / molar
MAPK	mitogen-activated protein kinase
MCN	mucinous cystic neoplasm
MEF	murine embryonic fibroblast
Mek	mitogen-activated protein kinase kinase
mg	milligram
min	minutes
ml	mililiter
mM	millimol / millimolar
MMF	Midazolam, Medetomidine, Fentanyl
mut	mutated
ng	nanogram
nm	nanometer
nM	nanomol / nanomolar
OD	optical density
o/n	over night
p	phospho
PanIN	pancreatic intraepithelial neoplasia
PBS	phosphate buffered saline
PCNA	proliferating cell nuclear antigen
PCR	polymerase chain reaction
PDAC	pancreatic ductal adenocarcinoma
Pdk1	3-phosphoinositide-dependent protein kinase 1
Pdx1	pancreatic and duodenal homeobox 1
PFA	paraformaldehyde
PI3K	phosphoinositide 3-kinase
PPT	pancreatic primary tumor
PTEN	phosphatase and tensin homolog
Ptf1a	pancreas transcription factor subunit alpha
R26	Rosa26
Rac1	RAS-related C3 botulinum substrate 1
RB	retinoblastoma

RNA	ribonucleic acid
rpm	rounds per minute
RT	room temperature
SDS	sodium dodecyl sulfate
sec	seconds
SMAD4	mothers against decapentaplegic homolog 4
TAE	tris acetate EDTA
TAM	tamoxifen
TEMED	*N*,*N*,*N*′,*N*′-Tetramethylethylenediamine
TGFα	transforming growth factor α
TGFβ	transforming growth factor β
Tris	tris-(hydroxymethyl)-aminomethan
Trp53	transformation related protein 53
U	units
V	volt
VEGF	vascular endothelial growth factor
WT	Wild type
µl	microliter
µm	micrometer
µM	micromolar

1. Introduction

1.1 Pancreatic ductal adenocarcinoma

Pancreatic cancer is the fourth leading cause of cancer associated death in the Western world. The estimation of 46.000 new cases and 39.000 deaths in 2014 shows the high mortality of this disease as well as the 5-year survival rate of 6% which did hardly improve over the last 30 years (Siegel et al., 2014). In contrast to the stable or declining trends for most cancer types, the incidence rates are increasing for pancreatic cancer (Siegel et al., 2014).

The most common form of pancreatic cancer is the pancreatic ductal adenocarcinoma (PDAC) accounting for more than 85% of neoplasms of the pancreas. Commonly, PDAC arises in the head of the pancreas. It typically infiltrates surrounding tissues like spleen and peritoneal cavity and metastasizes to lymph nodes, liver and lung. Another characteristic nature of PDAC is desmoplasia, the presence of dense stroma consisting of fibroblasts and inflammatory cells (Hezel et al., 2006).

The causes of pancreatic cancer still remain unclear. Only 5 - 10% of patients have a family history of this disease (Shi et al., 2009). Main risk factors of PDAC are advanced age, smoking, chronic pancreatitis, diabetes, obesity and non-O blood group (Berrington de Gonzalez et al., 2003; Everhart and Wright, 1995; Fuchs et al., 1996; Gapstur et al., 2000; Stolzenberg-Solomon et al., 2005; Wolpin et al., 2009). Due to unspecific symptoms and the lack of early diagnostic tools, only 15 - 20% of pancreatic cancer cases are diagnosed in an early stage and are therefore candidates for potentially curative surgery (Chames et al., 2010). And even of these patients with resectable disease, only 20% survive 5 years (Schneider et al., 2005).

The palliative treatment of patients with advanced unresectable disease ranges from systemic chemotherapy alone to combined forms with radiation therapy (chemoradiation). As a first-line treatment, gemcitabine, a nucleotide analogue, has been the standard of care for more than a decade (Burris et al., 1997; Hidalgo, 2010). Multiple new agents have been tested in combination with gemcitabine, but only erlotinib, a small-molecule inhibitor of the epidermal growth factor receptor (EGFR) has shown a small improvement in median survival (Gupta and El-Rayes, 2008; Moore et al., 2007). Unfortunately, a lot of pancreatic cancers do not respond to gemcitabine (Vincent et al., 2011). At the moment, FOLFIRINOX, a combination treatment with fluorouracil, folinic acid, irinotecan and oxaliplatin leads to the greatest survival benefit in patients by increasing the median survival to 11.1 months in comparison to 6.8 months with gemcitabine treatment (Conroy et al., 2011). However, this regimen has an increased toxicity, restricting the treatment to patients with good performance status. Another group showed that treatment of nab-Paclitaxel with gemcitabine

increases median survival to 8.5 months, but also causes more side effects (Von Hoff et al., 2013).

All these facts show that there is an urgent need for further improvement of our understanding of pancreatic tumor initiation and progression to develop new therapeutic strategies to optimize treatment of this deadly disease.

1.1.1 Progression model of pancreatic ductal adenocarcinoma

Development of PDAC is described as a multi-step process of histological and genetic defined changes. The most common non-invasive precursor lesions are the pancreatic intraepithelial neoplasias (PanINs). Besides, intraductal papillary mucinous neoplasms (IPMNs), mucinous cystic neoplasms (MCNs) and atypical flat lesions (AFL) are described as precursor lesions of PDAC (Aichler et al., 2012; Brugge et al., 2004; Esposito et al., 2012; Maitra et al., 2005). Also acinar-to-ductal metaplasia (ADM) has recently been suggested to be an initiating event in human and murine PDAC formation. It is defined as a condition where pancreatic differentiated acinar cells transdifferentiate into ductal cells (Aichler et al., 2012; Caldwell et al., 2012; Morris et al., 2010; Reichert and Rustgi, 2011).

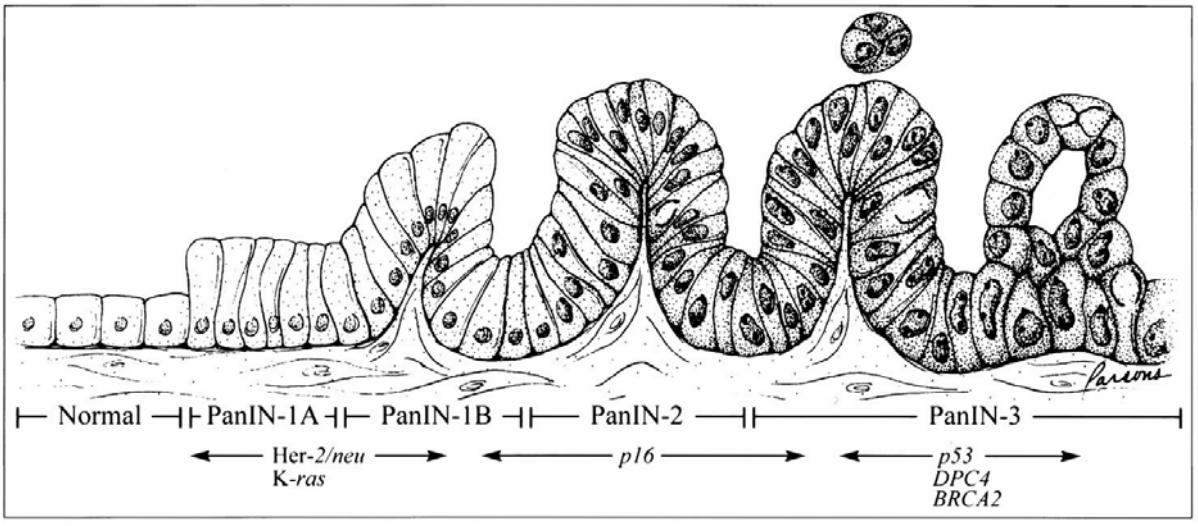

Figure 1-1: Progression model for pancreatic ductal adenocarcinoma
Normal ductal epithelium progresses to invasive pancreatic cancer through different stages of precursor lesions, the pancreatic intraepithelial neoplasias (PanINs). The overexpression of HER-2/neu and point mutations of Kras are the first events, followed by inactivation of p16, p53, DPC4, and BRCA2. Reprinted with permission from the American Association for Cancer Research (Hruban et al., 2000)

PanINs are divided into three different stages, characterized by increasing nuclear and architectural atypia (Figure 1-1) (Hruban et al., 2000). Normal ductal structures consist of cuboidal to low-columnar epithelium without cytoplasmatic mucin, whereas PanIN1A lesions, the earliest lesions, are built of tall-columnar cells with abundant mucin. When progressing to PanIN1B, these cells acquire a papillary, micropapillary or basally pseudostratified

architecture (Hruban et al., 2001). These low-grade PanINs are common and present in up to 40% of non-malignant pancreata in patients older then 50 years (Hruban et al., 2004; Schneider et al., 2005). In contrast to PanIN1, PanIN2 lesions have nuclear abnormalities like enlargement, loss of polarity or hyperchromatism. These lesions can be flat, but are most likely papillary like PanIN3, which are characterized by papillary or micropapillary structure with dystrophic goblet cells. Furthermore, PanIN3 lesions show several nuclear and structural abnormalities like abnormal mitosis and budding of cells into the lumen of ducts. PanIN3 lesions are considered as carcinoma *in situ* and directly progress to invasive PDAC (Hezel et al., 2006).

In line with these morphological changes, a consecutive accumulation of genetic alterations takes places during pancreatic cancer development. One of the first mutations observed is an activating point mutation of KRAS (Kirsten rat sarcoma). It is already present in 92% of PanIN1a lesions and the frequency increases slightly during further progression to PanIN1B (92.3%), PanIN2 (93.3%) and PanIN3 (95.4%) (Kanda et al., 2012). The *KRAS* proto-oncogene is a small GTPase and involved in many cellular functions like proliferation, differentiation and survival. In the active state it is bound to guanosine triphosphate (GTP) and thereby activates multiple effector pathways. The three major downstream pathways are the RAF-mitogen-activated kinase (MAPK; also Raf/Mek/Erk), the phosphoinositide-3-kinase/3-phosphoinositide-dependent protein kinase-1/AKT (PI3K/Pdk1/AKT) and the Ral guanine nucleotide exchange factor (RalGEFs) pathway (Collisson et al., 2012; Eser et al., 2013; Feldmann et al., 2010; Lim et al., 2005). The most frequent mutations at codon 12 lead to a substitution of glycine with aspartate or valine (G12D or G12V), resulting in a decrease of the intrinsic rate of GTP hydrolysis. The consequent insensitivity to GTPase-activating proteins (GAPs) causes a constitutive activation of KRAS independently of growth factor stimulation (Hezel et al., 2006).

In 80 - 95% of sporadic PDAC, the function of the $p16^{INK4A}$ and $p19^{ARF}$ is lost due to mutation, deletion or promoter hypermethylation. Both tumor suppressors are encoded by the *CDKN2A* locus via distinct first exons and alternative reading frames of shared exons. $p16^{INK4A}$ blocks the entry of the cell into the S phase of the cell cycle by inhibiting the phosphorylation of retinoblastoma (RB) protein mediated by cyclin-dependent kinases 4 and 6 (CDK4/6). $p19^{ARF}$ inhibits the MDM2-dependent proteolysis of p53, resulting in a stabilization of p53. As tumor suppressor, $p16^{INK4A}$ seems to play a more important role in PDAC, as mutations have been identified that affect $p16^{INK4A}$ but not $p19^{ARF}$(Bardeesy et al., 2006; Rozenblum et al., 1997).

In later stages, missense mutations in the DNA-binding domain of the tumor suppressor TP53 occur in approximately 57% of PanIN3 lesions and 50 - 75% of pancreatic tumors (Maitra and Hruban, 2008; Rozenblum et al., 1997). Because this mutation often goes along with loss of heterozygosity (LOH), TP53 wild type function is lost (Luttges et al., 2001). This

leads to uncontrolled cell proliferation and thereby accumulation of additional gene abnormalities, as wild-type TP53 regulates cell cycle, apoptosis and the DNA damage response (Maitra and Hruban, 2008).

Another important transcriptional regulator is SMAD4 (also DPC4, depleted in pancreatic carcinoma). As a rather late event during tumorigenesis, SMAD4 is lost by deletion or mutations in PanIN3 lesions and in about 55% of PDAC cases (Hahn et al., 1996; Hezel et al., 2006; Maitra and Hruban, 2008). SMAD4 is part of the transforming growth factor β (TGFβ) signaling pathway which regulates a variety of cellular functions including proliferation, differentiation, migration and apoptosis (Hezel et al., 2006). Therefore, loss of SMAD4 in pancreatic cancer cells contributes to tumor progression by selective growth advantages and effects on tumor-stroma interactions (Bardeesy and DePinho, 2002; Siegel and Massague, 2003).

Beside these alterations, mutations occur in LKB1/STK11 and BRCA2 tumor suppressors with a lower frequency. Furthermore, increased growth factor receptor signaling by overexpression of e.g. epidermal growth factor (EGF), fibroblast growth factor (FGF) and VEGF is observed (Hezel et al., 2006). Also developmental signaling pathways like Hedgehog and Notch are activated (Miyamoto et al., 2003; Thayer et al., 2003). Telomere length abnormalities, chromosomal alterations and epigenetic silencing are also characteristics of invasive pancreatic cancer (Hezel et al., 2006; Maitra and Hruban, 2008).

1.1.2 Genetically engineered mouse models for PDAC

Genetically engineered mouse models (GEMMs) have dramatically improved our understanding of the role of central genes and pathways during PDAC development, although there are differences between mice and man (Rangarajan and Weinberg, 2003). The first attempts to model human PDAC in mice by the induction of precursor lesions which progress to invasive and metastatic PDAC were made already in the 1980s. Transgenic mice expressing Hras (Quaife et al., 1987), SV40 large T antigen (Ornitz et al., 1987), c-myc (Sandgren et al., 1991) or TGFα (Sandgren et al., 1990; Wagner et al., 1998) under the control of the pancreas specific *elastase* (Ela) promoter failed to recapitulate the major hallmarks of the human disease. Due to acinar cell specific expression of the *Ela* promoter, these models developed acinar cell carcinoma or mixed acinar-ductal tumor histology. As mutations of Kras at codon 12 are found in nearly all PanIN lesions and PDAC, oncogenic Kras was expressed under the control of the *Ela* promoter (Grippo et al., 2003). Another group targeted mature ductal cells using the *cytokeratin 19* (CK19) promoter to express oncogenic Kras (Brembeck et al., 2003). Unfortunately, both models were not able to induce PanIN lesions and classical PDAC.

The recognition of the two transcription factors pancreatic and duodenal homeobox 1 (Pdx1) and pancreas-specific transcription factor 1a (Ptf1a, also known as p48) enabeled targeting of pancreatic progenitor cells by using the Cre/loxP sytem. The homeodomain protein Pdx1 can be first detected at embryonic day E8.5 in the mouse and is restricted to the dorsal gut endoderm. Later, at day E9.5 it is expressed in dorsal and ventral pancreatic buds and in the duodenal endoderm. In the adult animal, Pdx1 expression is found in insulin-producing islet cells, epithelial cells of the duodenum and in the epidermis (Guz et al., 1995; Mazur et al., 2010; Offield et al., 1996; Ohlsson et al., 1993). Expression of Ptf1a, a basic helix-loop-helix protein, can be first detected at E9.5 in pancreatic progenitor cells. In adult animals, Ptf1a expression is restricted to pancreatic acinar cells and the nervous system including brain, spine and retina (Kawaguchi et al., 2002; Krapp et al., 1998; Obata et al., 2001). As both Pdx1 and Ptf1a are expressed in pancreatic precursor cells, these transcription factors enable targeting of all pancreatic lineages using the Cre/loxP system (Orban et al., 1992).
For cell type specific expression of oncogenic $Kras^{G12D}$, a *LSL-*$Kras^{G12D/+}$ mouse line, in which the activating G12D point mutation is introduced into the endogenous *Kras* locus, was generated (Jackson et al., 2001). Ubiquitous expression of $Kras^{G12D}$ is prevented by insertion of a transcriptional stop element flanked by loxP sites (loxP-Stop-loxP; LSL) upstream of the modified *Kras* locus. This results in heterozygous expression of the wild type *Kras* allele, as the mutant allele is silenced by the LSL cassette. To achieve expression of the mutant allele in the pancreas, *LSL-*$Kras^{G12D/+}$ mice were crossed with *Pdx1-Cre* mice (Gannon et al., 2000), which express Cre as a transgene under the control of the murine *Pdx1* promoter, or $Ptf1a^{Cre/+}$ mice (Kawaguchi et al., 2002), which express Cre as a knock-in from the endogenous *Ptf1a* promoter. This leads to excision of the LSL cassette and therefore expression of mutant $Kras^{G12D}$ in pancreatic precursor cells and all pancreatic cell lineages. As the *Pdx1-Cre* is a transgenic mouse line, these animals only show mosaic expression of oncogenic $Kras^{G12D}$, whereas the $Ptf1a^{Cre/+}$ knock-in animals express $Kras^{G12D}$ in the whole pancreas. *Pdx1-Cre;LSL-*$Kras^{G12D/+}$ and $Ptf1a^{Cre/+}$*;LSL-*$Kras^{G12D/+}$ animals develop PanINs with complete penetrance, which increase in number and stage with advancing age. After longitudinally follow-up of a small cohort some of the animals progressed to invasive PDAC, which metastasizes to liver and lung (Hingorani et al., 2003). Other studies could show that nearly all animals developed invasive and metastatic PDAC after long latency with a median survival of 15 months in the $Ptf1a^{Cre/+}$*;LSL-*$Kras^{G12D/+}$ model (Eser et al., 2013) and 13 months in the *Pdx1-Cre;LSL-*$Kras^{G12D/+}$ model (Schönhuber et al., 2014). For the first time, this new GEMM is able to recapitulate all stages of human PanINs and classical metastatic human PDAC.
With advanced stage of human PanINs, accumulation of mutations increases. To analyze the effect of additional alterations in tumor suppressors found in human PDAC, several follow-up

mouse models were generated. In *Pdx1-Cre;LSL-Kras$^{G12D/+}$;CDKN2a$^{lox/lox}$* mice, in which excision of exon 2 and 3 leads to elimination of both the p16^{INK4A} and the p19^{ARF} protein, development of PanINs and PDAC is accelerated (Aguirre et al., 2003). Progression to aggressive, highly invasive and metastatic cancer results in death by 11 weeks of age in all cases.

Another opportunity to accelerate tumor formation is the introduction of a missense mutation in the endogenous *Trp53* locus, which is common in human PDAC (Olive et al., 2004). Hingorani et al. interbred *Pdx1-Cre;LSL-Kras$^{G12D/+}$* animals with the *LSL-Trp53^{R172H}* mouse line containing a LSL cassette upstream of mutant *Trp53^{R172H}* (Hingorani et al., 2005). After excision of LSL cassettes in pancreatic precursor cells, expression of mutant Kras^{G12D} and Trp53^{R172H} leads to formation of metastatic PDAC with a dramatically shortened median survival of approximately 5 months. Loss of wild type Trp53 occurred in all animals analysed, resembling the human disease where LOH is frequently observed. Tumors of *Pdx1-Cre;LSL-Kras$^{G12D/+}$;LSL-Trp53$^{R172H/+}$* animals display features of human PDAC in histopathology and metastatic profile and demonstrate a high rate of genomic instability, a hallmark of human carcinomas.

Taken together, pancreatic tumor formation is initiated by expression of oncogenic Kras^{G12D} in pancreatic precursor cells and accelerated by the loss of tumor suppressors like p16^{INK4A}, p19^{ARF} and Trp53. As they faithfully recapitulate the major hallmarks of the human disease, the *Pdx1-Cre;LSL-Kras$^{G12D/+}$;LSL-Trp53^{R172H}* and *Ptf1a$^{Cre/+}$;LSL-Kras$^{G12D/+}$;LSL-Trp53^{R172H}* models are widely accepted as an accurate and predictive model for human PDAC.

1.1.3 CreER^{T2}: a tamoxifen-inducible system

One limiting factor of Cre/loxP based mouse models is the missing possibility of time-specific inducible genetic manipulation of oncogenes or tumor suppressors. Consequently, there was a need for time-specific control of gene expression. To address this aim, the group of Pierre Chambon modified the Cre/loxP system. They fused the Cre recombinase to the ligand-binding domain (LBD) of the human estrogen receptor (ER). Thereby, the activity of Cre depends on the presence of estrogen or anti-estrogen (tamoxifen) (Metzger et al., 1995). This system is perfectly working in cultured cells, but in mice, endogenous estrogens are present. Therefore, they modified the system and generated a chimeric protein (CreER^{T}) with a mutated LBD (G521R), which only binds the synthetic ligands tamoxifen and 4-hydroxytamoxifen (4-OHT). In the absence of the ligand, CreER^{T} is bound to the heatshock protein HSP90 and therefore localized as inactive form in the cytoplasm (Figure 1-2). After administration and binding of tamoxifen to the ER^{T} domain, the CreER^{T} dissociates from the HSP90 and translocates to the nucleus. There, it mediates excision of DNA fragments

flanked by loxP sites. Feil et al. showed excision of a chromosomally integrated gene flanked by loxP sites in transgenic mice expressing the CreER^{T} under the control of the cytomegalovirus promoter (Feil et al., 1996). To further improve ligand-activated site-specific recombination, a triple-mutant CreER^{T2} (G400V/M543A/L544A) was generated, whose 4-OHT sensitivity was about 4-fold higher than that of CreER^{T} *in vitro* (Feil et al., 1997). Leone et al. showed tamoxifen-induced recombination in oligodendrocytes and Schwann cells of transgenic *PLP-CreER^{T2}* mice by using the *Rosa26 LacZ* reporter mouse line (Leone et al., 2003).

Other groups achieved temporal control of recombination events by fusing the progesterone receptor (CrePR) (Kellendonk et al., 1999) or the murine estrogen receptor (CreER^{TM}) (Danielian et al., 1998) to the Cre recombinase.

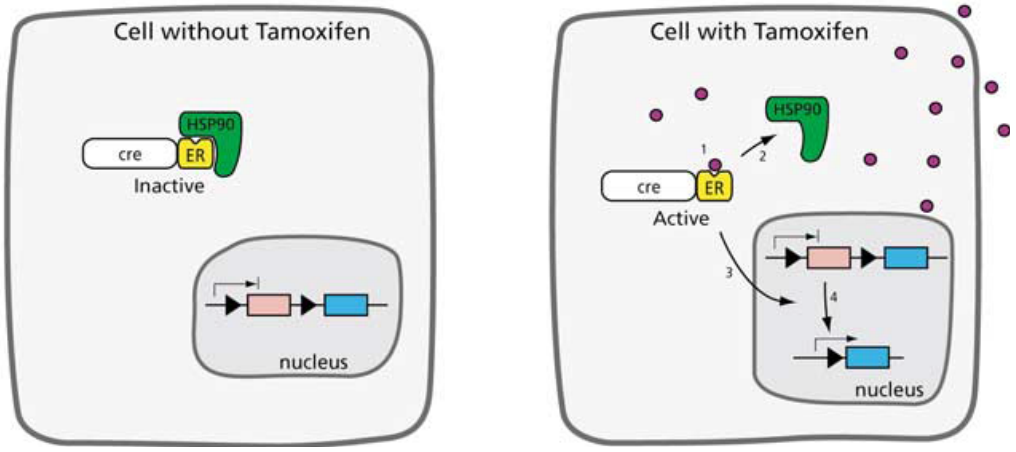

Figure 1-2: Model of the CreER^{T2} recombination system
In the absence of the ligand tamoxifen, the CreER fusion protein is bound to the heatshock protein HSP90. After tamoxifen administration and binding to the ER domain, HSP90 dissociates from the complex. Therefore, the CreER translocates into the nucleus and recombines loxP flanked DNA sequences. Violet circles represent tamoxifen. Reprinted by permission from Elsevier (Leone et al., 2003)

1.2 Kras-downstream signaling in pancreatic cancer

As depicted above, Kras is activated in most human PDAC and seems to be the initiating event. Oncogenic Kras is not only essential for the initiation and progression of pancreatic cancer but also for the maintenance. This was shown in a study using a mouse model in which oncogenic Kras can be switched on and off by doxycycline administration (Collins et al., 2012).

Kras downstream signaling is highly complex as oncogenic Kras activates a plethora of signaling pathways including canonical Raf/MEK/ERK, PI3K/Pdk1/AKT, RalGDS/p38MAPK, Rac and Rho, Rassf1, NF1, p120GAP and PLC-e (Castellano and Downward, 2011; Eser et

al., 2014; Pylayeva-Gupta et al., 2011). The three major effectors seem to be the Raf/MEK/ERK, PI3K/Pdk1/AKT and Ral guanine nucleotide exchange factor pathways.

Raf is a serine/threonine kinase which is located to the plasma membrane in the cytoplasm and is activated by Ras-GTP. Activated Raf then initiates a mitogen-activated protein kinase (MAPK) signal transduction cascade including MEK and ERK (Morrison and Cutler, 1997; Shields et al., 2000).

PI3K activates various downstream effectors by converting phosphatidylinositol (4,5)-bisphosphate (PIP2) into the second messenger PIP3. PIP3 then binds directly to proteins with pleckstrin homology domains such as Pdk1 and AKT (Cantley, 2002) and targets them to the cell membrane. In turn, Pdk1 activates AKT by phosphorylating threonine 308 (Alessi et al., 1997; Currie et al., 1999). AKT then phosphorylates and activates multiple downstream targets and thereby regulates cellular processes including growth, proliferation, survival and glucose metabolism.

Pancreas specific knock-out of the tumor supressor *Pten*, a negative regulator of PI3K signalling which converts PIP3 to PIP2 by its phosphatise activity, induced acinar to ductal metaplasia (ADM) and ductal malignancies at low frequency (Stanger et al., 2005). These data suggest a role of the PI3K/Pdk1/AKT pathway in pancreatic cancer initiation and progression. However, the repertoire of Pten has recently been expanded to include PI3K/Akt and phosphatase independent functions. Specifically, Pten has been shown to exert crucial functions within the nucleus which control genomic stability and cell cycle progression (Song et al., 2012). In addition, recent studies showed that loss of *Pten* does not phenocopy PI3K pathway activation by mutant PI3K isoforms like *PIK3CA* (p110α) (Vasudevan et al., 2009; Vivanco et al., 2007). Finally, both *PIK3CA* and *Pten* mutations often co-occur, suggesting that they may have distinct roles (Oda et al., 2005). Therefore, the role of the PI3K/Pdk1/AKT pathway in pancreatic cancer remains largely unclear.

The Ral guanine nucleotide exchange factor pathway also seems to play a role in pancreatic tumor formation. RalGEFs are relocated to the plasma membrane by Ras-GTP. These activators of Ras-related small GTPases RalA and RalB (Shields et al., 2000) promote the exchange of GDP to GTP (Kishida et al., 1997; Matsubara et al., 1999). In human PDAC, RalA and RalB are activated and are critical for invasion and metastasis which could be shown in cell culture experiments (Lim et al., 2006). In addition, inhibition of the cyclin-dependent kinase 5 (CDK5) in human pancreatic cancer cells blocks tumor growth and metastasis in an orthotopic xenograft model by interrupting the Ras-Ral signaling pathway (Feldmann et al., 2010). However, clean genetic *in vivo* data on the role of RalGEFs are lacking.

1.3 Aims of this work

It is still unclear which of the Kras downstream pathways are essential for Kras-driven PDAC formation and tumor maintenance. Therefore, the aim of this study was to analyze the major effectors of oncogenic Kras, the Raf/MEK/ERK and the PI3K/AKT signalling pathway.

Craf, a member of the Raf/MEK/ERK pathway, and *Pdk1*, an effector of the PI3K signalling pathway, were knocked out specifically in the pancreas by using the established *Ptf1a*$^{Cre/+}$*;LSL-Kras*$^{G12D/+}$ mouse model of pancreatic cancer. Both knock-out models were analyzed for PanIN and PDAC formation and median overall survival.

To be able to evaluate whether these genes and pathways are not only important for PDAC formation but also for tumor maintenance, a novel dual-recombinase system, which combines the Cre/loxP with the Flippase (Flp)/frt system, was generated and analyzed. A *Pdx1-Flp* mouse for pancreas specific expression of the Flp-recombinase and a frt-stop-frt (FSF) silenced *FSF-Kras*^{G12D} knock-in allele were generated. For site- and time-specific genetic manipulation of PanINs and PDAC, they were interbred with two tamoxifen-inducible CreER^{T2} mouse lines under the control of the ubiquitous *CAG* promoter as a knock-in at the *Rosa26* locus, or the proliferation marker *proliferating cell nuclear antigen* (*Pcna*) in the Flp-lineage.

With this new dual-recombinase model we are for the first time able to sequentially activate or inactive genes in the pancreas. Further, it is possible to manipulate pancreatic cancer subpopulations and target different pancreatic compartments and the host.

2. Materials

2.1 Technical equipment

Table 2-1: Technical equipment

Technical equipment	Source
Amersham Hyperprocessor™ automatic film processor	GE Healthcare Europe GmbH, München
Amersham VacuGene™ XL vacuum blotting system	GE Healthcare Europe GmbH, München
AxioCam MRc	Carl Zeiss AG, Oberkochen
CO_2 incubator HERAcell®	Heraeus Instruments GmbH, Osterode
Crystat Microm HM 560	Thermo Fisher Scientific Inc., Waltham, MA, USA
Elektrophoresis-power supply Power Pac 200	Bio-Rad Laboratories GmbH, München
Electroporation system Gene Pulser® II	Bio-Rad Laboratories GmbH, München
Gel Doc™ XR+ system	Bio-Rad Laboratories GmbH, München
Glucometer MediSense Precision Xtra	Abbott Laboratories, Wiesbaden
Heated paraffin embedding module EG1150 H	Leica Microsystems GmbH, Wetzlar
HERAsafe® biological safety cabinet	Thermo Fisher Scientific Inc., Waltham, MA, USA
Homogenizer Silent Crusher M with tool 6F	Heidolph Instruments GmbH, Schwabach
Magnetic stirrer MR2000	Heidolph Instruments GmbH, Schwabach
Microcentrifuge 5451 R	Eppendorf AG, Hamburg
Microplate Reader Anthos 2001	Anthos Mikrosysteme GmbH, Krefeld
Microscope Axio Imager.A1	Carl Zeiss AG, Oberkochen
Microscope Axiovert 25	Carl Zeiss AG, Oberkochen
Microtome Microm HM355S	Thermo Fisher Scientific Inc., Waltham, MA, USA
Microwave	Siemens, München
Neubauer hemocytometer	LO-Laboroptik GmbH, Bad Homburg
Odyssey® infrared imaging system	LI-COR Bioscience Corporate, Lincoln, NE, USA
Paraffin tissue floating bath Microm SB80	Thermo Fisher Scientific Inc., Waltham, MA, USA

Technical equipment	Source
pH-Meter 521	WTW GmbH, Weilheim
Pipetus®	Hirschmann Laborgeräte GmbH & Co. KG, Eberstadt
Power supply E844, E822, EV243	Peqlab Biotechnologie GmbH, Erlangen
Spectrophotometer NanoDrop 1000	Peqlab Biotechnologie GmbH, Erlangen
StepOnePlus™ Real-Time PCR system	Applied Biosystems Inc., Carlsbad, CA, USA
Stereomikroskope Stemi SV 11	Carl Zeiss AG, Oberkochen
Thermocycler TGradient	Biometra GmbH, Göttingen
Thermocycler Tpersonal	Biometra GmbH, Göttingen
Thermomixer compact	Eppendorf AG, Hamburg
Tissue processor ASP300	Leica Microsystems GmbH, Wetzlar
Vortex VF2	IKA-Werke GmbH, Staufen
Water bath 1003	GFL Gesellschaft für Labortechnik GmbH, Burgwedel
Western blot system SE 260 Mighty Small II	Hoefer, Inc., Holliston, MA, USA

2.2 Disposables

Table 2-2: Disposables

Disposable	Source
Amersham Hybond™-N membrane	GE Healthcare Europe GmbH, München
Amersham micro columns Illustra ProbeQuant™ G-50	GE Healthcare Europe GmbH, München
Amersham Rediprime™ II DNA labeling system	GE Healthcare Europe GmbH, München
Blood glucose test strips	Abbott GmbH & Co. KG, Ludwigshafen
Cell culture plastics	BD Bioscience, Franklin Lakes, NJ, USA; Greiner Bio-One, Frickenhausen
Cell scrapers	TPP Tissue Culture Labware, Trasadingen, Switzerland
Cell strainer	BD Bioscience, Franklin Lakes, NJ, USA
Combitips BioPur®	Eppendorf AG, Hamburg
Conical tubes, 15 ml	Greiner Bio-One, Frickenhausen

Disposable	Source
Conical tubes, 50 ml	Sarstedt AG & Co., Nümbrecht
Cover slips	Gerhard Menzel, Glasbearbeitungswerk GmbH & Co. KG, Braunschweig
Cryotubes™	Nunc™ Brand Products, Napeville, IL, USA
Cuvettes	Greiner Bio-One GmbH, Frickenhausen
Disposable scalpels	Feather Safety Razor Co., Ltd, Osaka, Japan
Gene Pulser®/MicroPulser™ cuvettes, 0.2 cm gap	Bio-Rad Laboratories GmbH, München
Filtropur S 0.2	Sarstedt AG & Co., Nümbrecht
Filtropur S 0.45	Sarstedt AG & Co., Nümbrecht
Glass slides Superfrost® Plus	Gerhard Menzel, Glasbearbeitungswerk GmbH & Co. KG, Braunschweig
MicroAmp® optical 96-well reaction plate	Applied Biosystems Inc., Carlsbad, CA, USA
Microtome blades S35, C35	Feather Safety Razor CO, LTD., Osaka, Japan
Pasteur pipettes	Hirschmann Laborgeräte GmbH & Co. KG, Eberstadt
PCR reaction tubes	Eppendorf AG, Hamburg
Petri dishes	Sarstedt AG & Co., Nümbrecht
Pipette tips	Sarstedt AG & Co., Nümbrecht
Reaction tubes, 0.5 ml, 1.5 ml and 2 ml	Eppendorf AG, Hamburg
Safe seal pipette tips, professional	Biozym Scientific GmbH, Oldenburg
Safe-lock reaction tubes BioPur®	Eppendorf AG, Hamburg
Serological pipettes	Sarstedt AG & Co., Nümbrecht
Single-use needles Sterican® 27-gauge	B. Braun Melsungen AG, Melsungen
Single-use syringes Omnifix®-F	B. Braun Melsungen AG, Melsungen
Spectra/Mesh® polypropylene filters	Spectrum Laboratories, Inc., Rancho Dominguez, CA, USA
Tissue embedding cassette system	MediteGmbH, Burgdorf
Transfer membrane Immobilon-P	Millipore GmbH, Schwalbach am Taunus

2.3 Reagents and enzymes

Table 2-3: Reagents and enzymes

Reagent	Source
1 kb extension ladder	Invitrogen GmbH, Karlsruhe
2-log DNA ladder	New England Biolabs, Frankfurt
2-Mercaptoethanol, 98%	Sigma-Aldrich Chemie GmbH, Steinheim
2-Propanol (isopropanol)	Carl Roth GmbH, Karlsruhe
4-hydroxytamoxifen (4-OHT)	Sigma-Aldrich Chemie GmbH, Steinheim
5-Bromo-2´-deoxyuridine (BrdU)	AppliChem GmbH, Darmstadt
Agarose	Sigma-Aldrich Chemie GmbH, Steinheim
Amersham Rapid-hyb™ buffer	GE Healthcare Europe GmbH, München
BBXF agarose gel loading dye mixture	BIO 101, Inc. Carlsbad, CA, USA
BI-D1870	Axon Medchem BV, Groningen, The Netherlands
Bovine serum albumin (BSA), fraction V	Sigma-Aldrich Chemie GmbH, Steinheim
Bradford reagent	Serva Electrophoresis GmbH, Heidelberg
Bromphenol blue	Sigma-Aldrich Chemie GmbH, Steinheim
BX-912	Axon Medchem BV, Groningen, The Netherlands
Complete, EDTA-free, protease inhibitor cocktail tablets	Roche Deutschland Holding GmbH, Grenzach-Wyhlen
Deoxycytidine 5'-triphosphate, [alpha-32P]- (EasyTides)	PerkinElmer, Rodgau
Dimethylsulfoxide (DMSO)	Carl Roth GmbH, Karlsruhe
dNTP mix, 10 mM each	Fermentas GmbH, St. Leon-Rot
Dulbecco's phosphate buffered saline, powder	Biochrom AG, Berlin
Ethanol, 100%	Merck KGaA, Darmstadt
Ethidium bromide	Sigma-Aldrich Chemie GmbH, Steinheim
Forene® isoflurane	Abbott GmbH & Co. KG, Ludwigshafen
GDC 0941 bismesylate	Axon Medchem BV, Groningen, The Netherlands
Gel loading dye, blue	New England Biolabs GmbH, Frankfurt
GelStar® nucleic acid gel stain	Biowhittaker Molecular Applications, Rockland, ME, USA
Gelatine	Carl Roth GmbH, Karlsruhe

Reagent	Source
GeneRuler™ 100 bp DNA ladder	Fermentas GmbH, St. Leon-Rot
Glucose	Sigma-Aldrich Chemie GmbH, Steinheim
Glycerol	Sigma-Aldrich Chemie GmbH, Steinheim
HotStarTaq DNA polymerase	Qiagen GmbH, Hilden
Hydrochloric acid (HCl)	Merck KGaA, Darmstadt
LB agar (Luria/Miller)	Carl Roth GmbH, Karlsruhe
LB broth (Luria/Miller)	Carl Roth GmbH, Karlsruhe
Magnesiumchloride	Carl Roth GmbH, Karlsruhe
Methanol	Merck KGaA, Darmstadt
MK-2206	Selleckchem, Houston, TX, USA
MLB-buffer	Millipore GmbH, Schwalbach am Taunus
Mouse diet LASCRdiet™ CreActive TAM400	LASvendi GmbH, Soest
Mouse diet Pancrex-Vet, #S2881-S713	ssniff Spezialdiäten GmbH, Soest
Nonidet NP-40	Sigma-Aldrich Chemie GmbH, Steinheim
NVP-BEZ235, Free Base	LC Laboratories, Woburn, MA, USA
Odyssey blocking reagent	LI-COR Corp. Offices, Lincoln, NE, USA
Orange G	Carl Roth GmbH, Karlsruhe
Peanut oil	Sigma-Aldrich Chemie GmbH, Steinheim
PfuUltra™ high fidelity DNA polymerase	Agilent Technologies, Inc., Santa Clara, CA, USA
Phosphatase inhibitor mix I	Serva Electrophoresis GmbH, Heidelberg
Precision Plus Protein™ all blue standard	Bio-Rad Laboratories GmbH, München
Proteinase K, recombinant, PCR grade	Roche Deutschland Holding GmbH, Grenzach-Wyhlen
QuantiFast® SYBR® green PCR master mix	Qiagen GmbH, Hilden
Raf-RBD protein GST beads	Cytoskeleton, Inc., Denver, Co, USA
rAPid alkaline phosphatase	Roche Deutschland Holding GmbH, Grenzach-Wyhlen
REDTaq® ReadyMix™ PCR reaction mix	Sigma-Aldrich Chemie GmbH, Steinheim
Restriction endonucleases	New England Biolabs GmbH, Frankfurt
Rnase-free DNase set	Qiagen GmbH, Hilden
RNaseA	Fermentas GmbH, St. Leon-Rot
Rotiphorese® gel 30	Carl Roth GmbH, Karlsruhe
Saponin	Sigma-Aldrich Chemie GmbH, Steinheim
S.O.C. medium	Invitrogen GmbH, Karlsruhe

Reagent	Source
Sodium chloride (NaCl)	Merck KGaA, Darmstadt
Sodium dodecyl sulphate (SDS)	Carl Roth GmbH, Karlsruhe
Sodium hydroxide solution (NaOH)	Merck KGaA, Darmstadt
SSC buffer 20x concentrate	Sigma-Aldrich Chemie GmbH, Steinheim
Sodiumdeoxycholate	Sigma-Aldrich Chemie GmbH, Steinheim
SuperScript II reverse transcriptase	Invitrogen GmbH, Karlsruhe
Sybr® Green	Applied Biosystems, Inc., Carlsbad, CA, USA
T4 DNA ligase	Invitrogen GmbH, Karlsruhe
Tamoxifen	Sigma-Aldrich Chemie GmbH, Steinheim
TaqMan® reverse transcriptase reagents	Applied Biosystems, Inc., Carlsbad, CA, USA
TE buffer, pH 8.0	AppliChem GmbH, Darmstadt
TEMED	Carl Roth GmbH, Karlsruhe
Tissue-Tek® O.C.T™ compound	Sakura Finetek Europe B.V, Alphen aan den Rijn, Netherlands
Triton® X-100	Sigma-Aldrich Chemie GmbH, Steinheim
Tween® 20	Carl Roth GmbH, Karlsruhe

2.4 Kits

Table 2-4: Kits

Kit	Source
EndoFree® plasmid maxi kit	Qiagen GmbH, Hilden
PIP_3 Mass ELISA Kit	Echelon Bioscience Inc., Salt Lake City, UT, USA
QIAamp DNA mini kit	Qiagen GmbH, Hilden
QIAfilter™ plasmid midi kit	Qiagen GmbH, Hilden
QIAprep® spin miniprep kit	Qiagen GmbH, Hilden
QIAquick® gel extraction kit	Qiagen GmbH, Hilden
QIA shredder	Qiagen GmbH, Hilden
Quick Blunting™ kit	New England Biolabs GmbH, Frankfurt
Ras activation assay kit	Millipore GmbH, Schwalbach am Taunus
RNeasy Mini kit	Qiagen GmbH, Hilden

Kit	Source
TaqMan® reverse transcription reagents	Applied Biosystems Inc., Foster City, CA, USA
Venor® *GeM* mycoplasma detection kit	Minerva Biolabs GmbH, Berlin

2.5 Antibodies

Table 2-5: Antibodies

Antibody	Source
Alexa Fluor® 488 anti-rabbit IgG (H+L)	Invitrogen GmbH, Karlsruhe
Alexa Fluor® 680 goat anti-rat IgG (H+L)	Invitrogen GmbH, Karlsruhe
Anti-mouse IgG (H+L) (DyLight® 680 Conjugate) #5470	Cell Signaling Technology, Inc, Danvers, MA, USA
Anti-mouse IgG (H+L) (DyLight® 800 Conjugate) #5257	Cell Signaling Technology, Inc, Danvers, MA, USA
Anti-rabbit IgG (H+L) (DyLight® 680 Conjugate) #5366	Cell Signaling Technology, Inc, Danvers, MA, USA
Anti-rabbit IgG (H+L) (DyLight® 800 Conjugate) #5151	Cell Signaling Technology, Inc, Danvers, MA, USA
Biotinylated Anti-rabbit	Vector Laboratories, Burlingame, CA, USA
Biotinylated Anti-rat	Vector Laboratories, Burlingame, CA, USA
BrdU, MCA2060	AbD Serotec, Düsseldorf
Craf, #9422	Cell Signaling Technology, Inc, Danvers, MA, USA
CK19 (Troma-III)	Developmental studies hybridoma bank, Iowa City, IA, USA
pan-AKT, #9272	Cell Signaling Technology, Inc, Danvers, MA, USA
pan-Ras, #05-516	Millipore GmbH, Schwalbach am Taunus
Pdk1, #3062	Cell Signaling Technology, Inc, Danvers, MA, USA
phospho-AKT Ser473, #9271 and #4060	Cell Signaling Technology, Inc, Danvers, MA, USA
phospho-AKT Thr308, #9275 and #2965	Cell Signaling Technology, Inc, Danvers, MA, USA

Antibody	Source
Phospho-GSK3β-S9 , #9336	Cell Signaling Technology, Inc, Danvers, MA, USA
α-Tubulin, # T9026	Sigma-Aldrich Chemie GmbH, Steinheim
β-Actin, # A5316	Sigma-Aldrich Chemie GmbH, Steinheim

2.6 Primers

All primers were synthesized by the company Eurofins MWG (Ebersberg) and dissolved in H_2O to a concentration of 10 µM.

Table 2-6: Primers for genotyping

Designation	Name	Sequence (5' – 3')
Genotyping *Ptf1a-Cre*	p48-Cre-GT-LP-URP	CCTCGAAGGCGTCGTTGATGGACTGCA
	p48-Cre-GT-wt-UP	CCACGGATCACTCACAAAGCGT
	p48-Cre-GT-mut-UP-neu	GCCACCAGCCAGCTATCAA
Genotyping *Pdx1-Cre*	Cre-neu-LP	CAGGGTGTTATAAGCAATCCC
	Cre-neu-UP	CCTGGAAAATGCTTCTGTCCG
Genotyping *LSL-Kras^{G12D}*	Kras-WT_UP1	CACCAGCTTCGGCTTCCTATT
	Kras-URP_LP1	AGCTAATGGCTCTCAAAGGAATGTA
	KrasG12Dmut_UP	CCATGGCTTGAGTAAGTCTGC
Genotyping *cRaf^{lox}*	Raf-lox_UP	AACATGAAGTGGTGTTCTCCGGGCGCC
	Raf-lox_LP	TGGCTGTGCCCTTGGAACCTCAGCACC
Genotyping *Pdk1^{lox}*	PDK1-UP	ATCCCAAGTTACTGAGTTGTGTTGGAAG
	PDK1-LP	TGTGGACAAACAGCAATGAACATACACGC
Genotyping *Pdx1-Flp*	Flpopt-scLP	CGTTGTAAGGGATGATGGTGAACT
	pdx5utr-scUP	AGAGAGAAAATTGAAACAAGTGCAGGT
Genotyping *FSF-Kras^{G12D}*	Kras-WT_UP1	CACCAGCTTCGGCTTCCTATT
	Kras-URP_LP1	AGCTAATGGCTCTCAAAGGAATGTA

Designation	Name	Sequence (5' – 3')
	R26-Tva-GT-SA-mut_LP	GCGAAGAGTTTGTCCTCAACC
Genotyping *FSF-R26^{CreERT2}*	CreERT2scUP3	GAATGTGCCTGGCTAGAGATC
	CreERT2scLP1	GCAGATTCATCATGCGGA
Genotyping *FSF-R26^{CreERT2}* Stop Cassette	Cre-neu-LP	CAGGGTGTTATAAGCAATCCC
	pGL3-pA-pause-4645-UP	TGAATAGTTAATTGGAGCGGCCGCAATA
Genotyping *FSF-R26^{CreERT2}* CAG promoter	R26-td-E-mutLP	TCAATGGGCGGGGGTCGTT
	R26-Tva-GT-UP	AAAGTCGCTCTGAGTTGTTAT
	R26-Tva-GT-WT-LP	GGAGCGGGAGAAATGGATATG
Genotyping *FSF-Pcna^{CreERT2}*	PCNA-FSF-LP	CAGCCAGACCTCGTTCCTCTTAG
	PCNA-FSFwt-UP	CTCAAAGCTGCAGGCATTTAATGA
	PCNA-FSFmut-UP1	GCTCCAGACTGCCTTGGGAA
Genotyping *R26^{mT-mG}*	CAG-sc-LP	GTACTTGGCATATGATACACTTGATGTAC
	R26-Tva-GT-UP	AAAGTCGCTCTGAGTTGTTAT
	R26-Tva-GT-WT-LP	GGAGCGGGAGAAATGGATATG
Genotyping *LSL-R26^{DTA}*	DTA-GT-UP	AACTTTTCTTCGTACCACGGGAC
	DTA-GT-LP	TTCCGTTCCGACTTGCTCC
Genotyping *FSF-R26^{hpAP}*	hp-AP-LP	TGTCTTGGACAGAGCCACATATG
	hp-AP-UP	GAGAACCCGGACTTCTGGAAC
Genotyping *R26$^{Tva/lacZ}$*	R26-Tva-GT-UP	AAAGTCGCTCTGAGTTGTTAT
	R26-Tva-GT-SA-mut-LP	GCGAAGAGTTTGTCCTCAACC
	R26-Tva-GT-WT-LP	GGAGCGGGAGAAATGGATATG

Table 2-7: Primers for cloning

Designation	Name	Sequence (5' – 3')
Cloning Screen PCR	pGL3-pA-pause-4645-UP	TGAATAGTTAATTGGAGCGGCCGCAATA
	pGL3-pA-pause-4812-UP	TCAGTTATCTAGAGAAATGTTCTGGCACCTGCA
Cloning Screen PCR	PCNA-ATG-UUP	GCACAGCTCGATTTGCCTG
	PCNA-ATG-WT-LP	CCCGACACCATAGACCAATCAG
Cloning Linker	rac-Asc-PBS-UP1	GTCGGCGCGCCAAATGCTGGGCTGGATGCAGGCGCG CCTTAAT
	rac-Asc-PBS-LP1	TAAGGCGCGCCTGCATCCAGCCCAGCATTTGGCGCGC CGACAT
Cloning Screen PCR	MB-f1-UP	GAGATAGGGTTGAGTGTTGTTCCA
	PCNA-sc-LP	TGCATCCAGCCCAGCATTT
	Soriano-SA-LP	CATCAAGGAAACCCTGGACTACTG
Cloning Screen PCR	PCNA-ES-sc-ATG-UP2	AAATGCTGGGCTGGATGCA
	FSF-sc-LP1	AAGCGAAGGAGCAAAGCTGCTAT
Cloning Screen PCR	rackua-LP1	CACCATATATCTAGGTATGCTGAGACA
	rackua-UP1	CTCCGTAGT GTTTAAAATA CTCTCCAG
Cloning Sequencing	pdxERT2-scUP1	ATGTGTAGAGGGCATGGTGGAGA
	pGL3-RV3-UP	CTAGCAAAATAGGCTGTCCC
	M13-FP	GTAAAACGACGGCCA
ES screening PCRs	PCNA-ES-sc-ATG-UP	GTTTAAATCTAGGCCCTCCGACCT
	PCNA-CRE-ES-LP1	AGCCCGGATCAAGCTTATCGATACCGTCGA
	PCNA-CRE-ES-LP4	AAAGACCGCGAAGAGTTTGTCCT

Table 2-8: Primers for qRT PCR

Designation	Name	Sequence (5' – 3')
Pdk1, mouse	Pdk1 forward	ACGCCCTGAAGACTTCAAGTTTG
	Pdk1 reverse	GCCAGTTCTCGGGCCAGA

Designation	Name	Sequence (5’ – 3’)
cyclophilin	Cyclophilin forward	ATGGTCAACCCCACCGTGT
	Cyclophilin reverse	TTCTGCTGTCTTTGGAACTTTGTC

2.7 Plasmids

Table 2-9: Plasmids

Plasmid	Abbreviation	Source
pBlue-Pcna	abr5	Generated in the laboratory of Prof. Saur, Munich; modification of pBluescript, Stratagene, La Jolla, CA, USA
pENTR-Rosafrt-CreERT2	ato2	Generated in the laboratory of Prof. Saur, Munich; modification of pENTR™/D-TOPO®, Invitrogen GmbH, Karlsruhe
pENTR-FSF-MCS-PA	atg	Generated in the laboratory of Prof. Saur, Munich; modification of pENTR™/D-TOPO®, Invitrogen GmbH, Karlsruhe
pFSF-Pcna^{CreERT2}	rac16	Generated in the laboratory of Prof. Saur, Munich; modification of pBluescript, Stratagene, La Jolla, CA, USA

2.8 Bacterials strains

Table 2-10: Bacterial strains

Bacterial strain	Source
One shot® Stbl3™ chemically competent *E. coli*	Invitrogen GmbH, Karlsruhe
One shot® TOP10 chemically competent *E. coli*	Invitrogen GmbH, Karlsruhe

2.9 Buffers and solutions

All buffers were prepared with bidistilled H_2O.

Table 2-11: Buffers and solutions

Buffer	Composition
Alcian blue, pH 2.5	1% Alcian blue
	3% Acetic acid
AP detection buffer	100 mM Tris-HCl pH 9.5
	100 mM NaCl
	50 mM $MgCl_2$
AP staining buffer	100 mM Tris-HCl pH 9.5
	100 mM NaCl
	50 mM $MgCl_2$
	Sodiumdesoxycholate
	NP-40
	Levimasole
	1:50 NBT/BCIP (add prior to use)
ES cell lysis buffer	100 mM Tris pH 8.5
	5 mM EDTA
	0.8 mM HCl
	2% SDS
	200 mM NaCl
	0.1 mg/mL proteinase K (add prior to use)
Gitschier's buffer (GB), 10x	670 mM Tris pH 8.8
	166 mM $(NH_4)_2SO_4$
	67 mM MgCl2
IP buffer, pH 7.9	50 mM HEPES
	150 mM NaCl
	1 mM EDTA
	0.5% NP-40
	10% glycerol
	1% phosphatase inhibitor (add prior to use)
	1% protease inhibitor (add prior to use)
KCM buffer, 5x	500 mM KCl
	150 mM $CaCl_2$
	250 mM $MgCl_2$

Buffer	Composition
Loading buffer orange G, 6x	60% glycerol 60 mM EDTA 0.24% orange G 0.12% SDS
Nuclear fast red	0.1% Nuclear fast red 2.5% Aluminium sulfate
PBS, pH 7.4	20 mM Na_2HPO_4 50 mM NaCl
PCR Lysis buffer	0.5% Triton X-100 1% 2-Mercaptoethanol 10% 10 x GB 400 µg/ml Proteinase K (add prior to use)
Protein loading buffer, 5x, pH 6.8	10% SDS 50% glycerol 228 mM TrisHCl 0.75 mM bromphenol blue 5% 2-mercaptoethanol
Solution C	3% BSA 1% Saponin 1% Triton-X
TAE buffer, 50x	2 M TRIS 100 mM EDTA 5.71% (v/v) Acetic acid (100%) pH 8.5
Transfer buffer	19 mM TrisHCl 192 mM glycin 0.1% SDS 20% methanol

2.10 Histology

Table 2-12: Reagents and kits for histological analysis

Reagent / kit	Source
Acetic acid	Merck KGaA, Darmstadt
Alcian Blue 8GX	Merck KGaA, Darmstadt
Aluminium sulfate	Sigma-Aldrich Chemie GmbH, Steinheim
Antigen unmasking solution	Vector Laboratories, Burlingame, CA, USA
Avidin / Biotin Blocking Kit	Vector Laboratories, Burlingame, CA, USA
Certistain® Nuclear fast red	Merck KGaA, Darmstadt
DAB peroxidase substrate kit	Vector Laboratories, Burlingame, CA, USA
Eosin	Waldeck GmbH & Co KG, Münster
Hematoxylin	Merck KGaA, Darmstadt
Hydrogen peroxide 30%	Merck KGaA, Darmstadt
Pertex mounting medium	Medite GmbH, Burgdorf
Roti® Histofix 4%	Carl Roth GmbH + Co. KG, Karlsruhe
Roti® Histol	Carl Roth GmbH + Co. KG, Karlsruhe
Sucrose (saccharose)	Merck KGaA, Darmstadt
TOPRO®3-iodid	Invitrogen GmbH, Karlsruhe
Vectashield® mounting medium	Vector Laboratories, Burlingame, CA, USA
Vectashield® mounting medium with DAPI	Vector Laboratories, Burlingame, CA, USA
Vectastain® elite ABC kit	Vector Laboratories, Burlingame, CA, USA

2.11 Cell culture reagents and media

Table 2-13: Reagents for cell culture

Reagent	Source
3,3′,5-Triiodo-L-thyronine sodium salt	Sigma-Aldrich Chemie GmbH, Steinheim
Antibiotic antimycotic	Invitrogen GmbH, Karlsruhe
Bovine serum albumin (BSA)	Sigma-Aldrich Chemie GmbH, Steinheim
Collagenase Type 2	Worthington Biochemical Corporation, Lakewood, NJ, USA
Collagenase P	Roche Deutschland Holding GmbH,

Reagent	Source
	Grenzach-Wyhlen
Dexamethasone	Sigma-Aldrich Chemie GmbH, Steinheim
Dulbecco's modified eagle medium (D-MEM) with L-glutamine	Invitrogen GmbH, Karlsruhe
Dulbecco's modified eagle medium (D-MEM) without L-glutamine (for ES cell medium)	Invitrogen GmbH, Karlsruhe
Dulbecco's phosphate buffered saline (PBS)	Invitrogen GmbH, Karlsruhe
Epidermal Growth Factor human (EGF)	Sigma-Aldrich Chemie GmbH, Steinheim
Fetal calf serum (FCS)	Biochrom AG, Berlin
Gelatine	Invitrogen GmbH, Karlsruhe
L-Glutamine	Invitrogen GmbH, Karlsruhe
Geniticin	Sigma-Aldrich Chemie GmbH, Munich
Hanks' balanced salt solution (HBSS)	Invitrogen GmbH, Karlsruhe
Hydrocortisone	Sigma-Aldrich Chemie GmbH, Steinheim
Insulin-transferrin-sodium selenite media supplement	Sigma-Aldrich Chemie GmbH, Steinheim
ESGRO® Leukemia inhibitory factor (LIF)	Merck KGaA, Darmstadt
Non-essential amino acids (100x)	Invitrogen GmbH, Karlsruhe
RPMI 1640 medium	HyClone Laboratories, Inc., Logan, UT, USA
Sodium pyruvate	Invitrogen GmbH, Karlsruhe
Soybean trypsin inhibitor (STI)	Sigma-Aldrich Chemie GmbH, Steinheim
Penicillin-Streptomycin	Invitrogen GmbH, Karlsruhe
rat tail collagen type I (RTC)	BD Bioscience, Franklin Lakes, NJ, USA
Trypsin-EDTA	Invitrogen GmbH, Karlsruhe

Table 2-14: Media for cell culture

Medium	
ACL3 medium	RPMI 1640 15% FCS 5 mg/ml BSA 10 µg/ml EGF 1% L-Glutamine 50 nM Hydrocortisone 5 mM Sodium pyruvate 1% Antibiotic antimycotic 1% Insuline-transferrine sodium selenite 0.4 µg/ml 3,3′,5-Triiodo-L-thyronine sodium salt
ES cell medium	D-MEM 15% EU-FCS 1% Penicillin-Streptomycin 1% L-Glutamine 1% Sodium pyruvate 1% Non-essential amino acids 0.1% 0.1 M 2-Mercaptoethanol 1000 U/mL LIF
Freezing medium	70 % D-MEM 20 % FCS 10 % DMSO
MEF medium	D-MEM 10% EU-FCS 1% Penicillin-Streptomycin 1% L-Glutamine
Tumor cell medium	D-MEM 10% FCS 1% Penicillin-Streptomycin

3. Methods

3.1 Molecular techniques

3.1.1 Cloning of the targeting construct

To achieve Cre expression in proliferating cells in the pancreas, the tamoxifen-inducible $CreER^{T2}$ was inserted into the *proliferating cell nuclear antigen* (*Pcna*) locus. For specific expression in the pancreas, the construct was silenced by a 5' frt-stop-frt (FSF) cassette.
The $CreER^{T2}$ fusion protein was cut out from the pENTR-Rosafrt-CreERT2 vector with EcoR I and Sac I and cloned into the pENTR-FSF-MCS-PA vector (digested with Sma I) containing the FSF cassette. By integration of a linker with the primer set rac-Asc-PBS-UP1 and rac-Asc-PBS-LP1 5' of the FSF cassette, two restriction sites were inserted for further cloning. The FSF-CreERT2 cassette was cut out with Sac II and cloned into the Pme I digested pBlue-Pcna vector containing the 3' and 5' homologous arms for homologous recombination. The resulting targeting vector was named $pFSF\text{-}Pcna^{CreERT2}$.

3.1.2 DNA analysis

3.1.2.1 Transformation of competent bacteria

Before transformation, the bacteria were thawed on ice. 200 - 500 ng of DNA were mixed with 20 µl 5x KCM buffer and H_2O was added to a final volume of 100 µl. To this solution, 100 µl of competent bacteria were added. After incubating the solution at 4°C for 20 min, a second incubation at room temperature (RT) for 10 min followed. Next, 1 ml S.O.C. medium was added and the bacteria were shaken for 1 h at 37°C (Top10) or 2 h at 25°C (Stbl3). Afterwards, the bacteria were streaked in different amounts on agar plates containing the appropriate antibiotic with a concentration of 100 µg/ml and incubated at 37°C o/n or 25°C for 24 h.

3.1.2.2 Cloning and isolation of plasmid DNA

Before amplification of plasmids, standard PCR (3.1.2.4) was performed to verify correct insertion and orientation. Therefore, colonies were picked from agar plates, streaked into a PCR tube and onto a fresh selective agar plate, the backup plate. In the PCR tube, 50 µl H_2O was added and bacteria were heated at 95°C for 5 min. This DNA and specific primers (Table 2-7) were used for screening PCR. Positive clones were taken to inoculate 5 ml of LB medium containing appropriate antibiotics and shaken o/n at 37°C or 25°C, respectively.

Glycerol stocks were prepared by mixing freshly grown bacteria and glycerol 1:1 and stored at -80°C. DNA preparation was done using the QIAprep® spin miniprep kit. For isolation of a higher amount of DNA, 50 ml or 250 ml of selective LB medium were inoculated and were used to carry out DNA preparation with the QIAfilter™ plasmid midi kit or the EndoFree® plasmid maxi kit. Concentration of the DNA was measured with the spectrophotometer NanoDrop 1000. For further cloning, restriction digests were performed. 30 µg of plasmid DNA were digested in a total volume of 120 µl at appropriate temperature. After adding GelStar® nucleic acid gel stain as loading dye, gel electrophoresis (3.1.2.5) with a 0.8% agarose gel was performed. The correct band was cut out and DNA extraction was done using the QIAquick® gel extraction kit. The Quick Blunting™ kit was used to remove nucleotide overhangs if required. DNA ends were dephosphorylated by the rAPid alkaline phosphatase.

3.1.2.3 Isolation of genomic DNA

For genotyping and recombination PCR analysis, a small piece of the mouse tail or tissue was lysed in PCR lysis buffer for 1.5 h at 55°C. Proteinase K was inactivated for 15 min at 95°C. After vortexing the sample, it was centrifuged at 14000 rpm for ten min and the supernatant containing the DNA was used for PCR analysis.

3.1.2.4 Polymerase chain reaction

For standard polymerase chain reaction (PCR), REDTaq® ReadyMix™ was used.

Table 3-1: Reaction mix and conditions for standard PCR

Reaction Mix		**Conditions**		
12.5 µl	REDTaq® Ready Mix™	95°C	5 min	
0.25 - 2 µl	Forward primer (10 µM)	95°C	45 sec	
0.25 - 2 µl	Reverse primer (10 µM)	55°C - 64°C	1 min	40x
1.5 µl	DNA	72°C	1min, 30 sec	
ad 25 µl	H_2O			

3.1.2.4.1 Genotyping

To determine the genotype, mouse tail DNA, isolated as described in 3.1.2.3 was used. For each allele, specific primers were designed (Table 2-6). Annealing temperatures and PCR products are indicated in Table 3-2.

Table 3-2: Annealing temperatures and PCR products of genotyping PCRs
mut = mutated allel; WT = wild type allele

Name of PCR	Annealing temperature	PCR products (bp)
Ptf1a^{Cre}	60°C	400 (mut) / 600 (WT)
LSL-Kras^{G12D}	55°C	170 (mut) / 270 (WT)
LSL-Trp53^{R172H}	60°C	270 (mut) / 570 (WT)
Pdk$^{f/+}$	63°C	280 (mut) / 200 (WT)
Craf$^{f/+}$	58°C	250 (mut) / 180 (WT)
R26^{mTmG}	62°C	450 (mut) / 650 (WT)
Pdx1-Flp	56°C	620 (mut) / 300 (internal control)
FSF-R26^{hpAP}	60°C	230 (mut)
FSF-Kras^{G12D}	55°C	350 (mut) / 270 (WT)
FSF-R26$^{-CreERT2}$	55°C	190 (mut)
FSF-R26-CAG	62°C	450 (mut) / 650 (WT)
FSF-Stop	60°C	600 (mut)
LSL-R26^{DTA}	60°C	320 (mut)
FSF-Pcna^{CreERT2}	64°C	310 (mut) / 550 (WT)

3.1.2.4.2 Recombination PCR

To check whether the FSF cassette is recombined, a piece of tissue was lysed as described in 3.1.2.3.

Table 3-3: Annealing temperatures and PCR products of recombination PCRs
rec = mutated allele without translational stop element after recombination; mut = mutated allele; WT = wild type allele

Name of PCR	Annealing temperature	PCR products
cRaf$^{f/+}$ del	58°C	350 (rec) / 250 (mut) / 180 (WT)
Pdk$^{f/+}$ del	63°C	250 (rec) / 280 (mut)
FSF-AP del	60°C	520 (rec)
FSF-Kras del	60°C	196 (rec)
FSF-Cre-Stop del	60°C	490 (rec)

3.1.2.4.3 Screening PCR for ES cell clones

Isolated genomic DNA from embryonic stem cell clones was used for screening PCR to check for correct homologous recombination of the targeting construct.

Table 3-4: Reaction mix for screening PCR

Reaction Mix	
11 µl	5x Q-Solution
5 µl	10x buffer
2 µl	dNTPs (10 mM each)
2 µl	Forward primer (10 µM)
2 µl	Reverse primer (10 µM)
2 µl	DNA
25.65 µl	H_2O
0.35 µl	Hot Star Taq

3.1.2.5 Gel electrophoresis

For analytical gel electrophoresis, TAE buffer was used for agarose gels and as running buffer. 0.8 - 2% agarose gels were prepared, depending on the size of the expected bands. 24 µl ethidium bromide (1 mg/ml) were added to the agarose gel and 150 µl to the running buffer. For PCR analysis, 12 µl of PCR reaction were loaded onto the gel. Orange G was added to restriction digests as loading dye. The gel was run at 120 V for 1 - 1.5 h or until the bands had been separated sufficiently. Subsequently analysis by UV transillumination was performed with the Gel Doc™ XR+ system.

3.1.3 RNA analysis

A small piece of pancreatic tissue was homogenized in 1 ml RLT buffer containing 10 µl 2-mercaptoethanol using the SilentCrusher M, snap frozen in liquid nitrogen and stored at -80°C until further use.

3.1.3.1 RNA isolation and cDNA synthesis

RNA isolation was carried out with the QIAshredder columns and the RNeasy mini kit according to manufacturer's protocol. DNA was digested using the RNase-free DNase set. RNA concentration was measured with the spectrophotometer NanoDrop 1000. Samples were stored at -80°C.

cDNA synthesis was performed using the TaqMan® reverse transcription reagents according to manufacturer's protocol. cDNA was stored at -20°C.

3.1.3.2 Quantitative real time PCR

Quantitative real time PCR was performed using the StepOnePlus™ real time PCR system and software (TaqMan, PE Applied Biosystems, Norwalk, CT) with Sybr Green as fluorescent dye. Using the Taq-Man Reverse Transcription Reagents according to manufacturer's protocol, cDNA samples for quantitative analysis were generated from 5 µg of total RNA. Primers used are listed in Table 2-8. The ubiquitously expressed housekeeping gene cyclophilin acted as endogenous reference.

3.1.4 Protein analysis

3.1.4.1 Protein isolation of tissue samples and tumor cells

Tumor cells were grown on a 10 cm plate to 80% confluency, washed with PBS and lysed in IP buffer containing phosphatase and proteinase inhibitors to obtain whole cell lysates. Samples were snap frozen in liquid nitrogen and stored at -80°C until further use. Protein isolation of murine tissue samples was performed as described in 3.2.2.
Before use, the lysates were thawed on ice, centrifuged for 20 min at 13200 rpm and 4°C. The supernatant was transferred into a new reaction tube. Bradford assay was used to measure the protein concentration. Therefore, the Bradford reagent was diluted 1:5 with H_2O and 300 µl per well were put into a 96-well plate. Measurement was carried out in triplicates by adding 1 µl of the samples per well. After incubation of 10 min, absorbance was measured in the microplate reader Anthos 2001 at 600 nm. Protein concentration was calculated using a BSA dilution series as reference. All samples were then adjusted to the same protein concentration by adding IP buffer. Protein loading buffer was added and the samples were denaturated for 5 min at 95°C. Samples were stored at -20°C until further analysis.

3.1.4.2 Western blot

To separate the proteins by size, standard sodium dodecyl sulphate polyacrylamide gel electrophoresis (SDS-PAGE) was performed. First, all reagents for a 10% or 12% separating gel were mixed according to table 3-6, TEMED was added at last for polymerization. The gel was poured into a gel caster and covered with 2-propanol until it polymerized. Then the stacking gel was prepared and added to the gel caster. After polymerization, 100 µg of

protein samples were loaded onto the gel. Protein separation was carried out at 80 – 120 V for 1.5 h in running buffer.

Table 3-5: SDS gel for electrophoresis of proteins

10% separating gel	12% separating gel	Stacking gel
2050 µl H_20	1700 µl H_20	1500 µl H_20
1300 µl Separating gel buffer	1300 µl Separating gel buffer	650 µl Stacking gel buffer
1650 µl Rotiphorese® gel 30	2000 µl Rotiphorese® gel 30	375 µl Rotiphorese® gel 30
50 µl 10% SDS	50 µl 10% SDS	25 µl 10% SDS
25 µl 10% APS	25 µl 10% APS	12.5 µl 10% APS
7.5 µl TEMED	7.5 µl TEMED	5 µl TEMED

For blotting, an immobilon-P membrane was activated in methanol. Wet blot was performed at 100 V for 3 h in transfer buffer. To block unspecific antibody binding, the membrane was incubated in Odyssey® blocking reagent diluted 1:1 in PBS for 30 min at RT. Next, the membrane was incubated by gently agitation with the first antibody o/n at 4°C. After washing the membrane three times for 10 min with PBS/Tween, the secondary antibody diluted 1:5000 was added for 1 h in the dark with gently shaking. The membrane was washed again three times with PBS/Tween before it was scanned at 700 nm or 800 nm using the Odyssey® infrared imaging system. As loading control, α-Tubulin or β-actin were used.

3.1.4.3 Ras activation assay

Tissue samples from 1 and 12 month old mice were lysed in MLB buffer supplemented with 10% glycerol, phosphatase- and protease-inhibitors. After normalizing the cleared lysates for protein, 1 mg of each sample was incubated with Raf-RBD protein GST beads for 2 h at 4°C with rotation. Beads were then collected by centrifugation at 13,000 rpm for 10 sec at 4°C. The pellet was washed twice, resuspended in Laemmli buffer and heated. The samples were loaded onto a 12% SDS-gel and detected as described in 3.6.2.

3.1.4.4 PIP3 assay

For PIP3 assay, pancreatic tissue samples from 6 weeks old mice were collected, weighed and homogenized in 0.5 M trichloracetic acid and prepared according to manufacturer's protocol. Measurement was carried out in duplicates and PIP3 levels were adjusted to input weight of the tissue samples. Absorbance was measured in the microplate reader FLUOstar OPTIMA at 450 nm.

3.2 Generation of the *FSF-Pcna*^{CreERT2} mouse

In this study, the *FSF-Pcna*^{CreERT2} mouse line was generated. The targeting construct was cloned as described in 3.1.1. To achieve homologous recombination, the construct was linarized and transfected into mouse embryonic stem cells by electroporation. After selecting the positive clones, they were cryopreserved and sent to PolyGene AG (Switzerland) for blastocyst injection and generation of chimeras.

3.2.1 Generation of transgenic embryonic stem cells

3.2.1.1 Preparation of the targeting vector

The vector containing the targeting construct was cloned as described in 3.1.1. Fresh LB medium was inoculated from a glycerol stock and bacteria were grown at 25°C o/n until OD 1.0 – 1.2. Plasmid preparation was performed according to manufacturer's protocol using EndoFree Plamid Maxi kit (Quiagen). After elution from the QIA-filter cartridge, the eluate was precipitated in isopropanol, dried and again precipitated in ethanol. The pellet was dissolved in sterile TE buffer. To linearize the vector, 30 µg of the plasmid DNA were digested with Asc I for 1.5 h at 37°C. The enzyme was heat inactivated for 20 min at 65°C. Linearization of the vector was confirmed by a 1% agarose gel electrophoresis.

3.2.1.2 Embryonic stem cell culture

ES cells need to be grown on a monolayer of mitotically inactivated mouse embryonic fibroblasts (MEFs). Inactivation of MEFs was achieved by irradiation with 34 gray. Generally, G418 resistant MEFs were seeded on gelatine-coated 10 cm dishes the day before the ES cells (129S6) were seeded. They were grown at 37°C and 5% CO_2 and ES cell medium was renewed daily.

3.2.1.3 Transfection and selection

The targeting construct was transfected into ES cells by electroporation. ES cells were washed with PBS, trypsinised and counted using a Neubauer hemocytometer. 1 x 10^7 cells were resuspended in 750 µl ice-cold PBS, pipetted into a pre-cooled electroporation cuvette (Bio-Rad) and carefully mixed with the linearized vector. Electroporation was performed at 250 V / 500 µF with the Bio-Rad Gene Pulser II. Afterwards, the suspension was resuspended in pre-warmed ES cell medium and pipetted on MEF-coated 10 cm dishes. The

remaining unelectroporated ES cells were seeded on a gelatine-coated 6-well plate for WT genomic stem cell DNA isolation.

After 18 h, ES cell medium was renewed and 250 µg/mL geniticine (G418) was added for selection of positive clones. Single clones were picked 7 days after electroporation. Cells were transferred on a MEF-coated 24-well plate for expansion and a gelatine-coated 96-well plate for DNA isolation. After screening PCR, positive clones were expanded and cryopreserved from a 6-well plate and 6 cm dish according to the scheme shown in Figure 3-1. For cryopreservation, ES cell medium containing 10% DMSO was used. Cryo tubes were frozen at -80°C in a Nalgene freezing container with isopropanol and transferred to liquid nitrogen after 24 h.

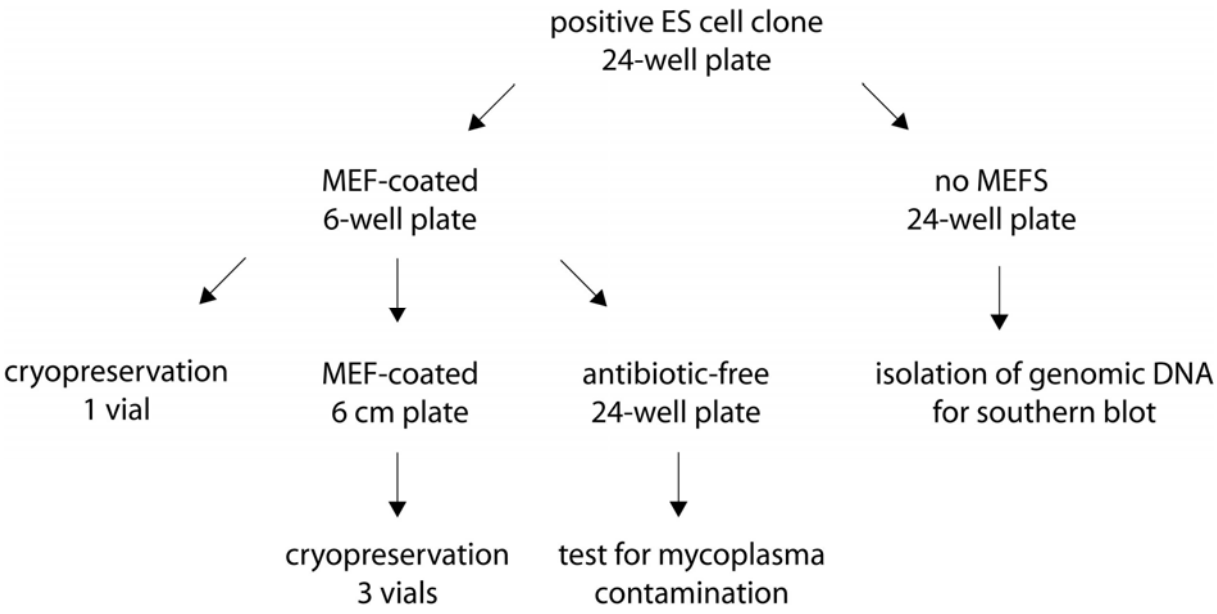

Figure 3-1: Culture procedures for positive ES cell clones

3.2.1.4 PCR screening of ES cells to identify homologous recombined clones

For PCR screening purpose, ES cell DNA was isolated out of gelatine-coated 96-well plate by incubation with 20 µl of PCR lysis buffer for 1 h at 55°C in a wet chamber. Afterwards, the DNA was transferred into new reaction tubes and proteinase K was inactivated at 95°C. PCNA-ES-sc-ATG-UP and PCNA-Cre-ES-LP4 primers and HotStarTaq were used for screening PCR (Table 3-4). Conditions are shown in Table 3-1. PCR products were loaded on an agarose gel to check for the correct size of 1978 bp.

Table 3-6: Conditions for ES cell screening PCR

Temperature	Time	Number of cycles
95°C	16 min	1
95°C	35 sec	10
63,8°C	1 min	
68°C	4 min	
95°C	35 sec	39
63,8°C	1 min	
68°C	4 min + 2 sec each cycle	

3.2.1.5 Genomic DNA isolation of ES cells for southern blot analysis

ES cells for DNA isolation were grown to 100% confluency on 6-well plate and medium was renewed daily. After washing them with PBS, cells were lysed in 2 ml PCR lysis buffer per 6-well over night at 55°C in a wet chamber. The next day, 4 ml of 100% ethanol were added and incubated over night at RT. Then, ethanol was removed, DNA was washed with PBS three times and dried at RT. After 40 min, DNA was dissolved in 300 µl H_2O and stored at 4°C until further analysis.

3.2.1.6 Testing for mycoplasma contamination

For testing for mycoplasma contamination ES cells were grown to 100% confluency on gelatine-coated 24-well plate with medium without P/S. Venor® *GeM* kit (Minerva biolabs) was used according to manufacturer's protocol.

3.2.2 Southern blot

Isolated genomic DNA from WT ES cells and PCR positive clones were digested with BamH I for 5' probe, Bgl II for 3' probe and BamH I and Kpn I for neo probe 24 h at 37°C. Southern blot was performed according to standard protocol (Southern, 1975). Samples, positive control and 1 kb extension ladder were loaded on 1% agarose gel after adding BBXF Agarose gel loading dye mixture. Agarose gel was running for 14 h at 40 V. The part of the gel containing extension ladder and a control digestion was cut out, stained with ethidium bromide (EtBr) and photographed under UV illumination. A transparent ruler was used as reference for the run length.

DNA was transferred on a Hybond™-N membrane using a vacuum blotter with 55 mbar. For 1 h, the gel was covered with 0.25 M HCl to improve transfer efficiency. Afterwards HCl was withdrawn and replaced by 0.4 M NaOH for denaturation. After blotting for 4 h, the membrane was washed with 2 x SSC buffer and baked at 80°C for 2 h.
Prehybridization of the membrane was performed in pre-warmed Amersham Rapid-hyb™ buffer (GE Healthcare) at 65°C for 2 h. 25 ng of each probe were labelled with [α^{32}P]-dCTP using the Amersham Rediprime™ II DNA Labeling System and purified with illustra ProbeQuant™ G-50 micro columns according to manufacturer's protocol. After denaturation at 95°C for 5 min and 5 min incubation on ice, the labelled probes were mixed with pre-warmed Amersham Rapid-hyb™ buffer and then added to the membrane. Hybridization was carried out with gentle agitation at 65°C over night.
The next day, membranes were washed 2 x SSC/0.1% SDS, 1 x SSC/0.1% SDS or 0.1 x SSC/0.1% SDS several times at 65°C for 15 - 45 min. Finally, the membranes were exposed to an X-ray film and developed after 3 - 10 days.

3.3 Animal experiments

All animal studies were conducted meeting the requirements of the European guidelines for the care and use of laboratory animals and were approved by the local authorities.

3.3.1 Mouse strains

For animal experiments the conditional Cre/loxP and Flp/frt systems were applied. Mice carrying a transgene silenced by a loxP-stop-loxP (LSL) or frt-stop-frt (FSF) cassette can be interbred with a mouse strain expressing the Cre or Flp recombinase under the control of a tissue-specific promoter to allow conditional deletion of the LSL or FSF cassette and tissue-specific expression of the target genes.
Combining the Cre/loxP and Flp/frt systems enables sequential gene activation or inactivation and targeting of different cellular compartments.

***Ptf1a*$^{Cre/+}$** (Nakhai et al., 2007). This knock-in mouse strain was kindly provided by Dr. Hassan Nakhai (Klinikum rechts der Isar, Technical Universiy Munich). The Ptf1a is a subunit of the so called "pancreas transcription factor" (Ptf) and plays a fundamental role in endocrine and exocrine pancreas development in mice. In this mouse strain, a Cre recombinase is expressed under the control of the *Ptf1a* promoter and is therefore specifically expressed in pancreatic precursor cells.

LSL-Kras^{G12D} (Hingorani et al., 2003; Jackson et al., 2001). This knock-in mouse strain was kindly provided by Prof. Tyler Jacks (Massachusetts Institute of Technology, Cambridge, MA, USA). It contains a G12D point mutation, which correspond to the mutation frequently found in human disease. After Cre-mediated deletion of the loxP-flanked stop cassette, oncogenic Kras is expressed leading to constitutive activation of Ras downstream pathways.

LSL-Trp53^{R172H} (Hingorani et al., 2005; Olive et al., 2004). This knock-in mouse strain was kindly provided by Prof. Tyler Jacks (Massachusetts Institute of Technology, Cambridge, MA, USA). It contains a conditional R172H point mutation of p53, which corresponds to human codon 175, and occurs in the Li-Fraumeni syndrome and sporadic tumors. After excision of the loxP-flanked stop cassette, the mutant p53 is is expressed.

Pdk1$^{f/+}$ (Lawlor et al., 2002). In this mouse strain, exon 3 and exon 4 are flanked by loxP sites. Deletion of these exons by Cre abolishes expression of Pdk1 protein.

Craf$^{f/+}$ (Jesenberger et al., 2001). In this mouse strain exon 3 is flanked by loxP sites and deleted by Cre abolishes expression of Craf protein.

R26$^{mT\text{-}mG}$ (Muzumdar et al., 2007). In this mouse strain, loxP-flanked membrane-targeted tdTomato is expressed under the control of the ubiquitously *CAG* promoter as a knock-in at the *R26* locus. After Cre recombination, the loxP-tdTomato-loxP cassette is deleted, resulting in expression of membrane-targeted EGFP.

Pdx1-Flp (Schönhuber et al., 2014). The *Pdx1-Flp* transgenic mouse strain was generated in the laboratory of Prof. Dr. Dieter Saur. The codon-optimized Flp-o recombinase is expressed under the control of the *Pdx1* promotor, which is active in pancreatic progenitor cells and in adult pancreatic islets.

FSF-R26$^{hpAP/+}$ (Awatramani et al., 2001). Expression of human placental alkaline phosphatase (hpAP) under the control of the ubiquitous *Rosa26* promoter is blocked by a 5' frt-flanked stop cassette. After deletion of the FSF cassette by Flp recombinase hpAP is expressed.

FSF-Kras$^{G12D/+}$ (Schönhuber et al., 2014). The *FSF-Kras$^{G12D/+}$* mouse strain was generated in the laboratory of Prof. Dr. Dieter Saur. In this mouse strain the expression of oncogenic Kras^{G12D} is blocked by a FSF cassette and can be activated by Flp recombinase.

FSF-R26$^{CAG\text{-}CreERT2}$ (Schönhuber et al., 2014). The FSF-R26$^{CAG\text{-}CreERT2}$ mouse strain was generated in the laboratory of Prof. Dr. Dieter Saur. After deletion of the FSF cassette, CreER^{T2} is expressed under the control of the *CAG* promoter as a knock-in at the *R26* locus. CreER^{T2} can be activated by Tamoxifen administration.

LSL-R26$^{DTA/+}$ (Ivanova et al., 2005). In this mouse strain the expression of diphtheria toxin fragment A is inhibited by a LSL cassette. After Cre-mediated excision of the LSL cassette, DTA is expressed and leads to ablation of these cells.

FSF-Pcna^{CreERT2} The *FSF-Pcna^{CreERT2}* mouse strain was generated in the laboratory of Prof. Dr. Dieter Saur. After deletion of the FSF cassette by the Flp recombinase, Cre recombinase can be activated by Tamoxifen administration in all proliferating cells.

3.3.2 Dissection of tumor mice and isolation of tumor cells from tissues and the circulation

2 - 4 h before being sacrificed, mice were injected i.p. with 50 mg/kg BrdU. Mice were anesthetized by Isofluran inhalation prior to cervical dislocation. After disinfection with 70% ethanol, dissection of the animal was carried out under sterile conditions. To collect circulating tumour cells the thorax was opened, the vena cava inferior was cut and blood was collected in a reaction tube containing sterile EDTA to prevent coagulation. The sample was centrifuged at 1000 rpm for 5 min. Afterwards, the supernatant was discarded and the cell pellet was resuspended in medium and cultured in a cell culture flask. Pancreatic tissue samples for RNA isolation were homogenized in RLT buffer containing 2-mercaptoethanol. A small piece of tissue was snap frozen for isolation of DNA. For protein isolation, samples were homogenized in IP buffer containing phosphatase and proteinase inhibitors. All samples were snap frozen and stored at -80°C. For isolation of tumor cells, pancreatic tissue samples were transferred to sterile PBS. Next, the tissue samples were sliced into small pieces and incubated in medium containing 200 U/ml collagenase type II at 37°C for 24 - 36 h until they were completely digested. Afterwards, they were centrifuged for 5 min at 100 rpm, the supernatant was discarded and the cells were cultured in a cell culture flask. Cell lines were seeded on 10 cm dishes for RNA, DNA and protein isolation and cryopreserved at passages three to four.

3.3.4 Blood glucose level determination

Blood glucose levels were measured with a glucometer by standard procedures.

3.3.5 Glucose tolerance test (GTT)

After an overnight fast, GTTs were performed by intraperitoneal injection of 1.5 g/kg body weight of glucose. Blood samples were taken at 0-, 10-, 20-, 30-, 60- and 120-min time points and glucose levels measured with a glucometer.

3.3.6 Tamoxifen treatment of mice

Pdx1-Flp;FSF-Kras$^{G12D/+}$;FSF-R26$^{CAG-CreERT2}$;LSL-R26^{DTA} animals were fed with tamoxifen-containing chow (400 mg tamoxifen citrate / kg chow; CreActive TAM400) and Pancrex-Vet food for four days respectively.
All other animals were fed tamoxifen-containing chow for two weeks.

3.3.7 High resolution ultrasound

Mice were screened for tumors by abdominal palpation. Tumors with a size of approximately 5 mm were verified by high-resolution ultrasound (Vevo 2100, VisualSonics) and enrolled in the treatment study. By automated three-dimensional (3D) B-mode imaging along the entire length of the tumor, volumes were determined. Reconstructed three-dimensional ultrasound imaging data sets were analyzed with the Vevo 2100 software package (VisualSonics).

3.4 Histological analysis

3.4.1 Paraffin and cryo sections

Samples for paraffin-histochemistry were fixed in Roti® Histofix for 16 h, dehydrated using a tissue processor ASP300 and embedded in paraffin. For further analysis, 3.5 µm thick serial sections were cut using the microtome Microm HM355S.
Samples for cryohistochemistry were fixed in Roti® Histofix for 2 h, washed with PBS for 20 min and followed by dehydration in sucrose series (4 h in 15% sucrose and o/n in 30% sucrose). Finally, cryo-samples were embedded in Tissue-Tek and stored at -80 °C. Sections for H&E staining were cut 3.5 µm, sections for confocal microscopy 20 µm thick.

3.4.2 Hematoxylin and eosin (H&E) staining of tissue sections

First, paraffin-embedded tissue sections were dewaxed in Roti® Histol two times for 5 min. Second, they were rehydrated in an ethanol series (2 x 99%, 2 x 96% and 2 x 80%) and washed in H_2O before they were stained in hematoxylin for 10 sec and eosin for 15 sec.

Afterwards they were washed in water for 10 min and dehydrated in an ethanol series (2 x 80%, 2 x 96% and 2 x 99%) and Roti® Histol. Finally, the sections were mounted in Pertex mounting medium.
Cryo sections were fixed in PFA for 10 min, washed two times with PBS and H_2O before they were stained in hematoxylin for 15 sec and eosin for 20 sec. Next, they were again dehydrated in an ethanol series as described for H&E staining for paraffin-embedded tissue sections, before mounted in Pertex.

3.4.3 Alcian blue (AB) staining

Paraffin-embedded tissue sections were dewaxed and rehydrated as described in 3.3.2. The sections were stained in alcian blue solution for 5 min. After washing them in H_2O, they were counterstained in a nuclear fast red solution for 5 min and rehydrated and mounted as described in 3.3.2.

3.4.4 Immunohistochemistry

Paraffin-embedded tissue sections were dewaxed and rehydrated as described in 3.3.2. To demask the antigens, the sections were boiled in unmasking solution for 10 min. After cooling down for 20 min and washing three times with PBS, they were blocked for 20 min in 3% H_2O_2 in the dark to inhibit endogenous peroxidase activity. Next, the sections were blocked for one h in 3 - 5% serum and Avidin (according to manufacturer's protocol) in PBS. In between they were washed three times with PBS. The sections were incubated with the first antibody diluted in 3 - 5% serum and Biotin in PBS o/n at 4°C. The next day, they were washed three times with PBS before they were incubated with the second antibody diluted 1:500 in 3 - 5% serum in PBS for 1 h at RT. Detection was performed using the Vectastain® elite ABC kit and the DAB peroxidase substrate kit according to manufacturer's protocol. Finally, the sections were counterstained with hematoxylin, dehydrated and mounted in Pertex as described in 3.3.2.

3.4.5 TOPRO®-3 staining of cryo sections

Sections for TOPRO®-3 staining were fixed in 4% Roti® Histofix for 1 min and washed two times in PBS for 5 min. After 1 h blocking in solution C at RT, the slides were incubated with TOPRO®-3-iodide, diluted 1:1000 in solution C, for 2 h at RT. Before they were mounted with Vectashield Mounting Medium, the sections were washed three times for 20 min with solution C and one time for 10 min with PBS. The TOPRO®-3 stained sections were stored

at 4°C. Stained cryosections were examined by confocal laser-scanning microscopy (LSM) with a Zeiss LSM 510 Axiovert 100 microscope (Zeiss, Oberkochen, Germany) equipment with a x 20/0.5 air and a x 40/1.3 oil-immersion objective (optical section thickness 4.4 mm).

3.4.6 Alkaline phosphatase (AP) staining of tissue

Tissues were fixed for 2 h in 4% Roti® Histofix. First, they were washed three times in PBS for 20 min at 4°C. Second, the tissues were incubated in AP detection buffer for 30 min at 70°C. Next, they were incubated in fresh AP detection buffer for 15 min at RT. For AP staining, the tissues were stored in the dark in AP staining buffer for 2 - 20 h at RT. When the tissues became purple, they were washed three times for 10 min in 25 mM EDTA/PBS, fixed for 20 h in Roti® Histofix at 4°C, dehydrated and embedded in paraffin. Sections were cut 3.5 µm thick and left to dry o/n. For counterstaining with nuclear fast red, the sections were rehydrated as described in 3.3.2 and stained with nuclear fast red for 10 min. Afterwards, the sections were dehydrated in an ethanol series and Roti® Histol before mounted in Pertex.

3.5 Cell culture

3.5.1 Culture conditions and handling of pancreatic tumor cells

Isolated tumor cells were cultured at 37°C and 5% CO_2 and passaged regularly. To subculture the cells, they were washed with PBS, trypsinised at 37°C until they dissociated and put into a new flask with fresh pre-warmed medium. For cryopreservation, cells were taken up in fresh medium after trypsinization and centrifuged at 1200 rpm for 5 min. After discarding the supernatant, the pellet was dissolved in ice-cold freezing medium, transferred into Cryo tubes and frozen at -80°C. After 24 h cells were proceeded to liquid nitrogen where they were stored until further use.

3.5.2 Tamoxifen treatment of tumor cells

For tamoxifen treatment, 5000 tumor cells per well were seeded in 96-well plate. On the next day, fresh medium with 500 nM 4-hydroxytamoxifen or vehicle (EtOH) was added. Cell counting using a Neubauer hemocytometer was done every second day.

3.5.3 Acinar cells

3.5.3.1 Isolation of acinar cells

Pancreatic acinar cells were isolated from *Ptf1a*$^{Cre/+}$;*Kras*$^{G12D/+}$ and *Ptf1a*$^{Cre/+}$;*Kras*$^{G12D/+}$;*Pdk1*$^{f/f}$ compound mutant pancreata. Human primary acinar cells were isolated from normal human pancreas obtained from surgical resections for malignant disease.

For isolation of acinar cells, 2.5 ml of a solution of 1.33 mg/ml collagenase P in HBSS were injected into the pancreas. Afterwards, the pancreas was put into a falcon tube with 5 ml of collagenase P solution on ice and cut into small pieces with a scissor. After an incubation step of 30 min at 37°C in a water bath, the reaction was stopped by adding 10 ml of 5% FCS in HBSS. The cell suspension was incubated for 10 min on ice for sedimentation of the cellular fraction. Next, the supernatant was aspirated and the cells were washed two times with 10 ml of 5% FCS in HBSS, centrifuged at 950 rpm at 4°C and resolved in 5 ml of 5% FCS in HBSS. This solution was filtered through a 500 µm mesh into a new falcon. The mesh was rinsed with 5 ml of 5% FCS in HBSS and the resulting suspension was transferred through a 100 µm mesh into a new falcon to separate the acinar cells from other cell types. Afterwards, the cell suspension was gently pipetted onto 20 ml of 30% FCS in HBSS and centrifuged at 950 rpm at 4°C. The pellet was resuspended in 1 ml of fresh pre-warmed medium. In a new falcon, 1183 µl medium, 16.6 µl 1N NaOH and 3400 µl rat tail collagen type I (RTC) were mixed and then added to the acinar cell suspension. 500 µl of this solution were seeded per well on a collagen-coated 24-well plate. After solidification of this layer, 500 µl medium were gently added. 24 h after isolation, acinar cells were maintained in the presence or absence of recombinant human transforming growth factor-α (TGFα) and inhibitors. Human isolated acini were cultured in ACL-3 medium with or without TGFα.

3.5.3.2 Acinar to ductal metaplasia (ADM) assay

Acinar cells were treated daily with and without 50 ng/ml TGFα (Sigma) and GDC 0941 (pan class I PI3K inhibitor), NVPBez235 (dual PI3K-mTOR inhibitor), BX912 (PDK1 inhibitor), MK2206 (AKT inhibitor), GSK690693 (AKT inhibitor), BI-D1870 (RSK inhibitor) or vehicle (DMSO). Acinar and ductal structures were counted after five days treatment.

3.6 Statistical analysis

Graphical depiction, data correlation and statistical analysis were done with GraphPad Prism5 software (La Jolla, USA).

Survival curves were done using Kaplan-Meier survival analysis. To analyze statistical significance log rank test was used. $P < 0.5$ was considered to be statistically significant.

4. Results

4.1 Analysis of Kras-downstream signaling in PDAC formation

Many tumors such as PDAC, non-small cell lung cancer (NSCLC) and colon cancer are driven by oncogenic Kras, but it is still largely unknown which Kras effectors play a critical role in the different tumor types. Because Kras is considered undrugable (Berndt et al., 2011), it is important to investigate the contribution of Kras effector pathways for tumor initiation and maintenance. In this study, the two major effector pathways, Raf/MEK/ERK and PI3K/AKT, were analyzed.

4.1.1 Craf is dispensable for Kras^{G12D}-driven PDAC initiation

It has recently been shown that Craf is essential for Kras^{G12D}-induced non-small cell lung cancer initiation (Blasco et al., 2011; Karreth et al., 2011). To analyze the role of Craf in pancreatic carcinogenesis, Craf was inactivated using floxed *Craf$^{f/f}$* mice (Jesenberger et al., 2001). Specific deletion of Craf in the epithelial compartment of the pancreas was achieved by using the well established *Ptf1a$^{Cre/+}$* line (Nakhai et al., 2007). Loss of Craf in the Kras^{G12D}-driven PDAC mouse model (*Ptf1a$^{Cre/+}$;LSL-Kras$^{G12D/+}$;Craf1$^{f/f}$*) had no inhibitory effect on tumor development or progression (Figure 4-1A and B). Also the median survival time of these mice is similar to the *Ptf1a$^{Cre/+}$;LSL-Kras$^{G12D/+}$* model and is significantly reduced in comparison to control animals (Figure 4-1C). PCR analysis of tail DNA was used to determine the genotype and DNA isolated from PDAC cells to show efficient deletion of both *Craf* alleles (Figure 4-1D). To verify loss of Craf protein, immunohistochemistry was performed. *Ptf1a$^{Cre/+}$;LSL-Kras$^{G12D/+}$;Craf1$^{f/+}$* mice showed expression of Craf, whereas in *Ptf1a$^{Cre/+}$;LSL-Kras$^{G12D/+}$;Craf1$^{f/f}$* mice Craf was not detectable (Figure 4-1E). Western Blot analysis of PDAC cell lines isolated from *Ptf1a$^{Cre/+}$;LSL-Kras$^{G12D/+}$;Craf1$^{f/f}$* mice also showed complete loss of Craf expression (Figure 4-1F).

Therefore, it could be excluded that tumors developed due to incomplete *Craf* deletion. In summary, these results indicate that signaling via Craf is dispensable for the initiation of Kras-driven PDAC.

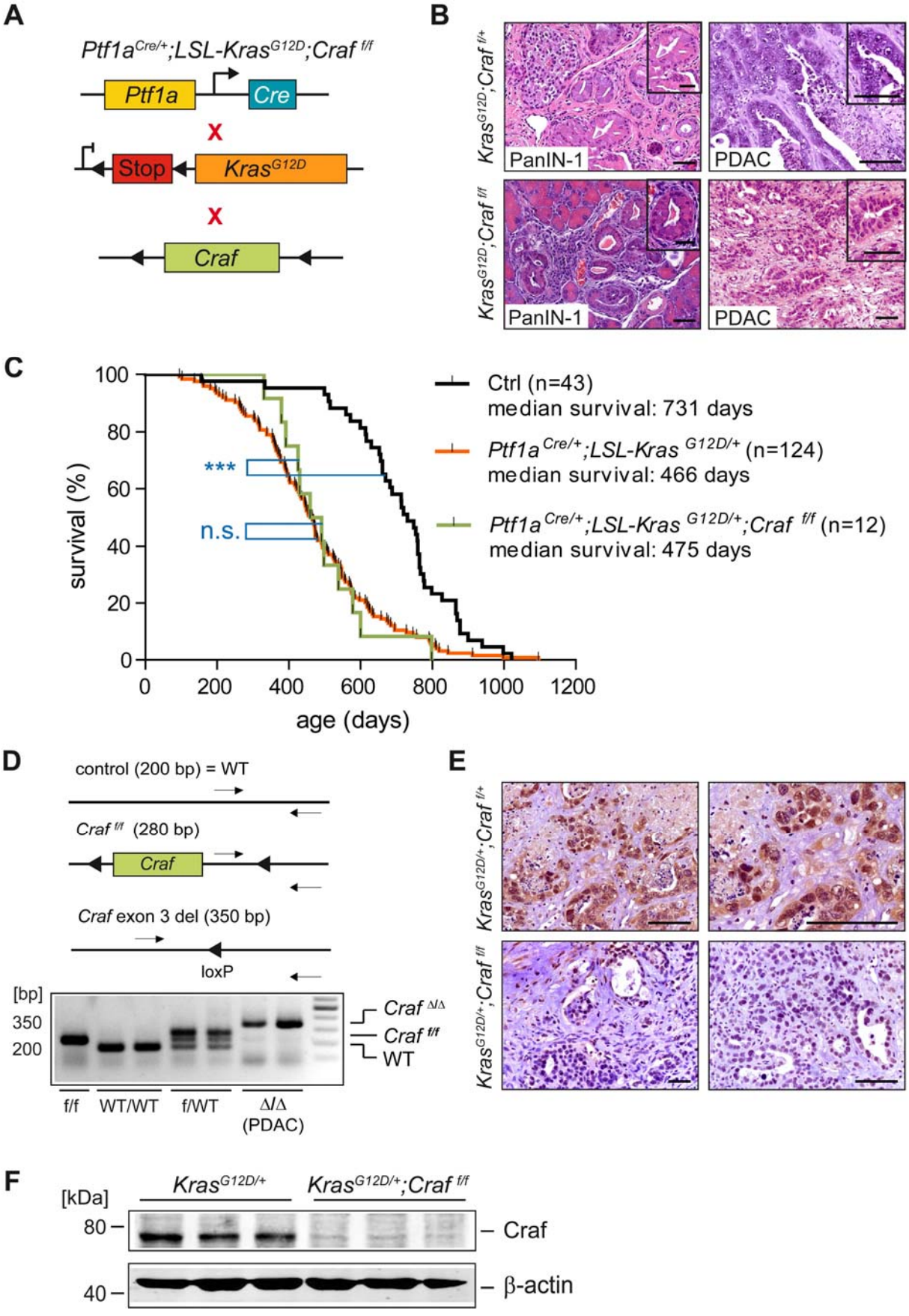

Figure 4-1: Craf is dispensable for KrasG12D-driven pancreatic carcinogenesis
A) Genetic strategy used to study the cell-autonomous role of Craf in Kras^{G12D}-driven pancreatic cancer formation. B) Representative H&E stains of control (*Ptf1a$^{Cre/+}$; LSL-Kras$^{G12D/+}$; Craf$^{f/+}$*) and conditional Craf knockout

(*Ptf1a*$^{Cre/+}$; *LSL-Kras*$^{G12D/+}$; *Craf*$^{f/f}$) mice. C) Kaplan-Meier survival analysis of the indicated genotypes. + denotes the wild-type allele, f the conditional allele (n.s.: not significant; ***p < 0.0001, log-rank test). D) Genotyping strategy of the floxed Craf allel (upper panel). PCR analysis of DNA from wild-type (WT), heterozygous (f/WT) and homozygous (f/f) conditional floxed Craf mice and *Ptf1a*^{Cre} mediated deletion of exon 3 of Craf (Craf$^{\Delta/\Delta}$) in pancreatic cancer cells (PDAC) (lower panel). Sizes of WT and mutant PCR products are indicated. E) Immunohistochemical analysis of Craf expression in PDAC of *Ptf1a*$^{Cre/+}$;*LSL-Kras*$^{G12D/+}$;*Craf*$^{f/f}$ and *Ptf1a*$^{Cre/+}$;*LSL-Kras*$^{G12D/+}$;*Craf*$^{f/+}$ mice. + denotes the WT allele, f the conditional allele. F) Immunoblot analysis of Craf expression in primary PDAC cells from mice with the indicated genotypes. B-actin was used as loading control.
Insets show representative lesions in high magnification. Scale bars 50 µm for micrographs, 20 µm for insets.

4.1.2 PI3K signaling is essential for PDAC formation

4.1.2.1 PI3K pathway activation in human ADM, PanIN and PDAC

PI3K/AKT activation is a classical and uniform feature in human PDAC (Jimeno et al., 2008; Kennedy et al., 2011; Reichert et al., 2007; Ying et al., 2011). However, it is still unclear whether PI3K/AKT signaling is important during early stages of human pancreatic carcinogenesis. To investigate PI3K/AKT signaling in the earliest step of pancreatic carcinogenesis, namely acinar to ductal metaplasia (ADM), human samples were stained for pAKT-T308 and pAKT-S473 (Figure 4-2A). All analyzed samples showed strong staing for both AKT phosphorylation sites confiming activation of the pathway. CK19 staining was used to validate ADM lesions (Figure 4-2A) (Osborn et al., 1986). In addition, human low and high grade PanINs and PDAC showed features of active PI3K/AKT signaling, as demonstrated by positive staining for pAKT-T308, pAKT-S473 and the AKT target pGSK3β-S9 (Figure 4-2B).
In summary, these data show that PI3K/AKT signaling is already activated at the earliest stages of tumor development in humans and seems to control pancreatic carcinogenesis.

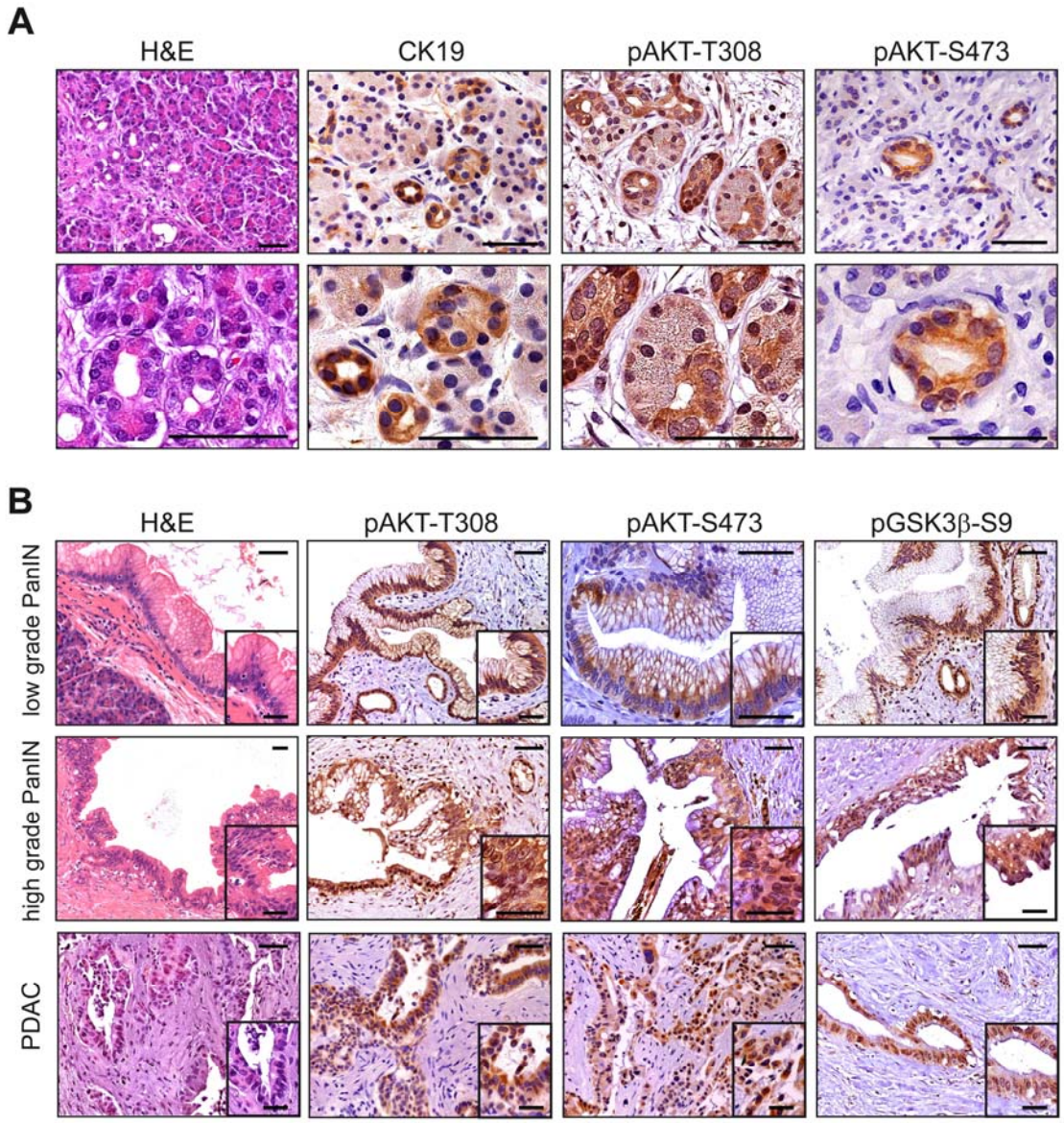

Figure 4-2: PI3K/AKT pathway activation in human pancreatic ADM and Neoplasia
A) H&E stains and immunohistochemical analysis of CK19 and PI3K/AKT pathway activation in human ADM. B) H&E stains and immunohistochemical PI3K/AKT pathway analysis of human low and high grade PanINs and PDAC. Insets show representative lesions in high magnification. Scale bars 50 µm for micrographs, 20 µm for insets.

4.1.2.2 Elimination of Pdk1 blocks Kras-driven ADM, PanIN and PDAC *in vivo*

To investigate the role of the direct PI3K downstream target Pdk1 by genetics, a floxed *Pdk1*$^{f/f}$ mouse line was used to inactivate *Pdk1* in the pancreas (Figure 4-3A) (Lawlor et al., 2002). *Ptf1a*^{Cre}-mediated excision of the floxed exons 3 and 4 of Pdk1 in the pancreas could be verified by genotyping and recombination PCR (Figure 4-3B). As expected, there was no recombination of *Pdk1* in spleen, liver, stomach, duodenum, heart, lung and kidney (Figure

4-3B). Deletion of Pdk1 in the pancreas was also confirmed by Western Blot analysis and correlated with the inactivation of the target AKT (Figure 4-3C).

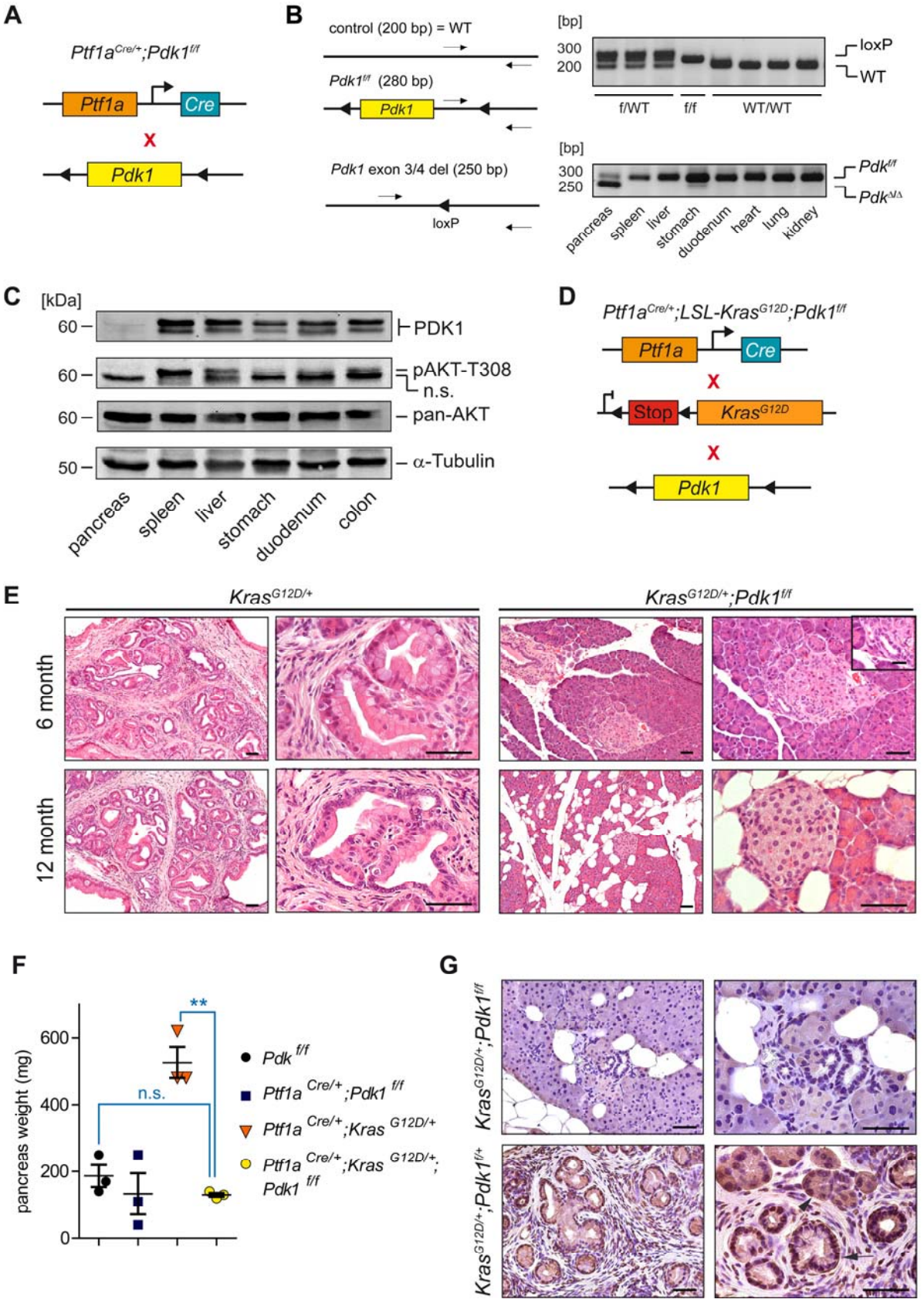

Figure 4-3: Epithelial Pdk1 is essential for Kras^{G12D}-driven pancreatic carcinogenesis

A) Genetic strategy used to delete Pdk1 in the pancreas. B) Genotyping strategy (left panel). PCR analysis of tail tip DNA from wild-type (WT), heterozygous (f/WT) and homozygous (f/f) conditional floxed Pdk1 mice (upper right panel). PCR analysis of DNA of the indicated organs show *Ptf1a*^{Cre} mediated pancreas-specific deletion of exon 3 and 4 of Pdk1 (Pdk1$^{\Delta/\Delta}$) in *Ptf1a*$^{Cre/+}$*;Pdk1*$^{f/f}$ mice (lower right panel). Sizes of wild-type and mutant PCR products are indicated. C) Immunoblot analysis of Pdk1 expression and PI3K/AKT pathway activation in indicated tissues of 3 month old *Ptf1a*$^{Cre/+}$*;Pdk1*$^{f/f}$ animals. α-Tubulin was used as a loading control. n.s.: non specific band. D) Genetic strategy used to study the cell-autonomous role of the PI3K substrate Pdk1 in Kras^{G12D}-driven pancreatic cancer formation. E) Representative H&E stains of control (*Ptf1a*$^{Cre/+}$*;LSL-Kras*$^{G12D/+}$) and conditional Pdk1 knockout (*Ptf1a*$^{Cre/+}$*;LSL-Kras*$^{G12D/+}$*;Pdk1*$^{f/f}$) mice. F) pancreatic weight of 6-month-old mice with the indicated genotypes (n.s.: not significant; **p < 0.01, Student's t test). G) Immunohistochemical analysis of Pdk1 expression in the pancreas of *Ptf1a*$^{Cre/+}$*;LSL-Kras*$^{G12D/+}$*;Pdk1*$^{f/f}$ (upper panel) and *Ptf1a*$^{Cre/+}$*;LSL-Kras*$^{G12D/+}$*;Pdk1*$^{f/+}$ (lower panel) pancreata. + denotes the wild-type allele, f the conditional allel. The arrowhead indicates an ADM and the arrow indicates a PanIN-1 lesion. Scale bars 50 µm.

To test whether Pdk1 is essential for the Kras-driven pancreatic plasticity and PDAC formation, *Ptf1a*$^{Cre/+}$*;Pdk*$^{f/f}$ mice were bred with the *LSL-Kras*^{G12D} mouse line (Figure 4-3D), allowing specific expression of activated Kras in the pancreas (Hingorani et al., 2003). In contrast to *Ptf1a*$^{Cre/+}$*;LSL-Kras*$^{G12D/+}$ mice, *Ptf1a*$^{Cre/+}$*;LSL-Kras*$^{G12D/+}$*;Pdk*$^{f/f}$ mice developed neither PanINs nor PDAC (Figure 4-3E). Pancreata showed normal morphology and weight (Figure 4-3E and F). In some of the 12 month old animals fatty degeneration of the pancreas, a sign of cellular stress due to oncogenic Kras expression, could be observed (Figure 4-3E). Immunohistochemical staining confirmed complete loss of Pdk1 in *Ptf1a*$^{Cre/+}$*;LSL-Kras*$^{G12D/+}$*;Pdk*$^{f/f}$ mice (Figure 4-3G) whereas *Ptf1a*$^{Cre/+}$*;LSL-Kras*$^{G12D/+}$*;Pdk*$^{f/+}$ mice still show expression of Pdk1.

With a median survival time of 720 days, the life expectancy of *Ptf1a*$^{Cre/+}$*;LSL-Kras*$^{G12D/+}$*;Pdk*$^{f/f}$ mice was similar to control animals. In contrast, loss of only one allele of *Pdk1* did not increase median survival time compared to *Ptf1a*$^{Cre/+}$*;LSL-Kras*$^{G12D/+}$ mice (Figure 4-4A). Further, *Ptf1a*$^{Cre/+}$*;LSL-Kras*$^{G12D/+}$*;Pdk*$^{f/+}$ mice developed PanINs and PDAC due to active PI3K signaling as indicated by the unaltered phosphorylation of GSK3β-S9 and AKT at T308 and S473 (Figure 4-4B).

However, deletion of *Pdk1* resulted in PI3K/AKT pathway inactivation as evidenced by AKT dephosphorylation (Figure 4-4B and C) without affecting PIP3 levels (Figure 4-4D) and Ras activity (Figure 4-4E).

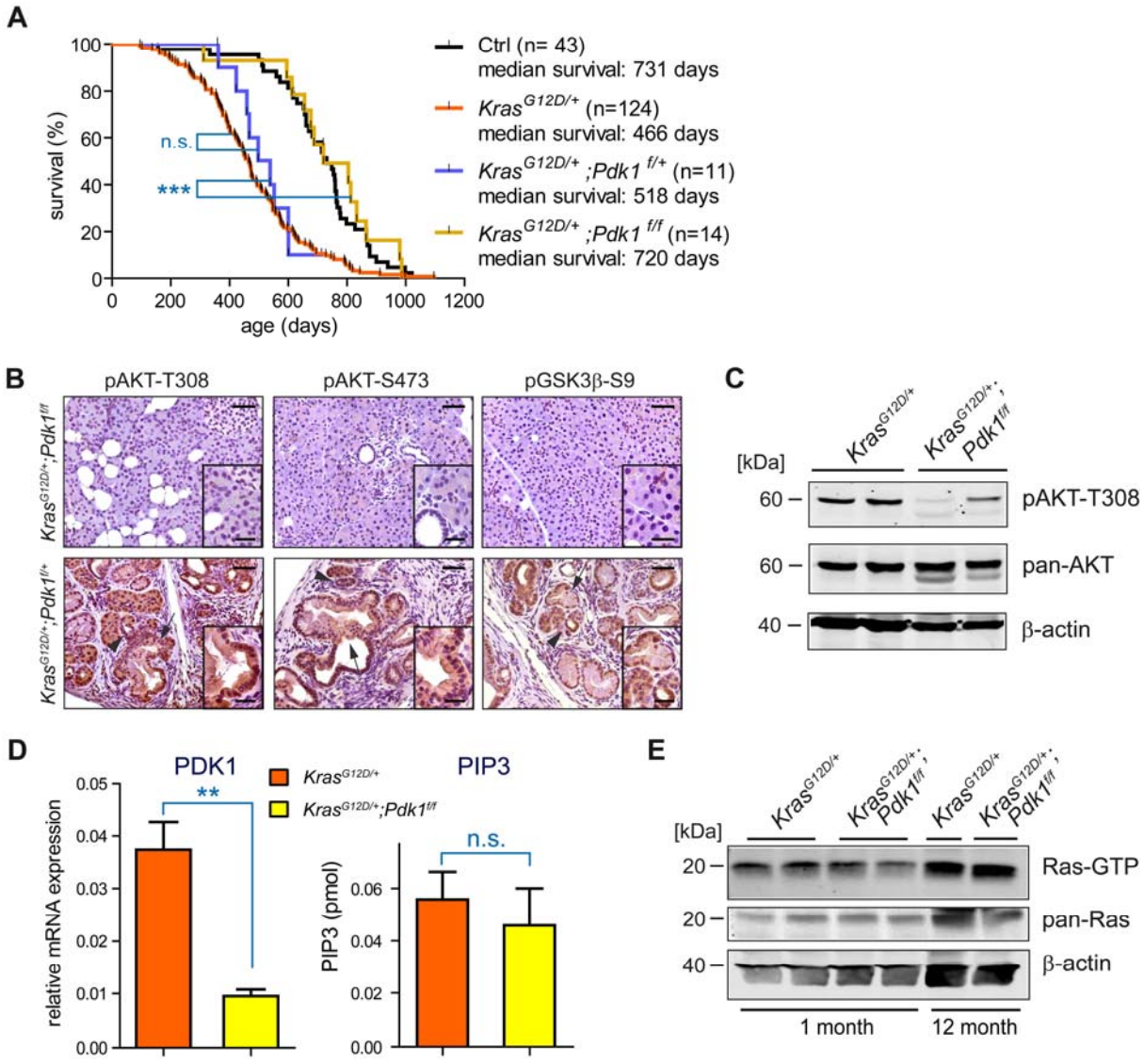

Figure 4-4: Ablation of Pdk1 blocks Kras^{G12D}-driven PDAC formation
A) Kaplan-Meier survival analysis of the indicated geotypes. + denotes the wild type allele, f the condictional allele (n.s., not significant; *** p<0.001, log-rank test). B) qRT-PCR analysis of PDK1 mRNA expression in the pancreas of *Ptf1a$^{Cre/+}$;LSL-Kras$^{G12D/+}$* and *Ptf1a$^{Cre/+}$;LSL-Kras$^{G12D/+}$;Pdk1$^{f/f}$* mice (left panel; ** p<0.01, Students t-test) and analysis of the pancreatic PIP3 level of the indicated genotypes (right panel; n.s., not significant; Students t-test). C) Analysis of activated Ras (Ras-GTP) in the pancreas of 1 and 12 month old *Ptf1a$^{Cre/+}$;LSL-Kras$^{G12D/+}$* and *Ptf1a$^{Cre/+}$;LSL-Kras$^{G12D/+}$;Pdk1$^{f/f}$* mice. D) Immunohistochemical analysis of PI3K/AKT pathway activation in the pancreas of 12 month old mice with the indicated genotypes. Arrowheads indicate ADM and arrows PanIN-1 lesions. E) Immunoblot analysis of PI3K7AKT pathway activation in pancreata of 12 month old *Ptf1a$^{Cre/+}$;LSL-Kras$^{G12D/+}$* and *Ptf1a$^{Cre/+}$;LSL-Kras$^{G12D/+}$;Pdk1$^{f/f}$* mice.

Other groups reported hypoplasia or developmental defects of the pancreas, pancreatic islets and beta cells or overt hyperglycemia and lethality due to *Pdk1* deletion in the pancreas (Hashimoto 2006; Westmoreland 2009). In contrast to these data, the *Ptf1a$^{Cre/+}$;LSL-Kras$^{G12D/+}$;Pdk$^{f/f}$* mice used in this study showed normal histology of the pancreas and similar blood glucose levels when compared to control animals (Figure 4-5A).

However, impaired glucose tolerance could be observed, but did not progress to diabetes mellitus (Figure 4-5B).

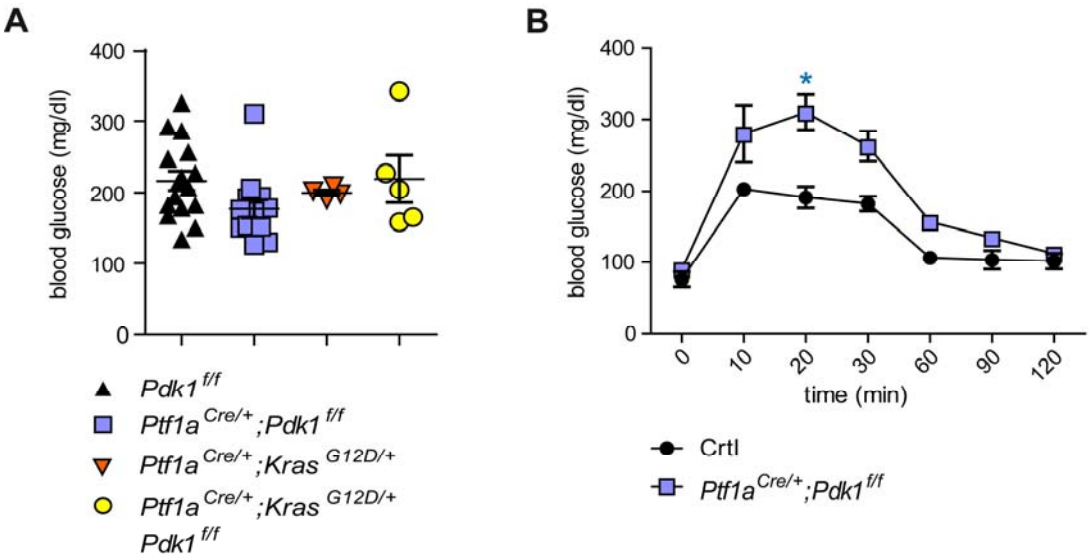

Figure 4-5: Loss of Pdk1 results in impaired glucose tolerance
A) Blood glucose levels of 9-12 month old mice with the indicated genotypes in fed state. B) Glucose tolerance test of control and *Ptf1a*$^{Cre/+}$*; Pdk1*$^{f/f}$ mice fasted overnight (* p<0.05, Students t-test).

4.1.3 Disruption of Pdk1 or inhibition of PI3K signaling blocks murine and human ADM *in vitro*

To investigate the cellular mechanisms of Kras^{G12D}-PI3K-Pdk1-induced transformation, early events of pancreatic carcinogenesis, namely ADM were analyzed. As demonstrated in previous studies, the transforming growth factor α (TGFα)/epidermal growth factor receptor and Ras activation induce ADM *in vitro* (Means et al., 2005; Morris et al., 2010; Reichert and Rustgi, 2011). To test whether Pdk1 signaling has an impact on Kras-induced ADM *in vitro*, acinar cells were isolated from *Ptf1a*$^{Cre/+}$*;LSL-Kras*$^{G12D/+}$ and *Ptf1a*$^{Cre/+}$*;LSL-Kras*$^{G12D/+}$*;Pdk1*$^{f/f}$ mice. In an *in vitro* ADM assay, acinar cells isolated from *Ptf1a*$^{Cre/+}$*;LSL-Kras*$^{G12D/+}$ mice showed ADM in the presence and absence of TGFα (Figure 4-6A and C). Consistent with the in vivo data, deletion of Pdk1 completely blocked ADM in vitro, even if treated with TGFα (Figure 4-6A and C). ADM of *Ptf1a*$^{Cre/+}$*;LSL-Kras*$^{G12D/+}$ derived cells was also blocked by the pan class I PI3K inhibitor GDC 0941, the Pdk1 inhibitor BX912, the dual pan class I PI3K-mTOR inhibitor NVP-Bez235 and the AKT inhibitor MK-2206 (Figure 4-6B). In contrast, the RSK inhibitor BI-D1870 had no effect on ADM formation in vitro, even at concentrations as high as 10 μM (Figure 4-6B). Taken together, these data confirm the *in vivo* results and

indicate that disruption of the PI3K-Pdk1-AKT, but not the Pdk1-RSK axis, blocks ADM and therefore tumor initiation in the pancreas.

To test whether these data are also relevant to humans, acinar cells from human pancreas were isolated. As expected, TGFα treatment induced ADM of human acinar cells, as confirmed by CK19 staining (Figure 4-6D). Phosphorylation of AKT-T308 showed activation of the PI3K pathway in ductal structures. Inhibition of PI3K signaling by treatment with GDC 0941 blocked ADM in human acinar cells (Figure 4-6E) and inhibited CK19 expression and phosphorylation of AKT-T308 (data not shown). Overall, these data clearly demonstrate that PI3K/Pdk1 signaling is essential for tumor initiation in the pancreas.

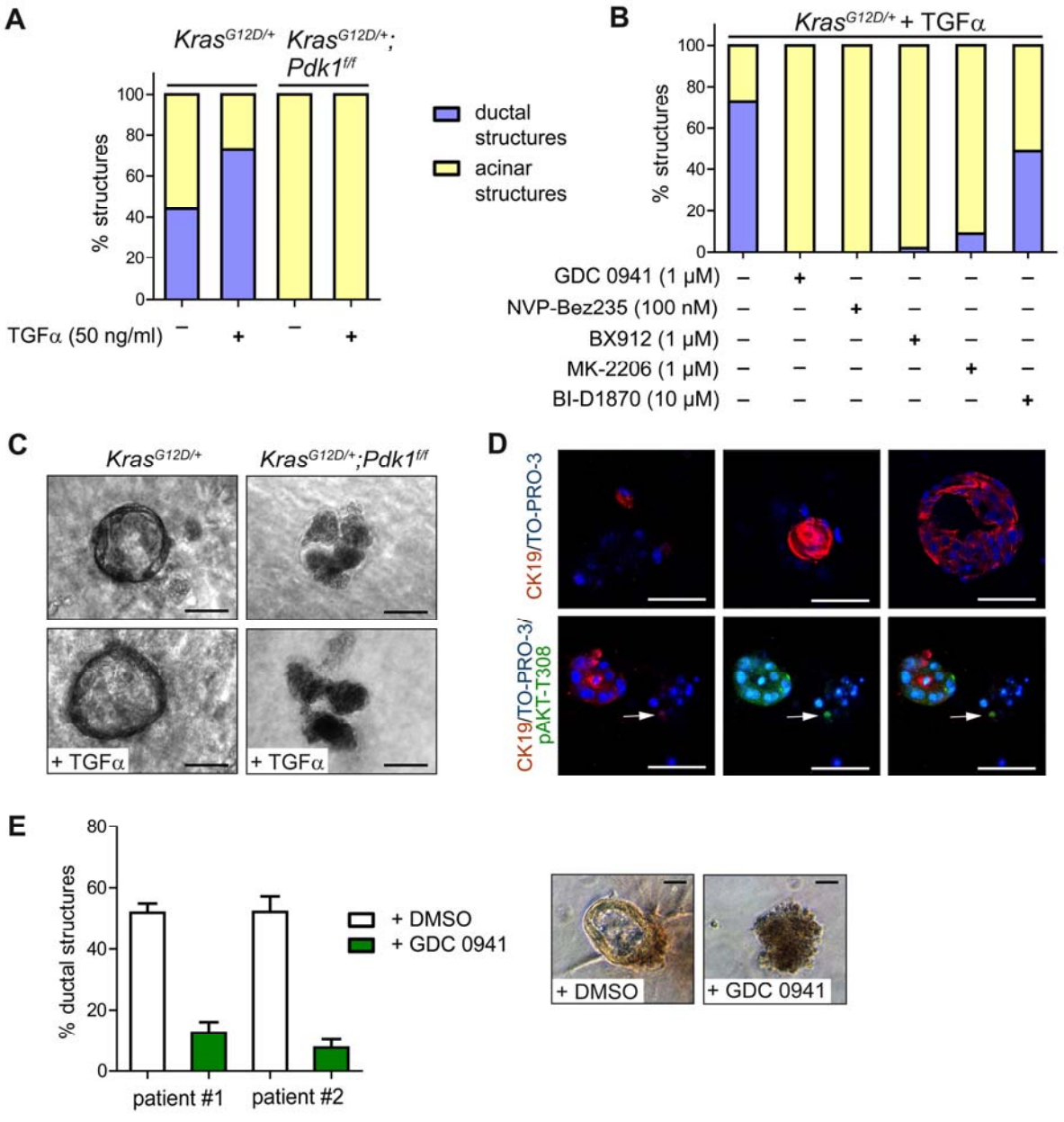

Figure 4-6: PI3K signalling regulates human and murine ADM

A) Quantification of ductal and acinar structures after 5 days in culture. Bar graphs show percentage of structures of the indicated genotypes with and without TGF-α treatment. B) Quantification of ductal and acinar structures after 5 days in culture with and without treatment of the indicated chemicals. Bar graphs show percentage of structures of indicated genotype treated with TGF-α and the indicated chemicals. C) Phase contrast images of pancreatic acinar cells with the indicated genotypes 5 days after isolation and treatment with or without TGF-α (50 ng/ml). D) Confocal microscopic images of TGF-α induced human ADM. Upper panel: CK19 expression (red) in ADM after 5 days of TGF-α (50 ng/ml) treatment. Lower panel: CK19 expression (red) and AKT-T308 phosphorylation (green) after 5 days TGF-α treatment. Arrow indicates a cell with acinar morphology but positive staining for CK19 and pAKT-T308. Nuclei were counterstained with TO-PRO-3 (blue). E) Left panel: Quantification of human ductal and acinar structures from two independent patients after 5 days in culture with and without GDC 0941 treatment. Scale bars: 50 µm. Error bars: ± SEM. Right panel: Phase contrast images of human pancreatic acinar cells 5 days after isolation and treatment with TGF-α (50 ng/ml) with or without GDC 0941 (1 µM). Scale bars 50 µm.

4.2 Generation and analysis of a novel genetic-engineered mouse model for sequential and host specific targeting of pancreatic cancer

Genetically engineered Cre/loxP-based mouse models have dramatically improved our understanding of pancreatic carcinogenesis. However, modeling of sequential multi-step carcinogenesis, genetic manipulation of tumor subpopulations like cancer stem cells, selective targeting of different tumor compartments and genetic validation of therapeutic targets in established tumors is almost impossible. In this study, a novel dual-recombinase system which combines the Cre/loxP with the Flp/frt system was analyzed. Thereby it is possible to manipulate gene expression in a time specific fashion and target different pancreatic compartments and the host.

4.2.1 The dual-recombinase PDAC model

4.2.1.1 Analysis of the Pdx1-Flp line

We used the the murine Pdx1 promoter to target expression of the codon optimized Flp-o recombinase to the pancreas (Gannon et al., 2000) (Figure 4-7A). Pronuclear injection of a *Pdx1-Flp-o* construct yielded two mouse lines (8153.16 and 8153.46) with transgene integration. DNA fluorescence in situ hybridization (FISH) localized the transgene to chromosome 1C3-5 and 12C1-3, respectively (Figure 4-7A). Genotyping PCR of DNA from the tail tip was used to determine the genotype (Figure 4-7B).

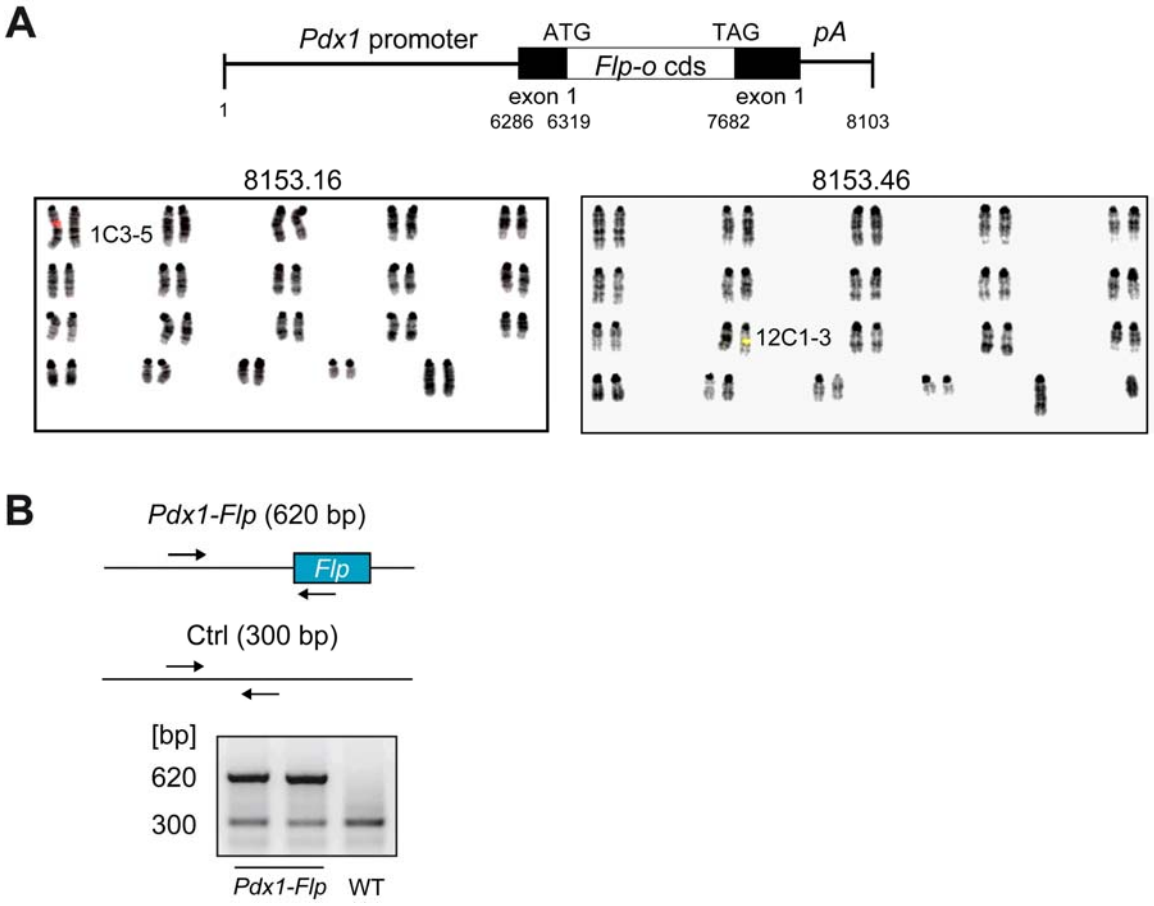

Figure 4-7: Generation of the transgenic *Pdx1-Flp* mouse line
A) Upper panel: Scheme of the structure of the *Pdx1-Flp-o* transgene. The ATG of the Flp-o coding sequence is directly fused with the Pdx1 ATG start codon. Lower panels: Fluorescence in situ hybridization (FISH) analysis shows integration of the transgene in chromosome 1 (C3-5; 8153.16 line) and chromosome 12 (C1-3; 8153.46 line). B) Genotyping strategy of the Pdx1-Flp-o transgene. PCR analysis of DNA from wild-type (WT) and transgenic Pdx1-Flp animals (lower panel). Sizes of WT and mutant PCR products are indicated.

To confirm expression of transgenic Flp recombinase in the pancreas, a Flp activatable alkaline phosphatase reporter allele (*FSF-R26*$^{hpAP/+}$) (Awatramani et al., 2001) was used. Alkaline phosphatase staining demonstrated Flp-mediated recombination in pancreatic acini, ducts and islets (Figure 4-8A and B). Extra-pancreatic recombination was observed in duodenum, stomach and bile duct by PCR analysis (Figure 4-8C). These patterns are similar to the transgene expression of the *Pdx1-Cre* lines (Gannon et al., 2000; Hingorani et al., 2003). For further experiments, the 8153.46 mouse line was used.

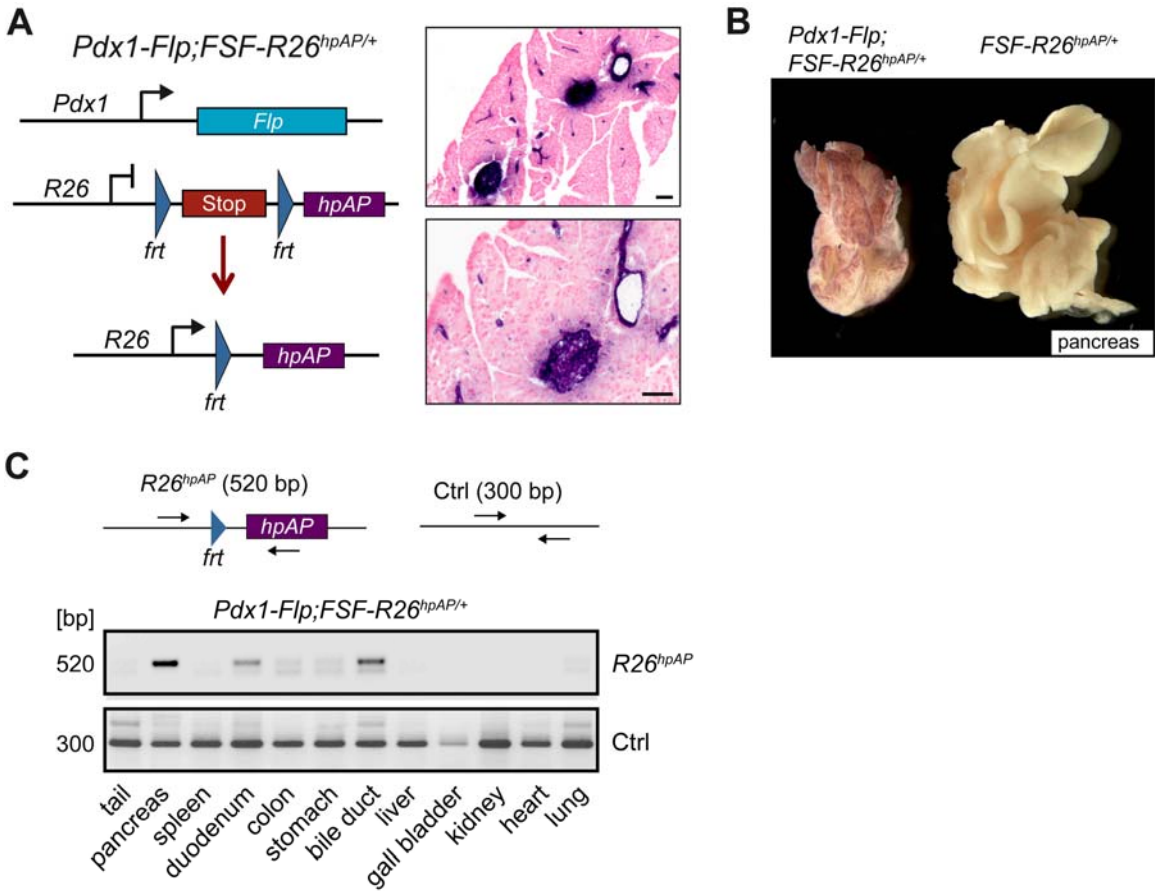

Figure 4-8: Pdx1-Flp recombinase expression
A) Flp/frt recombination system based lineage tracing strategy for the transgenic *Pdx1-Flp* mouse line with a human placental alkaline phosphatase (hpAP) reporter line (left panel). Alkaline phosphatase staining (purple color) of pancreatic sections demonstrates *Pdx1-Flp* mediated recombination of pancreatic islets, ducts and acini (right panel). B) Alkaline phosphatase staining (purple color) of pancreatic whole mount tissues of indicated genotypes. C) PCR analyses of *Pdx1-Flp* mediated deletion of the frt-stop-frt (FSF) cassette in the indicated tissues of *Pdx1-Flp;FSF-R26*$^{hpAP/+}$ mice.

4.2.1.2 *Pdx1-Flp;FSF-Kras*$^{G12D/+}$ mice develop PanIN lesions that progress to metastatic PDAC

To achieve expression of oncogenic Kras in the *Pdx1-Flp* lineage, a FSF silenced oncogenic *Kras*^{G12D} allele was generated as a knock-in at the endogenous *Kras* locus (Figure 4-9A). This *FSF-Kras*$^{G12D/+}$ mouse line carries a codon 12 glycine (G) to aspartic acid (D) (G12D) mutation, which is often found in human PDAC (Hezel et al., 2006; Rozenblum et al., 1997). This mutation leads to constitutive activation of Ras signaling by interfering with the interaction of Kras and GTPase-activating proteins (Pylayeva-Gupta et al., 2011). PCR analysis of DNA extracted from the tail tip was used for genotyping of this mouse line (Figure 4-9B).

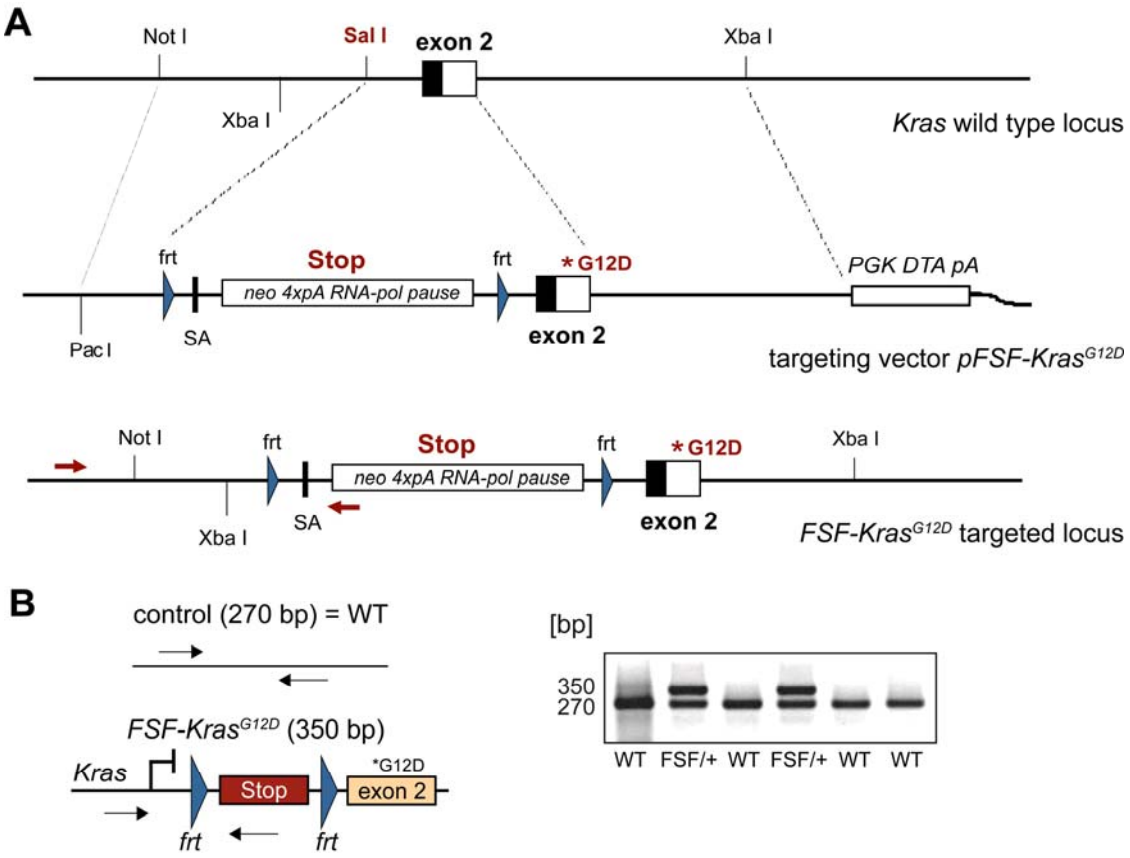

Figure 4-9: Generation of the *FSF-Kras^{G12D}* mouse line
A) Targeting the endogenous *Kras* locus. From top to bottom, diagrams of: *Kras* wild type locus; the *pFSF-Kras^{G12D}* targeting vector with the promoterless frt-stop-frt gene trapping cassette 5´ of Kras exon 2 with the oncogenic codon 12 (G12D) mutation; the targeted *FSF-Kras^{G12D}* locus. Restriction sites and the exon structure of the *Kras* locus are indicated. B) Genotyping strategy. PCR analysis of DNA from wild type (WT) and heterozygous (FSF/+) *FSF-Kras$^{G12D/+}$* mice. Sizes of WT and mutant PCR products are indicated.

Expression of oncogenic Kras in *Pdx1-Flp;FSF-Kras$^{G12D/+}$* mice revealed no overt phenotype after birth. Analysis of 1, 3, 6, 9 and 12 months old animals showed presence of acinar to ductal metaplasia and pancreatic intraepithelial neoplasia (Figure 4-10A). These precursor lesions of PDAC were also observed in the well established Cre/loxP based *Pdx1-Cre;LSL-Kras$^{G12D/+}$* model (Hingorani et al., 2003; Hruban et al., 2006) (Figure 4-10A). The amount and grade of PanIN lesions increased over time similar to the *Pdx1-Cre;LSL-Kras$^{G12D/+}$* model. To confirm origin of PanIN lesions and PDAC from the Pdx1-Flp lineage, the conditional *FSF-R26^{hpAP}* reporter and alkaline phosphatase staining was used (Figure 4-10B).

The novel Flp/frt based *Pdx1-Flp;FSF-Kras$^{G12D/+}$* mouse model showed very similar patterns of PanIN progression and PDAC development as the already established Cre/loxP based *Pdx1-Cre;LSL-Kras$^{G12D/+}$* model. Comparison of tumor latency, survival and metastasis revealed striking similarities in both models, with nearly identical survival times and similar rates of metastasis (data not shown, bachelor's thesis of Christina Schachtler). Tumors of both models showed full spectrum of human disease, ranging from well-differentiated ductal

PDAC to undifferentiated tumors and metastasis to liver, lung and lymph nodes (data not shown, bachelor's thesis of Christina Schachtler).

In summary, these data show that the novel *Pdx1-Flp;FSF-Kras*$^{G12D/+}$ mouse model phenocopies human PanIN and PDAC development as shown before for the *Pdx1-Cre;LSL-Kras*$^{G12D/+}$ mouse model (Hingorani et al., 2003; Olive et al., 2009).

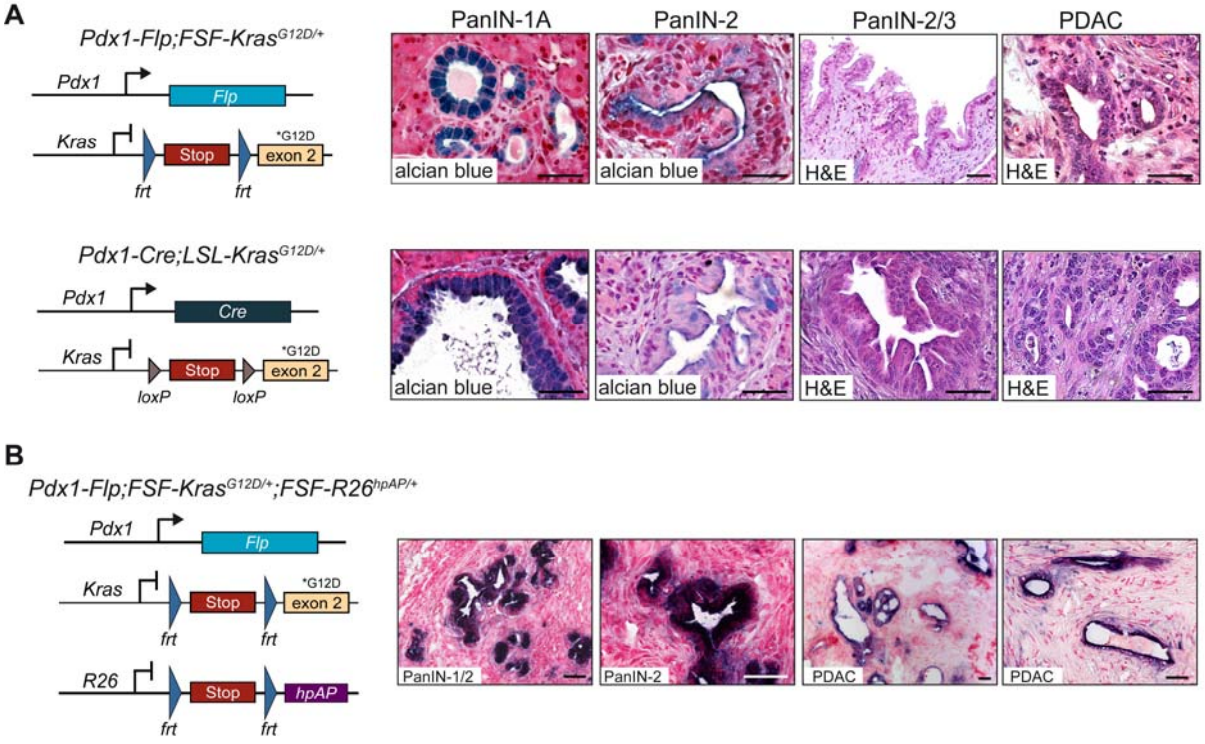

Figure 4-10: Activation of oncogenic Kras^{G12D} expression in the pancreas in the *Pdx1-Flp* lineage induces PanIN and PDAC

A) Representative alcian blue and hematoxylin and eosin (H&E) stained sections of different grades of pancreatic intraepithelial neoplasia (PanIN) and invasive PDAC in *Pdx1-Flp;FSF-Kras*$^{G12D/+}$ (upper panel) and the established *Pdx1-Cre;LSL-Kras*$^{G12D/+}$ (lower panel) mutant animals. B) Genetic strategy used to induce oncogenic Kras^{G12D} and hpAP reporter gene expression in the *Pdx1-Flp* lineage (left panel). Representative alkaline phosphatase expression (purple color) in PanIN lesions and PDAC cells of *Pdx1-Flp;FSF-Kras*$^{G12D/+}$*;FSF-R26*$^{hpAP/+}$ animals (right panel).

4.2.1.3 Time specific genetic manipulation of PDAC cells *in vitro* using the dual-recombinase system

To manipulate Flp recombined cells sequentially using the Cre recombination system, the *FSF-R26*$^{CAG\text{-}CreERT2/+}$ mouse line was generated. In this mouse line, a latent tamoxifen-inducible CreER^{T2} allele silenced by a frt-stop-frt (FSF) cassette under the control of the strong *CAG* promoter was targeted as knock-in at the mouse *Rosa26* locus.

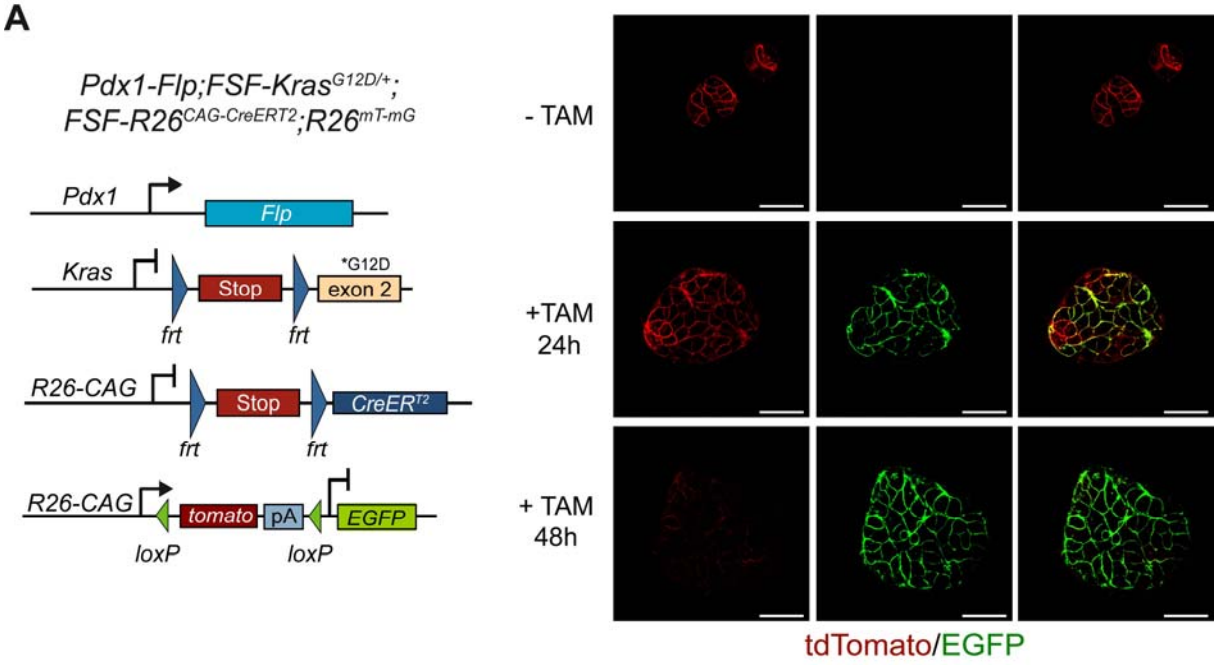

Figure 4-11: Secondary genetic manipulation of established Kras^{G12D}-induced PanIN lesions and PDAC cells in the *Pdx1-Flp* lineage
A) Genetic strategy used to induce EGFP expression by tamoxifen-mediated CreER^{T2} activation (left panel). PDAC cells isolated from a *Pdx1-Flp;FSF-Kras$^{G12D/+}$;FSF-R26$^{Cag-CreERT2}$;R26^{mT-mG}* mouse, which has not been treated with tamoxifen, were incubated with 0.1 µM 4-hydroxitamoxifen *in vitro*. tdTomato (red color, non Cre recombined cells) and Cre-induced EGFP (green color) expression was analyzed by confocal microscopy at indicated time points (right panel). Scale bars 50 µm.

To monitor tamoxifen-induced CreER^{T2}-mediated recombination in the Flp lineage, the floxed double colour fluorescent tdTomato-EGFP Cre reporter line (*R26^{mT-mG}*) (Muzumdar et al., 2007) that replaces the expression of tdTomato with EGFP following Cre-mediated excision, was used. *Pdx1-Flp;FSF-Kras$^{G12D/+}$;FSF-R26$^{CAG-CreERT2}$;R26^{mT-mG}* mice were aged and after PDAC formation, tumor cell lines were isolated. These animals had not been exposed to tamoxifen, so the floxed tdTomato reporter allele remained non-recombined in these cells. *In vitro* administration of tamoxifen led to recombination of the *R26^{mT-mG}* reporter and therefore to EGFP expression already after 24 hours of treatment (Figure 4-11A). Vehicle treated cells (-TAM) showed no recombination (Figure 4-11A), excluding Cre activity in the absence of tamoxifen.

4.2.1.4 Time specific depletion of PDAC cells *in vitro* and *in vivo*

As a proof of concept that the novel dual-recombination mouse model can define therapeutic targets on the genetic level *in vitro* and *in vivo*, *Pdx1-Flp;FSF-Kras$^{G12D/+}$;FSF-R26$^{CAG-CreERT2}$* mice were bred with the *LSL-R26^{DTA}* mouse line (Figure 4-12A). These animals carry a LSL

silenced diphtheria toxin A (DTA) expression cassette, which enables depletion of the recombined cells.

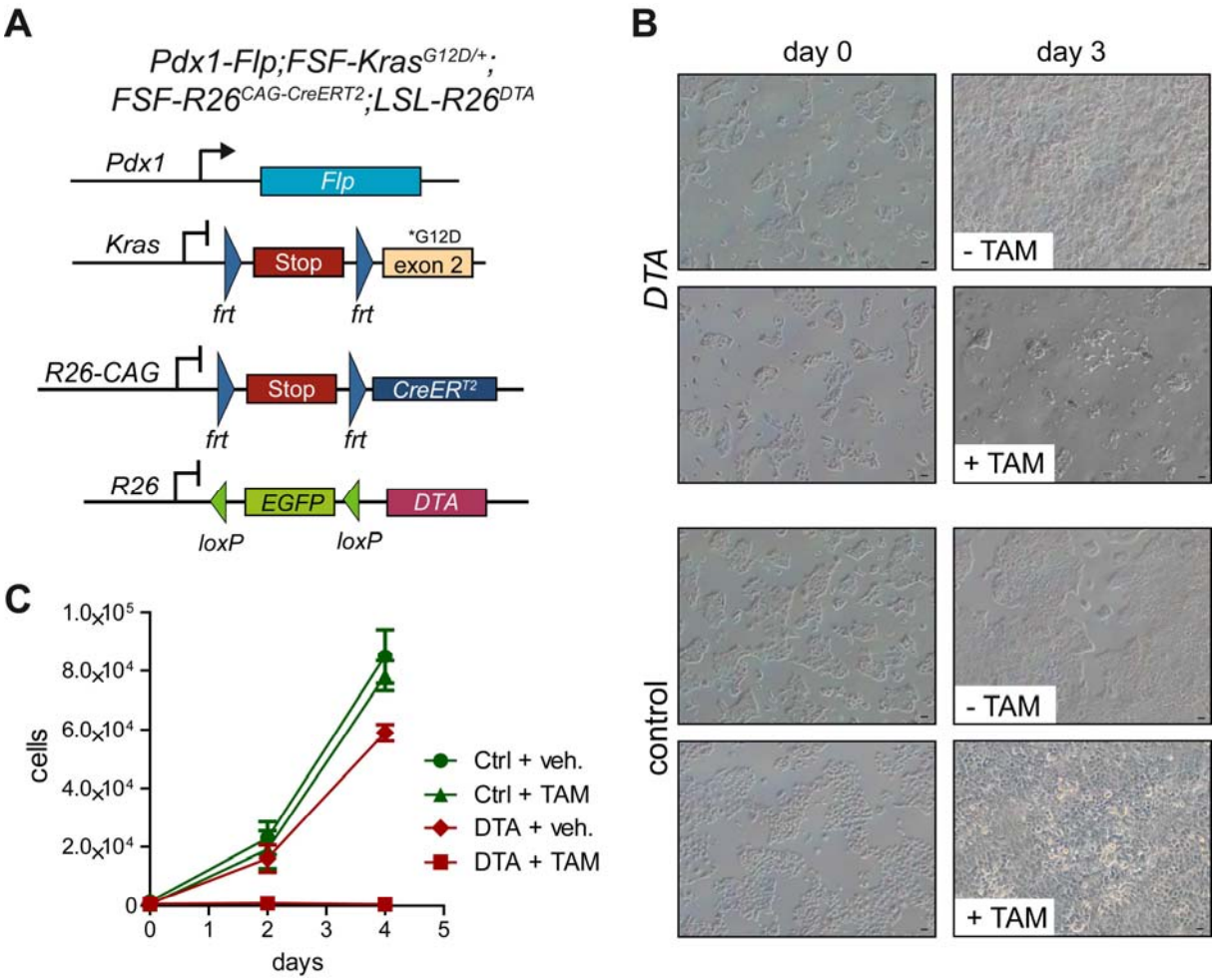

Figure 4-12: Cre-induced expression of DTA in PDAC cells induces apoptosis
A) Genetic strategy used to induce diphtheria toxin A (DTA) expression in established PDAC by tamoxifen-mediated CreER^{T2} activation. B) PDAC cells isolated from tamoxifen naïve *Pdx1-Flp;FSF-Kras$^{G12D/+}$;FSF-R26$^{CAG-CreERT2}$;LSL-R26^{DTA}* (*DTA*) and *Pdx1-Flp;FSF-Kras$^{G12D/+}$;FSF-R26$^{CAG-CreERT2}$* (control) mouse, were incubated with 0.5 µM 4-hydroxytamoxifen (+ TAM) or vehicle (- TAM) *in vitro*. Microscopic white light images of PDAC cells before and after 3 days of tamoxifen treatment are shown. C) Proliferation of 4-hydroxytamoxifen (+ TAM) and vehicle (- TAM) treated *DTA* and control cells monitored over time by cell counting. Scale bars 50 µm. Error bars ±SEM.

Cell lines from tumors of *Pdx1-Flp;FSF-Kras$^{G12D/+}$;FSF-R26$^{CAG-CreERT2}$;LSL-R26^{DTA}* mice which were not exposed to tamoxifen were isolated. CreER^{T2} activation by tamoxifen administration induced massive cell death *in vitro* due to DTA expression (Figure 4-12B and C) whereas tamoxifen treated control cells and the vehicle treated DTA cells showed no difference in proliferation.

To investigate PDAC cell depletion *in vivo*, *Pdx1-Flp;FSF-Kras$^{G12D/+}$;FSF-R26$^{CAG-CreERT2}$* mice with (*DTA*) and without (control) the *LSL-R26^{DTA}* allele were monitored by high resolution ultrasound. When the animals developed tumors of comparable size, they were treated with

tamoxifen to activate the Cre recombinase and induce DTA expression. High resolution ultrasound showed rapid regression of the tumor volume of DTA animals (Figure 4-13A and B). Macroscopic pathological examination and histopathology revealed often no pancreatic masses in the DTA cohort (Figure 4-13C and D). In contrast, tumor volume in animals lacking the LSL-R26^{DTA} allele increased over time (Figure 4-13A and B) and pathological examination and histopathology showed full blown PDAC (Figure 4-13C and D).

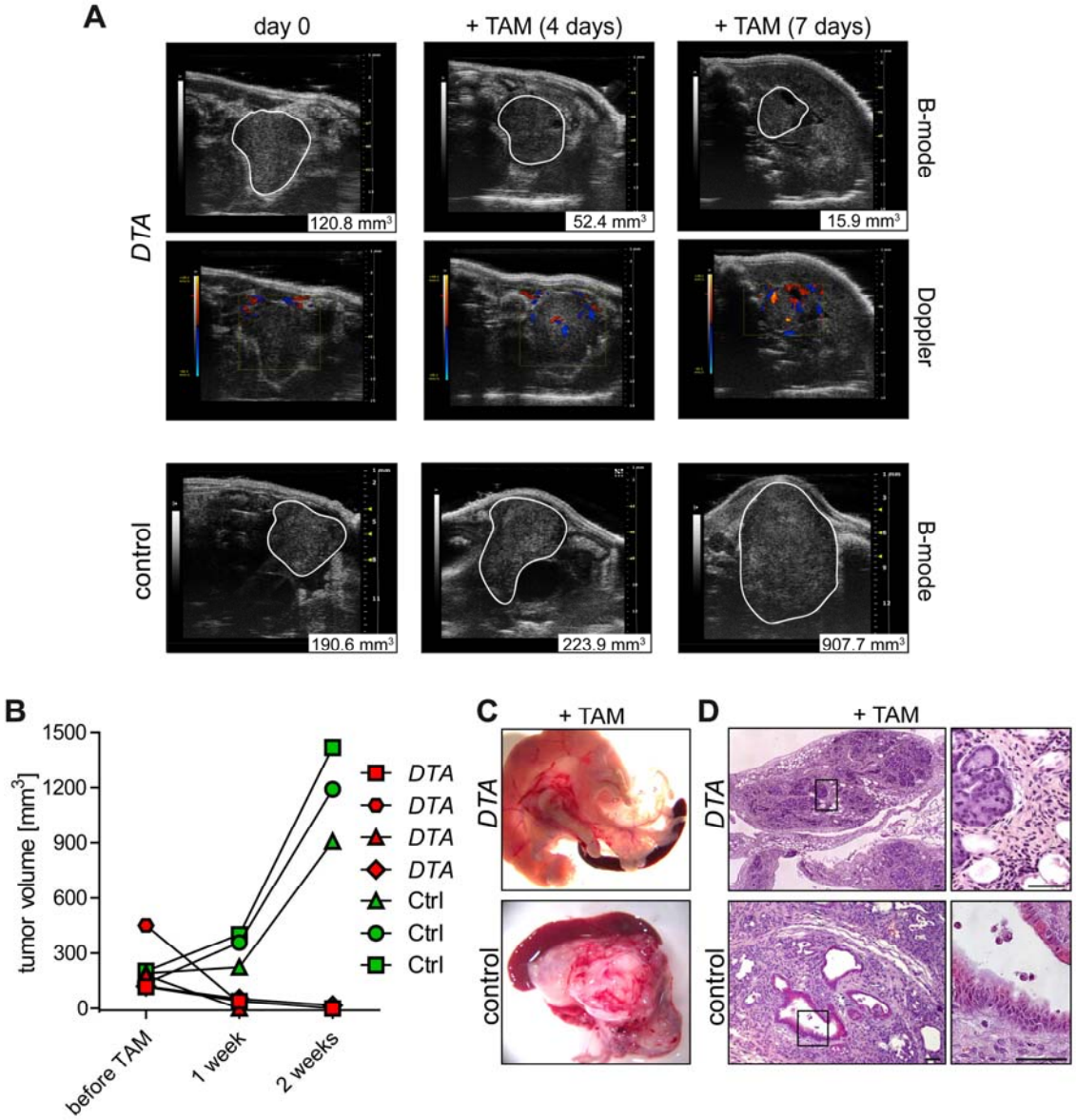

Figure 4-13: Cre-induced expression of DTA in PDAC cells induces tumor shrinkage in vivo
A) Tumor growth was monitored by high-resolution ultrasound (Vevo 2100 System, Visual Sonics) in vivo. DTA and control mice with mean tumor diameters > 5 mm were enrolled and treated with tamoxifen (+ TAM). Representative high-resolution ultrasound images from mice pre-treatment (left, day 0) and after 4 and 7 days of TAM treatment (middle and right panel) are shown. Tumor vascularization was evaluated by Doppler ultrasound. Visible lesions are outlined in white and tumor burden determined by automated three-dimensional (3D) B-mode imaging is shown in mm^3 in the lower right corner. B) Quantification of tumor volume using three-dimensional high-resolution ultrasound shows rapid tumor regression in TAM treated DTA, but not control (Ctrl) mice. C) Representative macroscopic view of pancreas from tamoxifen treated DTA (upper panel) and control (lower panel) mouse. D) Representative H&E stains of tamoxifen treated DTA (upper panel) and control mice (lower panel). Scale bars 50 µm.

Other pancreata of *Pdx1-Flp;FSF-Kras*$^{G12D/+}$*;FSF-R26*$^{CAG\text{-}CreERT2}$*;LSL-R26*^{DTA} mice displayed some residual small tumor nodules (Figure 4-14A) with histopathological signs of intact tumor tissue (Figure 4-14B). Approaches to extend the tamoxifen treatment for analysis of long term consequences of DTA activation failed. All animals developed pancreatitis and subsequently pancreatic atrophy with loss of acinar cells and islets (Figure 4-13D and 4-14B). To determine whether pancreatitis induction is due to DTA expression, *Pdx1-Flp;FSF-R26*$^{CAG\text{-}CreERT2}$*;LSL-R26*^{DTA} (*DTA*) and *Pdx1-Flp;FSF-R26*$^{CAG\text{-}CreERT2}$ (Ctrl) mice were treated with tamoxifen. Histopathological analysis showed signs of pancreatitis in DTA mice, whereas control animals showed normal pancreatic tissue and no signs of inflammation or atrophy (Figure 4-14C). Abnormally elevated serum lipase levels confirmed pancreatitis induction by DTA expression (Figure 4-14D).

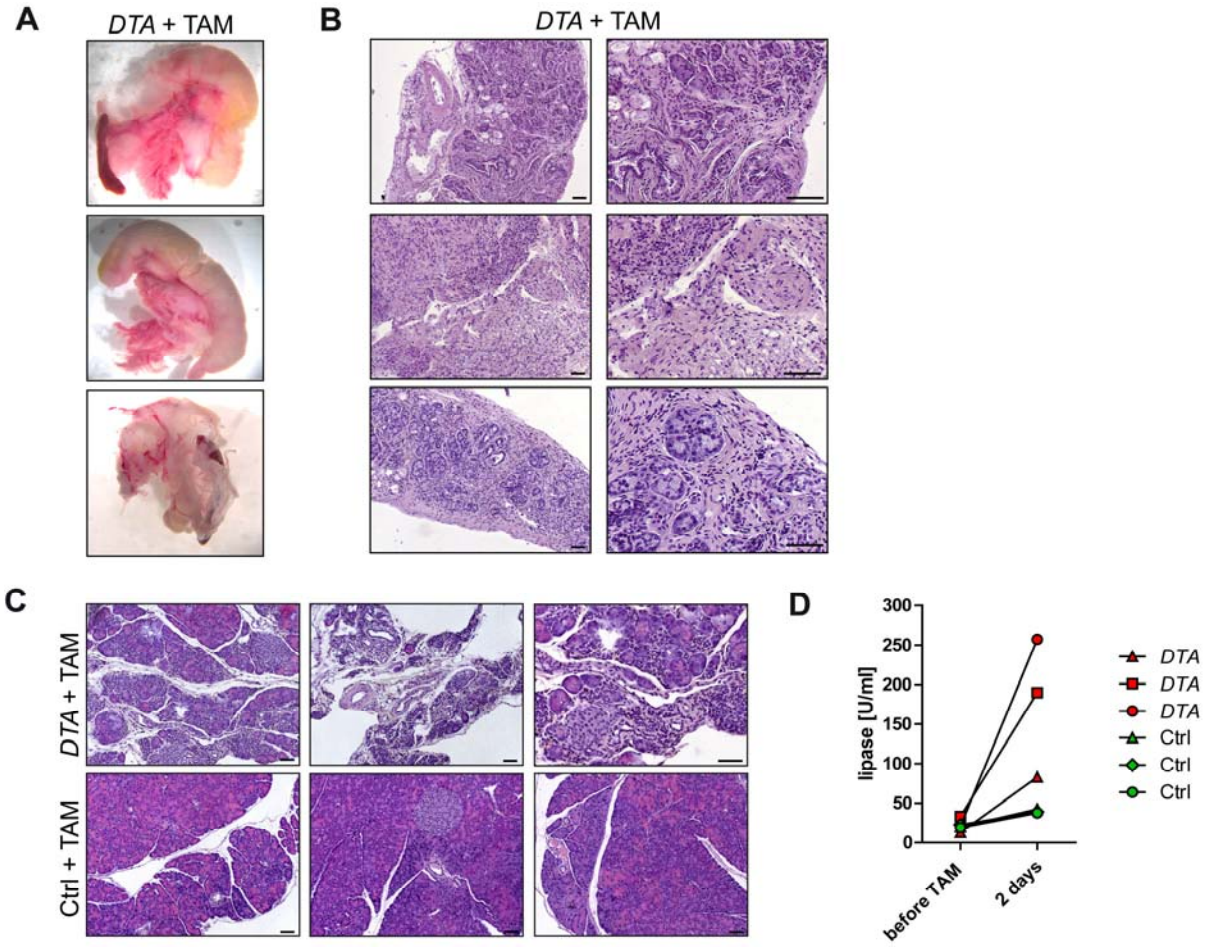

Figure 4-14: Secondary Cre-mediated DTA expression in established PDAC tumors induces tumor shrinkage *in vivo*
A) Representative macroscopic view of pancreata from tamoxifen treated *DTA* mice. B) Representative H&E stains of tamoxifen treated *DTA* mice in A. C) *Pdx1-Flp;FSF-R26*$^{CAG\text{-}CreERT2}$*;LSL-R26*^{DTA} (*DTA,* upper panel) and *Pdx1-Flp;FSF-R26*$^{CAG\text{-}CreERT2/+}$ control (Ctrl, lower panel) animals were treated for 14 days with tamoxifen (+ TAM) and pancreata were analyzed by H&E staining. D) Serum lipase levels of *Pdx1-Flp;FSF-R26*$^{CAG\text{-}CreERT2}$*;LSL-R26*^{DTA} (*DTA*) and *Pdx1-Flp;FSF-R26*$^{CAG\text{-}CreERT2/+}$ control (Ctrl) animals treated with tamoxifen (TAM). Scale bars 50 µm.

4.2.2 Time specific targeting of proliferating cells

The *Pdx1-Flp;FSF-Kras$^{G12D/+}$;FSF-R26$^{CAG\text{-}CreERT2}$* mouse model allows targeting of all recombined cells in the Flp lineage. To target only a subpopulation of these cells, namely proliferating cells, a *FSF-Pcna^{CreERT2}* mouse line was designed.

To create this mouse line, a frt-stop-frt silenced CreER^{T2} cassette was targeted to the *proliferating cell nuclear antigen (Pcna*) locus by homologous recombination in embryonic stem cells.

The targeting vector *pFSF-Pcna^{CreERT2}* (Figure 4-15A) was electroporated into ES cells and 228 geneticin-resistant clones were picked. After checking them by screening PCR (data not shown), five positive clones were identified and further analysed by Southern Blot. Three of them showed correct integration (Figure 4-15B) and clone 2 was injected into blastocysts (PolyGene AG). The resulting chimeras were bred with *C57BL/6J* mice to achieve germline transmission and obtain heterozygous *FSF-Pcna^{CreERT2}* animals. Genotyping PCR of tail DNA was used to determine the geneotype of this line (Figure 4-15C).

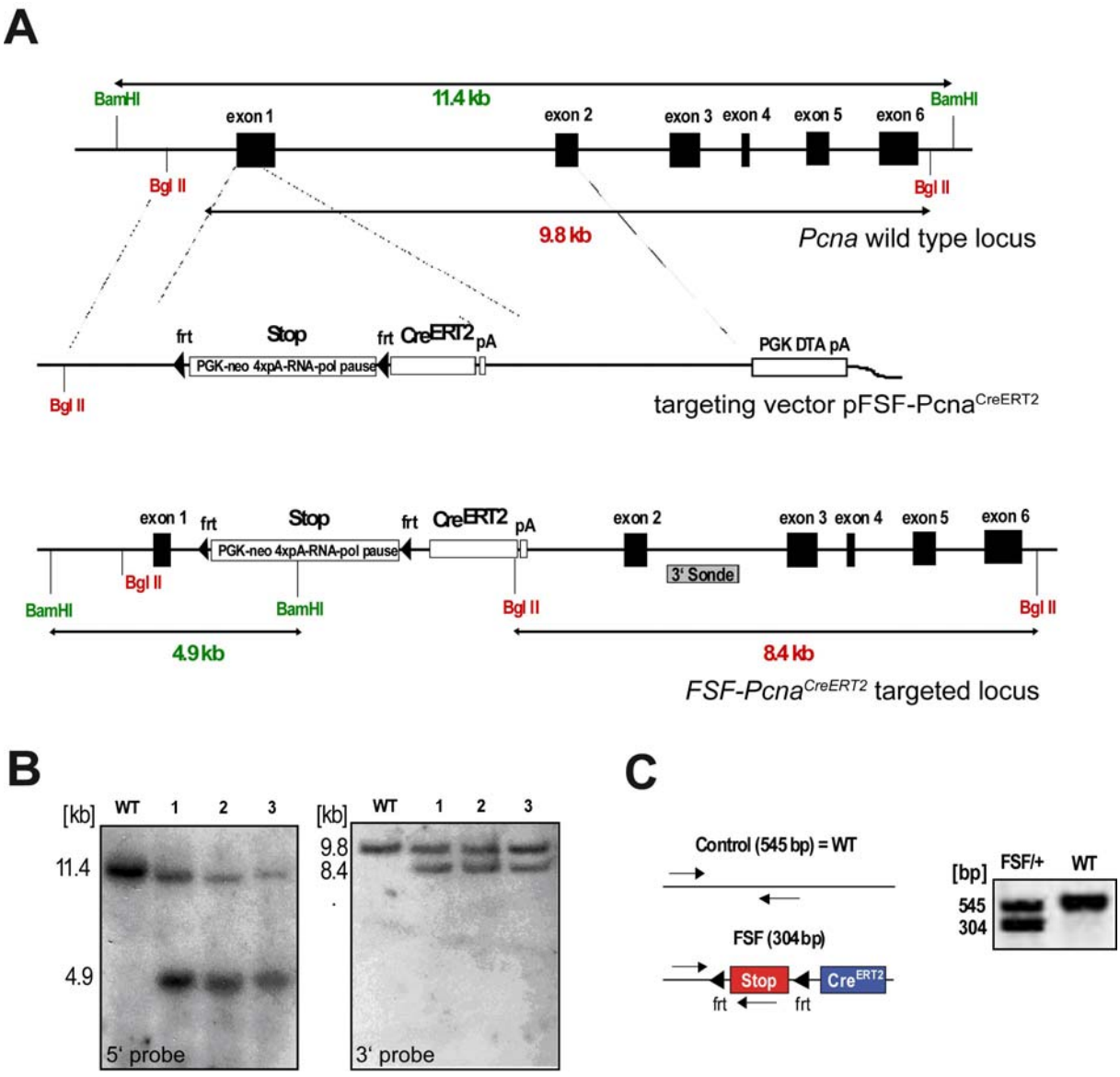

Figure 4-15: Generation of the *FSF-Pcna*^{CreERT2} mouse line.
A) Targeting the endogenous *Pcna* locus by homologous recombination in ES cells. From top to bottom, diagrams of: *Pcna* wild type locus; the *pFSF-Pcna*^{CreERT2} targeting vector with the frt-stop-frt cassette 5' of the *CreER*^{T2} recombinase; the targeted *FSF-Pcna*^{CreERT2} locus. Restriction sites, location of the 5' and 3' probes and sizes of DNA fragments are indicated. B) Southern Blot analysis of DNA from wild type (WT) and targeted ES cells (1-3) after BamHI (5' probe) and Bgl II (3' probe) digestion. For the 5' probe, a 11.4 kb band for the WT and a 4.9 kb band for the mutant allele were expected. For the 3' probe, a 9.8 kb band for the WT and a 8.4. kb band for the mutant allele were expected. C) Genotyping strategy. PCR analysis of DNA from wild type (WT) and heterozygous (FSF/+) *FSF-Pcna*^{CreERT2} mice. Sizes of WT (control) and mutant (FSF) PCR products are indicated.

4.2.3 Characterization of the *FSF-Pcna*^{CreERT2} mouse line

To analyze CreER^{T2} meditated recombination *in vivo*, *FSF-Pcna*^{CreERT2} mice were crossed with *Pdx1-Flp;R26*$^{mT-mG}$ mice (Figure 4-16A). In first preliminary experiments very few Cre recombined cells could be observed, as indicated by the expression of membrane-tagged EGFP (Figure 4-16B). This is in accordance with prior publications demonstrating very low

proliferation rates in the pancreas. Currently, we are in the process to obtain *Pdx1-Flp;FSF-Kras*$^{G12D/+}$*;FSF-Pcna*^{CreERT2}*;R26*$^{mT\text{-}mG}$ animals which develop PDAC to analyze the value of the new mouse line to manipulate proliferating PDAC cells *in vivo*.

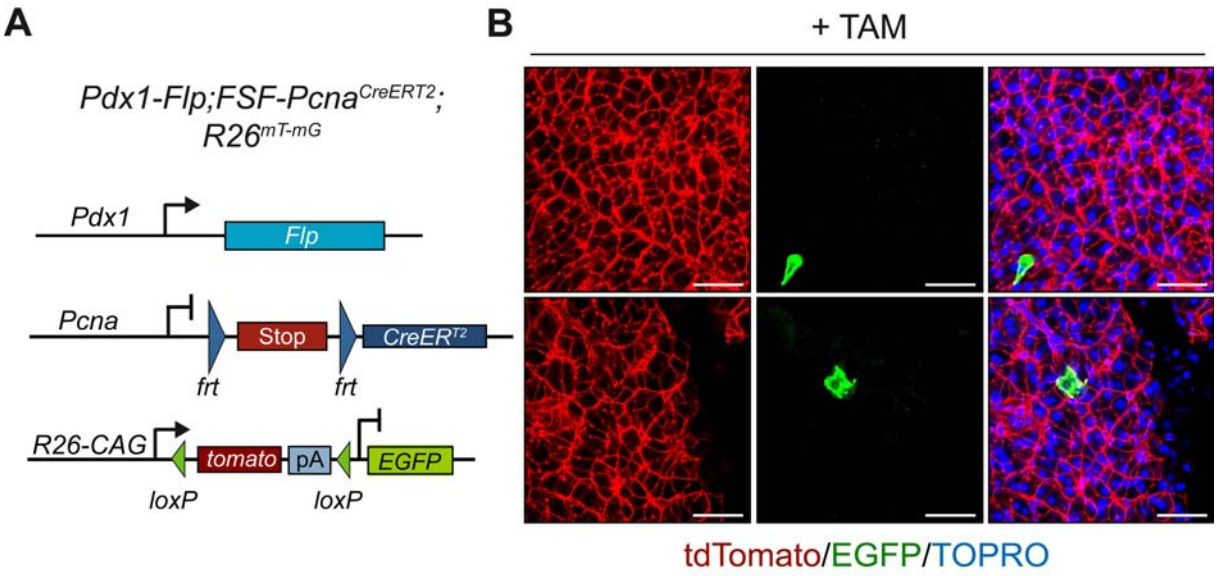

Figure 4-16: Secondary genetic manipulation of proliferating cells in the *Pdx1-Flp* lineage
A) Genetic strategy used to induce EGFP expression by tamoxifen mediated CreER^{T2} activation (left panel). B) Representative confocal microscopic images of tdTomato (red color, non Cre recombined cells) and Cre-induced EGFP (green color) expression in the pancreas of Tamoxifen (+ TAM) treated *Pdx1-Flp;FSF-Pcna*^{CreERT2}*;R26*$^{mT\text{-}mG}$ animals (right panel). Nuclei were stained with TOPRO-3-iodide. Scale bars 50 µm.

5. Discussion

Oncogenic Kras mutations are the signature event in human PDAC, but all strategies to target activated Kras failed in the clinic. Therefore, it is important to identify essential Kras effector pathways which can be targeted more easily using inhibitors that are currently under clinical investigation.

In this work the PI3K/Pdk1 signaling pathway was identified as an essential tumor-initiating event and a potential target for therapy in pancreatic cancer. To further analyze the role of Pdk1 in pancreatic cancer maintenance, a novel dual-recombinase system was developed. By combining the Flp/frt and the Cre/loxP recombination system, genes can be activated or deleted at a given time and thereby the effect on PanIN or PDAC formation can be evaluated. With the help of different Cre driver lines tumor cell subpopulations like cancer stem cells, immune cells or the tumor microenvironment can be manipulated genetically. In addition, tumor cells can be ablated in established tumors by the use of a Flp-dependent *FSF-R26*$^{CAG\text{-}CreERT2}$ and a latent *diphtheria toxin A* allele. First preliminary results also demonstrate that targeting of proliferating cells is possible with the help of the novel *FSF-Pcna*^{CreERT2} mouse line.

5.1 Craf is dispensable for Kras-driven PDAC development

Recent studies identified Craf signaling as essential for Kras^{G12D}-induced NSCLC (Blasco et al., 2011; Karreth et al., 2011). It was shown that Craf ablation leads to decreased amount of tumors in the lung and therefore suggested Craf, but not Braf as a suitable target for NSCLC therapy.

In contrast, this study shows that deletion of Craf in a Kras^{G12D}-driven mouse model of PDAC has no significant effect on PanIN and PDAC formation. Also PDAC progression and overall survival was not affected in these animals. These results show that Kras downstream signalling is tissue specific and may explain the different response of various Kras-driven tumor types to targeted therapies. Indeed, Engelman and colleagues demonstrated that mouse NSCLC, which is driven by oncogenic Kras, does not respond to NVP-BEZ235, a dual pan PI3K/mTOR inhibitor (Engelman et al., 2008). In contrast, inhibition of the PI3K pathway in the Kras^{G12D}-driven PDAC model efficiently blocks ADM, PanIN and PDAC formation (Eser et al., 2013). These data support the view that Kras exerts its oncogenic effects in a tissue-specific manner.

Collisson et al. showed that specific expression of oncogenic Braf^{V600E} in the pancreas leads to PanIN lesions in mice. Moreover, additional expression of TP53^{R270H} resulted in development of PDAC. As median survival of mice is statistically significant prolonged by inhibition of MEK1/2, they concluded that Raf/MEK/ERK signaling plays a central role in

initiation and maintenance of PDAC (Collisson et al., 2012). The role of Braf in PanIN and PDAC formation in the Kras^{G12D}-driven model still needs to be investigated.

5.2 Loss of Pdk1 blocks ADM, PanIN and PDAC formation

One of the three major pathways downstream of Kras is the PI3K/Pdk1/AKT pathway. It has been shown by our group that selective activation of this pathway in the pancreas induces PanIN and PDAC formation *in vivo* (Eser et al., 2013). Expression of an oncogenic class IA PI3K (PIK3CA^{H1047R} (p110α^{H1047R})) enabled selective activation of the PI3K/Pdk1/AKT pathway in Ptf1a positive cells. This model phenocopied Kras^{G12D}-driven pancreatic carcinogenesis with a high rate of metastasis.

This contrasts findings by Collisson and colleagues in another murine model. They used a transgenic *Pdx1-CreER^{T2}* mouse line for tamoxifen-induced expression of p110α^{H1047R} in the pancreas and failed to induce PanIN and PDAC. These conflicting results might be due to different target cells of the Cre-driver lines used in these two studies, different recombination efficacies and different expression and signaling levels of p110α (Collisson et al., 2012).

It has been shown that tumor cells are addicted to oncogenic Kras signaling, as inactivation of Kras^{G12D} in established PanINs and PDAC led to reversion of these lesions (Collins et al., 2012). Lim and Counter demonstrated that once tumors formed, the PI3K/Pdk1/AKT pathway replaced dependency on Ras activity (Lim and Counter, 2005). These data suggest that the addiction of pancreatic cancer to Kras signaling depends critically on the PI3K/AKT pathway.

Because Pdk1 is a central protein in the PI3K signaling pathway (Castellano and Downward, 2011) its role in Kras^{G12D}-induced pancreatic cancer was analyzed in this study. Inactivation of Pdk1 in the epithelium of the pancreas completely blocked ADM, PanIN and PDAC formation. ADM is considered as the initiating event of PDAC formation. It could be blocked by PI3K, PI3K-mTOR, AKT and Pdk1 inhibitors *in vitro*, supporting the *in vivo* data that disruption of the PI3K-Pdk1-AKT axis is essential for tumor initiation in the pancreas.

It has been shown already for other tumor types like melanoma, breast, colorectal and head and neck cancer that Pdk1 may be a suitable therapeutic target (Bhola et al., 2012; Maurer et al., 2009; Scortegagna et al., 2013; Tan et al., 2010). To test whether this is also true for pancreatic cancer, our group used the *Ptf1a$^{Cre/+}$;LSL-Kras$^{G12D/+}$;LSL-Trp53$^{R172H/f}$* mouse model of pancreatic cancer (Olive et al., 2009). Mice with established tumors were treated with a pan class I PI3K inhibitor, resulting in reduced phosphorylation of AKT and blockade of proliferation. In further experiments, *Pdk1* was deleted in a Kras-driven NSCLC model in the epithelial compartment of the lung. In contrast to the pancreas, loss of Pdk1 had no inhibitory effect on development and progression of Kras^{G12D}-induced NSCLC (Eser et al., 2013).

These results support the conclusion that Kras engages specific and distinct effector pathways in a tissue- and context-specific fashion *in vivo*.

The important role of PI3K signaling in pancreatic cancer was confirmed in the meantime by others. Wu and colleagues reported that complete deletion of p110α in the *Ptf1a$^{Cre/+}$;LSL-Kras$^{G12D/+}$* model completely blocked tumorigenesis whereas p110β was dispensable (Wu et al., 2014). They suggest that Rac1, a PI3K downstream effector is required for tumorigenesis. Rac1 was already described to be important for ADM and PanIN formation in Kras-driven PDAC (Heid et al., 2011). In contrast, we could not induce PanINs and PDAC formation by expressing a dominant active Rac^{G12V} gain of function mutant in the pancreas (Eser et al., 2013).

Interestingly, acini isolated from *Ptf1a$^{Cre/+}$;LSL-Kras$^{G12D/+}$;p110α$^{-/-}$* mice were still able to undergo ADM *in vitro* (Wu et al., 2014) whereas this study showed that a pan class I PI3K inhibitor was able to block ADM. However, Wu et al. observed unchanged AKT phosphorylation levels in *Ptf1a$^{Cre/+}$;LSL-Kras$^{G12D/+}$;p110α$^{-/-}$* acini, indicating that AKT activity is critical for ADM *in vitro*.

Another group used the *Pdx1-Cre;LSL-Kras$^{G12D/+}$* mouse model to analyze the role of the kinase activity of p110α in PDAC initiation and progression. They used a *p110α$^{lox/lox}$* mouse line in which the exons encoding the kinase domain are flanked by loxP sites. Cre meditated recombination of these exons generates a kinase dead p110α enzyme, which closely mimicks pharmacological p110α inhibition. Thereby, they could show that inactivation of the kinase activity of p110α blocked ADM, PanIN and PDAC formation *in vivo* and ADM *in vitro*. In contrast to Wu et al., they observed decreased phosphorylation levels of AKT (Baer et al., 2014). These differences may be due to compensatory effects in the complete p110α knock-out model, as deletion of PI3K components leads to the upregulation of the other catalytic and regulatory subunits of PI3K (Vanhaesebroeck et al., 2005).

In summary, these data suggest that PI3K/Pdk1/AKT signaling is the major downstream pathway of Kras in PDAC. Thus, Pdk1 may serve as a suitable target for therapeutic interventions in pancreatic cancer.

5.3 Manipulating the tumor entity and its microenvironment

Genetically engineered mouse models which recapitulate the hallmarks of human pancreatic cancer have dramatically improved our understanding of PDAC. All these models are based on a single Cre recombination step which activates oncogenic Kras^{G12D}. Additional mutations or deletions of tumor suppressors like Trp53, p16^{INK4A} and p19^{ARF} accelerate PanIN formation and PDAC progression in this model, but occur at the same time due to Cre activity. In contrast, the human disease is the result of a multi-step process in which mutations

accumulate over time (Hruban et al., 2000). Mimicking the step-wise occurance of such genetic alterations is not possible with the classical Cre/loxP-based mouse models. In addition, it is challenging to validate possible targets genetically to block PanIN progression or treat PDAC after tumors have formed.

In this study, a novel dual-recombinase system combining the established Cre/loxP with the Flp/frt recombination system was developed and analyzed. *Pdx1-Flp;FSF-Kras$^{G12D/+}$* animals develop PanINs and metastatic PDAC, similar to the well established *Pdx1-Cre;LSL-Kras$^{G12D/+}$* model (Schönhuber et al., 2014). To mimick multi-step carcinogenesis and manipulate established tumors genetically, a *FSF-R26$^{CAG\text{-}CreERT2/+}$* mouse line was generated. Effective secondary genetic targeting was demonstrated using the *R26$^{mT\text{-}mG}$* reporter. After Tamoxifen treatment, nearly all tumor cells isolated from *Pdx1-Flp;FSF-Kras$^{G12D/+}$;FSF-R26$^{CAG\text{-}CreERT2/+}$;R26$^{mT\text{-}mG}$* animals showed expression of membrane-tagged EGFP as evidence for Cre-mediated recombination.

As a proof of concept, a latent *diphtheria toxin A* allele was used to mimick therapeutic interventions. Tamoxifen-induced ablation of tumor cells in *Pdx1-Flp;FSF-Kras$^{G12D/+}$;FSF-R26$^{CAG\text{-}CreERT2}$;LSL-R26^{DTA}* mice showed that such an approach is possible in this model.

In the first part of this study, Pdk1 was identified as an essential mediator of Kras-driven tumor initiation in the pancreas. But the question remained whether Pdk1 is still required for tumor maintenance. Deletion of Pdk1 in *Pdx1-Flp;FSF-Kras$^{G12D/+}$;FSF-R26$^{CAG\text{-}CreERT2}$;Pdk1$^{lox/lox}$* mice at the age of 3 months blocked PDAC progression. Pancreata showed normal size and weight, in contrast to heterozygous Pdk1 deleted control animals (Schönhuber et al., 2014). These data support the view that the dual recombinase system can be used to evaluate potential drug targets *in vivo*.

Furthermore, it can be also used to analyze the contribution of the tumor microenvironment for PDAC initiation and maintenance. The PDAC stroma is clearly relevant to the development of new therapies as it is known to support tumor growth and mediate drug resistance (Kraman et al., 2010; Olive et al., 2009; Perez-Mancera et al., 2012; Provenzano et al., 2012). Therefore, it is important to understand the role of the different stromal compartments. With the help of different Cre-driver lines it is possible to target fibroblast, stellate cells, mast cells, immune cells and other cell types to analyze their role in clean genetic models.

5.4 Targeting proliferating cells

Cancer cells are characterized by deregulated proliferation. Thus, it is of interest to target only proliferating cells in the tumor. Proliferating cell nuclear antigen (Pcna) is a well established proliferation marker. Accordingly, a *FSF-Pcna^{CreERT2}* mouse line was generated in

this study. First results using a *R26*$^{mT\text{-}mG}$ reporter allele showed recombination of single cells in the pancreas which reflect the few proliferating cells in the normal healthy organ. Further experiments are needed to fully characterize this novel mouse line and its value to target proliferating cells in a time specific fashion.

5.5 Outlook

In this study, Pdk1 was shown to be essential for the initiation of PDAC. Further experiments in our group demonstrated that deletion of *Pdk1* blocked tumor progression *in vivo* (Schönhuber et al., 2014). Now the question arises which downstream targets of Pdk1 are responsible for these effects.

Interestingly, in contrast to PI3K, Pdk1 and AKT inhibitors, a RSK inhibitor was not able to block ADM of acinar cells isolated from *Ptf1a*$^{Cre/+}$*;LSL-Kras*$^{G12D/+}$ animals. The Pdk1 protein contains two different regulatory domains. A pleckstrin homology (PH) domain and a substrate binding site termed PIF-pocket. The PH domain is essential to activate AKT whereas the PIF-pocket domain is necessary to activate S6K, RSK, SGK and PKC isoforms (Bayascas, 2008). There are two knock-in mice available which affect the activity of these domains. The Pdk1[K465E] mutant allele harbours a point mutation in the PH domain leading to substantially reduced activation of AKT (Bayascas et al., 2008). In contrast, Pdk1[L155E] mutant mice show normal AKT phosphorylation, but impaired activation of other ACG kinases such as RSK, SGK, PKC isoforms and S6K (Collins et al., 2003). Crossing these two mouse lines into the *Ptf1a*$^{Cre/+}$*;LSL-Kras*$^{G12D/+}$ model will hopefully identify downstream targets of Pdk1 which are able to block ADM, PanIN and PDAC formation and thereby enable the development of a more effective therapy for this deadly disease.

The dual-recombinase mouse model is a multifunctional tool. It enables evaluation of potential drug targets *in vivo*, as it was already shown for Pdk1 (Schönhuber et al., 2014). Furthermore, different stromal compartments and their role in PDAC progression can be investigated using this novel mouse model. Therefore, it has the potential to advance cancer research in the future.

6. Summary

Pancreatic ductal adenocarcinoma (PDAC) is nearly uniformly fatal despite maximal treatment, with less than 6% of patients surviving 5 years. A wealth of molecular studies have identified mutant KRAS as the initiating event. Although infrequently mutated, the PI3K/AKT pathway is uniformly activated in human PDAC and mouse models of Kras-driven pancreatic cancer.

To investigate the role of PI3K/Pdk1/AKT and Raf/MEK/ERK signaling for pancreatic cell plasticity and PDAC formation, the fist aim was to inactivate these signaling pathways specifically in the epithelial compartment of the pancreas. Deletion of *Craf* using a pancreas-specific Cre-driver line (*Ptf1a*$^{Cre/+}$) had no inhibitory effect on tumor development and progression and did not improve median survival of mice. In contrast, loss of Pdk1 blocked acinar to ductal metaplasia, PanIN and PDAC formation. *Ptf1a*$^{Cre/+}$*;LSL-Kras*$^{G12D/+}$*;Pdk1*$^{f/f}$ mice have normal life expectancy, normal histology and weight of the pancreas. Impaired glucose tolerance could be observed in these mice, but no overt diabetes, hypoplasia or developmental defects of the pancreas.

However, this Cre/loxP based strategy to delete Pdk1 has important limitations. It relies on a single Cre recombination step to activate mutant Kras and inactivate Pdk1. This has the significant drawback that it is not possible to evaluate and validate PI3K signaling as a suitable target for the treatment of pancreatic cancer at the level of genetics. Therefore, the second aim of this work was to create and analyze a novel conditional dual recombination PDAC model for sequential gene activation and inactivation and targeting of different pancreatic compartments by combining the Flp/frt with the Cre/loxP system. To induce pancreatic tumor development, a transgenic *Pdx1-Flp* line for pancreas specific expression of Flp-recombinase and a *FSF-Kras*^{G12D} knock-in mouse line, expressing a latent frt-stop-frt (FSF) silenced oncogenic *Kras*^{G12D} allele were generated. These *Pdx1-Flp;FSF-Kras*$^{G12D/+}$ mice developed PanIN lesions and PDAC similar to the well known Cre/loxP based *Pdx1-Cre;LSL-Kras*$^{G12D/+}$ mouse model. For site and time-specific Cre-activation, two FSF silenced knock-in mouse strains were generated, which express a tamoxifen-inducible CreER^{T2} fusion protein in the Flp-lineage under the control of the ubiquitous *CAG* promoter or the proliferation marker *Pcna*. With the help of the double fluorescent reporter mouse *R26*$^{mT-mG}$ tamoxifen-induced Cre mediated recombination could be shown *in vitro* and *in vivo.* As a proof of concept, cells isolated from *Pdx1-Flp;FSF-Kras*$^{G12D/+}$*;FSF-R26*$^{CAG-CreERT2}$*;LSL-R26*^{DTA} mice were depleted by tamoxifen induced diphtheria toxin A expression. Further, tumor shrinkage in established PDAC could be shown after tamoxifen treatment *in vivo*.

The results of this work clearly demonstrate the essential role of Pdk1 in the initiation of pancreatic cancer and introduce a novel dual recombinase system which can be used to evaluate potential drug targets like Pdk1 in established autochtonous tumors *in vivo*.

7. Zusammenfassung

Das duktale Pankreaskarzinom ist mit einer 5-Jahres Überlebensrate unter 6% eine der aggressivsten und tödlichsten Krebserkrankungen. Studien haben KRAS Mutationen als initiierendes Ereignis identifiziert. Häufig spielt der PI3K/AKT Signalweg im humanen PDAC und in Kras-induzierten Mausmodellen eine wichtige Rolle.

Im ersten Teil dieser Arbeit wurde der PI3K/Pdk1/AKT und der Raf/MEK/ERK Signalweg spezifisch im Pankreas inaktiviert, um ihre Rolle bei der Entstehung des duktalen Pankreaskarzinoms zu untersuchen. Die Inaktivierung von Craf mittels einer Pankreas-spezifischen Cre-Linie (*Ptf1a*$^{Cre/+}$) zeigte keinen Effekt auf die Tumorentstehung, Progression und die mittlere Überlebenszeit der Tiere. Im Gegensatz dazu verhinderte der Verlust von Pdk1 die Entstehung von ADM, PanIN und PDAC. *Ptf1a*$^{Cre/+}$*;LSL-Kras*$^{G12D/+}$*;Pdk1*$^{f/f}$ Tiere haben eine normale Lebenserwartung und Pankreata dieser Tiere weisen eine normale Histologie und ein normales Gewicht auf. Diese Tiere zeigten eine verminderte Glukosetoleranz, entwickelten jedoch keinen Diabetes mellitus. Auch konnten weder eine Hypoplasie noch Entwicklungsdefekte des Pankreas festgestellt werden.

Mit Hilfe dieses Mausmodells kann jedoch nicht untersucht werden, ob der PI3K Signalweg ein mögliches Angriffsziel für die Behandlung des Pankreaskarzinoms darstellt. Daher wurde im zweiten Teil dieser Arbeit ein induzierbares duales Rekombinationsmodell für das PDAC generiert und analysiert. Hierfür wurden die Flp/frt und Cre/loxP Rekombinationssysteme kombiniert, um in verschiedenen Kompartimenten des Pankreas sequenziell Gene an- oder abzuschalten. Um Pankreaskarzinome zu induzieren, wurde zum einen eine *Pdx1-Flp* Maus generiert, welche die Flp-Rekombinase spezifisch im Pankreas exprimiert und zum anderen eine *FSF-Kras*^{G12D} Mauslinie, welche onkogenes Kras nach Rekombination der frt-Stop-frt (FSF) Kassette exprimiert. Die PanIN und PDAC Entstehung in *Pdx1-Flp;FSF-Kras*$^{G12D/+}$ Tieren ist vergleichbar mit der im etablierten *Pdx1-Cre;LSL-Kras*$^{G12D/+}$ Modell. Um eine Gewebe- und Zeit-spezifische Cre-Aktivierung zu ermöglichen, wurden zwei Mauslinien generiert. Diese exprimieren ein Tamoxifen-induzierbares CreER^{T2} Fusionsprotein unter der Kontrolle des ubiquitär exprimierten *CAG* Promotors oder des Proliferationsmarkers *Pcna*. Mit Hilfe der fluoreszierenden Reportermauslinie *R26*$^{mT-mG}$ konnte die Tamoxifen-induzierte Cre Aktivierung und Rekombination *in vitro* und *in vivo* gezeigt werden. Um die Funktionalität des Systems zu zeigen, wurden Tumorzelllinien aus *Pdx1-Flp;FSF-Kras*$^{G12D/+}$*;FSF-R26*$^{CAG-CreERT2}$*;LSL-R26*^{DTA} Tieren isoliert, welche nach Tamoxifen-Induktion Diphtherie Toxin A exprimieren und daraufhin sterben. Weiterhin konnte eine Regression von etablierten Tumoren *in vivo* nach Tamoxifen-Gabe gezeigt werden.

Die Erkenntnisse dieser Arbeit zeigen die essentielle Rolle von Pdk1 bei der Entstehung des duktalen Pankreaskarzinoms auf. Mit Hilfe des neuen dualen Rekombinationsmodells

können potentielle Zielstrukturen für molekulare Therapieansätze, wie zum Beispiel Pdk1, *in vivo* getestet werden.

8. References

Aguirre, A. J., Bardeesy, N., Sinha, M., Lopez, L., Tuveson, D. A., Horner, J., Redston, M. S., and DePinho, R. A. (2003). Activated Kras and Ink4a/Arf deficiency cooperate to produce metastatic pancreatic ductal adenocarcinoma. Genes Dev *17*, 3112-3126.

Aichler, M., Seiler, C., Tost, M., Siveke, J., Mazur, P. K., Da Silva-Buttkus, P., Bartsch, D. K., Langer, P., Chiblak, S., Durr, A.*, et al.* (2012). Origin of pancreatic ductal adenocarcinoma from atypical flat lesions: a comparative study in transgenic mice and human tissues. J Pathol *226*, 723-734.

Alessi, D. R., James, S. R., Downes, C. P., Holmes, A. B., Gaffney, P. R., Reese, C. B., and Cohen, P. (1997). Characterization of a 3-phosphoinositide-dependent protein kinase which phosphorylates and activates protein kinase Balpha. Curr Biol *7*, 261-269.

Awatramani, R., Soriano, P., Mai, J. J., and Dymecki, S. (2001). An Flp indicator mouse expressing alkaline phosphatase from the ROSA26 locus. Nat Genet *29*, 257-259.

Baer, R., Cintas, C., Dufresne, M., Cassant-Sourdy, S., Schonhuber, N., Planque, L., Lulka, H., Couderc, B., Bousquet, C., Garmy-Susini, B.*, et al.* (2014). Pancreatic cell plasticity and cancer initiation induced by oncogenic Kras is completely dependent on wild-type PI 3-kinase p110alpha. Genes Dev *28*, 2621-2635.

Bardeesy, N., Aguirre, A. J., Chu, G. C., Cheng, K. H., Lopez, L. V., Hezel, A. F., Feng, B., Brennan, C., Weissleder, R., Mahmood, U.*, et al.* (2006). Both p16(Ink4a) and the p19(Arf)-p53 pathway constrain progression of pancreatic adenocarcinoma in the mouse. Proc Natl Acad Sci U S A *103*, 5947-5952.

Bardeesy, N., and DePinho, R. A. (2002). Pancreatic cancer biology and genetics. Nat Rev Cancer *2*, 897-909.

Bayascas, J. R. (2008). Dissecting the role of the 3-phosphoinositide-dependent protein kinase-1 (PDK1) signalling pathways. Cell Cycle *7*, 2978-2982.

Bayascas, J. R., Wullschleger, S., Sakamoto, K., Garcia-Martinez, J. M., Clacher, C., Komander, D., van Aalten, D. M., Boini, K. M., Lang, F., Lipina, C.*, et al.* (2008). Mutation of the PDK1 PH domain inhibits protein kinase B/Akt, leading to small size and insulin resistance. Mol Cell Biol *28*, 3258-3272.

Berndt, N., Hamilton, A. D., and Sebti, S. M. (2011). Targeting protein prenylation for cancer therapy. Nat Rev Cancer *11*, 775-791.

Berrington de Gonzalez, A., Sweetland, S., and Spencer, E. (2003). A meta-analysis of obesity and the risk of pancreatic cancer. Br J Cancer *89*, 519-523.

Bhola, N. E., Freilino, M. L., Joyce, S. C., Sen, M., Thomas, S. M., Sahu, A., Cassell, A., Chen, C. S., and Grandis, J. R. (2012). Antitumor mechanisms of targeting the PDK1 pathway in head and neck cancer. Mol Cancer Ther *11*, 1236-1246.

References

Blasco, R. B., Francoz, S., Santamaria, D., Canamero, M., Dubus, P., Charron, J., Baccarini, M., and Barbacid, M. (2011). c-Raf, but not B-Raf, is essential for development of K-Ras oncogene-driven non-small cell lung carcinoma. Cancer Cell *19*, 652-663.

Brembeck, F. H., Schreiber, F. S., Deramaudt, T. B., Craig, L., Rhoades, B., Swain, G., Grippo, P., Stoffers, D. A., Silberg, D. G., and Rustgi, A. K. (2003). The mutant K-ras oncogene causes pancreatic periductal lymphocytic infiltration and gastric mucous neck cell hyperplasia in transgenic mice. Cancer Res *63*, 2005-2009.

Brugge, W. R., Lauwers, G. Y., Sahani, D., Fernandez-del Castillo, C., and Warshaw, A. L. (2004). Cystic neoplasms of the pancreas. N Engl J Med *351*, 1218-1226.

Burris, H. A., 3rd, Moore, M. J., Andersen, J., Green, M. R., Rothenberg, M. L., Modiano, M. R., Cripps, M. C., Portenoy, R. K., Storniolo, A. M., Tarassoff, P.*, et al.* (1997). Improvements in survival and clinical benefit with gemcitabine as first-line therapy for patients with advanced pancreas cancer: a randomized trial. J Clin Oncol *15*, 2403-2413.

Caldwell, M. E., DeNicola, G. M., Martins, C. P., Jacobetz, M. A., Maitra, A., Hruban, R. H., and Tuveson, D. A. (2012). Cellular features of senescence during the evolution of human and murine ductal pancreatic cancer. Oncogene *31*, 1599-1608.

Cantley, L. C. (2002). The phosphoinositide 3-kinase pathway. Science *296*, 1655-1657.

Castellano, E., and Downward, J. (2011). RAS Interaction with PI3K: More Than Just Another Effector Pathway. Genes Cancer *2*, 261-274.

Chames, P., Kerfelec, B., and Baty, D. (2010). Therapeutic antibodies for the treatment of pancreatic cancer. ScientificWorldJournal *10*, 1107-1120.

Collins, B. J., Deak, M., Arthur, J. S., Armit, L. J., and Alessi, D. R. (2003). In vivo role of the PIF-binding docking site of PDK1 defined by knock-in mutation. Embo J *22*, 4202-4211.

Collins, M. A., Bednar, F., Zhang, Y., Brisset, J. C., Galban, S., Galban, C. J., Rakshit, S., Flannagan, K. S., Adsay, N. V., and Pasca di Magliano, M. (2012). Oncogenic Kras is required for both the initiation and maintenance of pancreatic cancer in mice. J Clin Invest *122*, 639-653.

Collisson, E. A., Trejo, C. L., Silva, J. M., Gu, S., Korkola, J. E., Heiser, L. M., Charles, R. P., Rabinovich, B. A., Hann, B., Dankort, D.*, et al.* (2012). A central role for RAF-->MEK-->ERK signaling in the genesis of pancreatic ductal adenocarcinoma. Cancer Discov *2*, 685-693.

Conroy, T., Desseigne, F., Ychou, M., Bouche, O., Guimbaud, R., Becouarn, Y., Adenis, A., Raoul, J. L., Gourgou-Bourgade, S., de la Fouchardiere, C.*, et al.* (2011). FOLFIRINOX versus gemcitabine for metastatic pancreatic cancer. N Engl J Med *364*, 1817-1825.

Currie, R. A., Walker, K. S., Gray, A., Deak, M., Casamayor, A., Downes, C. P., Cohen, P., Alessi, D. R., and Lucocq, J. (1999). Role of phosphatidylinositol 3,4,5-trisphosphate in regulating the activity and localization of 3-phosphoinositide-dependent protein kinase-1. Biochem J *337 (Pt 3)*, 575-583.

Danielian, P. S., Muccino, D., Rowitch, D. H., Michael, S. K., and McMahon, A. P. (1998). Modification of gene activity in mouse embryos in utero by a tamoxifen-inducible form of Cre recombinase. Curr Biol *8*, 1323-1326.

Engelman, J. A., Chen, L., Tan, X., Crosby, K., Guimaraes, A. R., Upadhyay, R., Maira, M., McNamara, K., Perera, S. A., Song, Y.*, et al.* (2008). Effective use of PI3K and MEK inhibitors to treat mutant Kras G12D and PIK3CA H1047R murine lung cancers. Nat Med *14*, 1351-1356.

Eser, S., Reiff, N., Messer, M., Seidler, B., Gottschalk, K., Dobler, M., Hieber, M., Arbeiter, A., Klein, S., Kong, B.*, et al.* (2013). Selective requirement of PI3K/PDK1 signaling for Kras oncogene-driven pancreatic cell plasticity and cancer. Cancer Cell *23*, 406-420.

Eser, S., Schnieke, A., Schneider, G., and Saur, D. (2014). Oncogenic KRAS signalling in pancreatic cancer. Br J Cancer *111*, 817-822.

Esposito, I., Konukiewitz, B., Schlitter, A. M., and Kloppel, G. (2012). [New insights into the origin of pancreatic cancer. Role of atypical flat lesions in pancreatic carcinogenesis]. Pathologe *33 Suppl 2*, 189-193.

Everhart, J., and Wright, D. (1995). Diabetes mellitus as a risk factor for pancreatic cancer. A meta-analysis. Jama *273*, 1605-1609.

Feil, R., Brocard, J., Mascrez, B., LeMeur, M., Metzger, D., and Chambon, P. (1996). Ligand-activated site-specific recombination in mice. Proc Natl Acad Sci U S A *93*, 10887-10890.

Feil, R., Wagner, J., Metzger, D., and Chambon, P. (1997). Regulation of Cre recombinase activity by mutated estrogen receptor ligand-binding domains. Biochem Biophys Res Commun *237*, 752-757.

Feldmann, G., Mishra, A., Hong, S. M., Bisht, S., Strock, C. J., Ball, D. W., Goggins, M., Maitra, A., and Nelkin, B. D. (2010). Inhibiting the cyclin-dependent kinase CDK5 blocks pancreatic cancer formation and progression through the suppression of Ras-Ral signaling. Cancer Res *70*, 4460-4469.

Fuchs, C. S., Colditz, G. A., Stampfer, M. J., Giovannucci, E. L., Hunter, D. J., Rimm, E. B., Willett, W. C., and Speizer, F. E. (1996). A prospective study of cigarette smoking and the risk of pancreatic cancer. Arch Intern Med *156*, 2255-2260.

Gannon, M., Herrera, P. L., and Wright, C. V. (2000). Mosaic Cre-mediated recombination in pancreas using the pdx-1 enhancer/promoter. Genesis *26*, 143-144.

Gapstur, S. M., Gann, P. H., Lowe, W., Liu, K., Colangelo, L., and Dyer, A. (2000). Abnormal glucose metabolism and pancreatic cancer mortality. Jama *283*, 2552-2558.

Grippo, P. J., Nowlin, P. S., Demeure, M. J., Longnecker, D. S., and Sandgren, E. P. (2003). Preinvasive pancreatic neoplasia of ductal phenotype induced by acinar cell targeting of mutant Kras in transgenic mice. Cancer Res *63*, 2016-2019.

Gupta, S., and El-Rayes, B. F. (2008). Small molecule tyrosine kinase inhibitors in pancreatic cancer. Biologics *2*, 707-715.

Guz, Y., Montminy, M. R., Stein, R., Leonard, J., Gamer, L. W., Wright, C. V., and Teitelman, G. (1995). Expression of murine STF-1, a putative insulin gene transcription factor, in beta cells of pancreas, duodenal epithelium and pancreatic exocrine and endocrine progenitors during ontogeny. Development *121*, 11-18.

Hahn, S. A., Schutte, M., Hoque, A. T., Moskaluk, C. A., da Costa, L. T., Rozenblum, E., Weinstein, C. L., Fischer, A., Yeo, C. J., Hruban, R. H., and Kern, S. E. (1996). DPC4, a candidate tumor suppressor gene at human chromosome 18q21.1. Science *271*, 350-353.

Heid, I., Lubeseder-Martellato, C., Sipos, B., Mazur, P. K., Lesina, M., Schmid, R. M., and Siveke, J. T. (2011). Early requirement of Rac1 in a mouse model of pancreatic cancer. Gastroenterology *141*, 719-730, 730 e711-717.

Hezel, A. F., Kimmelman, A. C., Stanger, B. Z., Bardeesy, N., and Depinho, R. A. (2006). Genetics and biology of pancreatic ductal adenocarcinoma. Genes Dev *20*, 1218-1249.

Hidalgo, M. (2010). Pancreatic cancer. N Engl J Med *362*, 1605-1617.

Hingorani, S. R., Petricoin, E. F., Maitra, A., Rajapakse, V., King, C., Jacobetz, M. A., Ross, S., Conrads, T. P., Veenstra, T. D., Hitt, B. A*., et al.* (2003). Preinvasive and invasive ductal pancreatic cancer and its early detection in the mouse. Cancer Cell *4*, 437-450.

Hingorani, S. R., Wang, L., Multani, A. S., Combs, C., Deramaudt, T. B., Hruban, R. H., Rustgi, A. K., Chang, S., and Tuveson, D. A. (2005). Trp53R172H and KrasG12D cooperate to promote chromosomal instability and widely metastatic pancreatic ductal adenocarcinoma in mice. Cancer Cell *7*, 469-483.

Hruban, R. H., Adsay, N. V., Albores-Saavedra, J., Anver, M. R., Biankin, A. V., Boivin, G. P., Furth, E. E., Furukawa, T., Klein, A., Klimstra, D. S*., et al.* (2006). Pathology of genetically engineered mouse models of pancreatic exocrine cancer: consensus report and recommendations. Cancer Res *66*, 95-106.

Hruban, R. H., Adsay, N. V., Albores-Saavedra, J., Compton, C., Garrett, E. S., Goodman, S. N., Kern, S. E., Klimstra, D. S., Kloppel, G., Longnecker, D. S*., et al.* (2001). Pancreatic intraepithelial neoplasia: a new nomenclature and classification system for pancreatic duct lesions. Am J Surg Pathol *25*, 579-586.

Hruban, R. H., Goggins, M., Parsons, J., and Kern, S. E. (2000). Progression model for pancreatic cancer. Clin Cancer Res *6*, 2969-2972.

Hruban, R. H., Takaori, K., Klimstra, D. S., Adsay, N. V., Albores-Saavedra, J., Biankin, A. V., Biankin, S. A., Compton, C., Fukushima, N., Furukawa, T*., et al.* (2004). An illustrated consensus on the classification of pancreatic intraepithelial neoplasia and intraductal papillary mucinous neoplasms. Am J Surg Pathol *28*, 977-987.

Ivanova, A., Signore, M., Caro, N., Greene, N. D., Copp, A. J., and Martinez-Barbera, J. P. (2005). In vivo genetic ablation by Cre-mediated expression of diphtheria toxin fragment A. Genesis *43*, 129-135.

Jackson, E. L., Willis, N., Mercer, K., Bronson, R. T., Crowley, D., Montoya, R., Jacks, T., and Tuveson, D. A. (2001). Analysis of lung tumor initiation and progression using conditional expression of oncogenic K-ras. Genes Dev *15*, 3243-3248.

Jesenberger, V., Procyk, K. J., Ruth, J., Schreiber, M., Theussl, H. C., Wagner, E. F., and Baccarini, M. (2001). Protective role of Raf-1 in Salmonella-induced macrophage apoptosis. J Exp Med *193*, 353-364.

Jimeno, A., Tan, A. C., Coffa, J., Rajeshkumar, N. V., Kulesza, P., Rubio-Viqueira, B., Wheelhouse, J., Diosdado, B., Messersmith, W. A., Iacobuzio-Donahue, C.*, et al.* (2008). Coordinated epidermal growth factor receptor pathway gene overexpression predicts epidermal growth factor receptor inhibitor sensitivity in pancreatic cancer. Cancer Res *68*, 2841-2849.

Kanda, M., Matthaei, H., Wu, J., Hong, S. M., Yu, J., Borges, M., Hruban, R. H., Maitra, A., Kinzler, K., Vogelstein, B., and Goggins, M. (2012). Presence of somatic mutations in most early-stage pancreatic intraepithelial neoplasia. Gastroenterology *142*, 730-733 e739.

Karreth, F. A., Frese, K. K., DeNicola, G. M., Baccarini, M., and Tuveson, D. A. (2011). C-Raf is required for the initiation of lung cancer by K-Ras(G12D). Cancer Discov *1*, 128-136.

Kawaguchi, Y., Cooper, B., Gannon, M., Ray, M., MacDonald, R. J., and Wright, C. V. (2002). The role of the transcriptional regulator Ptf1a in converting intestinal to pancreatic progenitors. Nat Genet *32*, 128-134.

Kellendonk, C., Tronche, F., Casanova, E., Anlag, K., Opherk, C., and Schutz, G. (1999). Inducible site-specific recombination in the brain. J Mol Biol *285*, 175-182.

Kennedy, A. L., Morton, J. P., Manoharan, I., Nelson, D. M., Jamieson, N. B., Pawlikowski, J. S., McBryan, T., Doyle, B., McKay, C., Oien, K. A.*, et al.* (2011). Activation of the PIK3CA/AKT pathway suppresses senescence induced by an activated RAS oncogene to promote tumorigenesis. Mol Cell *42*, 36-49.

Kishida, S., Koyama, S., Matsubara, K., Kishida, M., Matsuura, Y., and Kikuchi, A. (1997). Colocalization of Ras and Ral on the membrane is required for Ras-dependent Ral activation through Ral GDP dissociation stimulator. Oncogene *15*, 2899-2907.

Kraman, M., Bambrough, P. J., Arnold, J. N., Roberts, E. W., Magiera, L., Jones, J. O., Gopinathan, A., Tuveson, D. A., and Fearon, D. T. (2010). Suppression of antitumor immunity by stromal cells expressing fibroblast activation protein-alpha. Science *330*, 827-830.

Krapp, A., Knofler, M., Ledermann, B., Burki, K., Berney, C., Zoerkler, N., Hagenbuchle, O., and Wellauer, P. K. (1998). The bHLH protein PTF1-p48 is essential for the formation of the exocrine and the correct spatial organization of the endocrine pancreas. Genes Dev *12*, 3752-3763.

Lawlor, M. A., Mora, A., Ashby, P. R., Williams, M. R., Murray-Tait, V., Malone, L., Prescott, A. R., Lucocq, J. M., and Alessi, D. R. (2002). Essential role of PDK1 in regulating cell size and development in mice. Embo J *21*, 3728-3738.

Leone, D. P., Genoud, S., Atanasoski, S., Grausenburger, R., Berger, P., Metzger, D., Macklin, W. B., Chambon, P., and Suter, U. (2003). Tamoxifen-inducible glia-specific Cre mice for somatic mutagenesis in oligodendrocytes and Schwann cells. Mol Cell Neurosci *22*, 430-440.

Lim, K. H., Baines, A. T., Fiordalisi, J. J., Shipitsin, M., Feig, L. A., Cox, A. D., Der, C. J., and Counter, C. M. (2005). Activation of RalA is critical for Ras-induced tumorigenesis of human cells. Cancer Cell *7*, 533-545.

Lim, K. H., and Counter, C. M. (2005). Reduction in the requirement of oncogenic Ras signaling to activation of PI3K/AKT pathway during tumor maintenance. Cancer Cell *8*, 381-392.

Lim, K. H., O'Hayer, K., Adam, S. J., Kendall, S. D., Campbell, P. M., Der, C. J., and Counter, C. M. (2006). Divergent roles for RalA and RalB in malignant growth of human pancreatic carcinoma cells. Curr Biol *16*, 2385-2394.

Luttges, J., Galehdari, H., Brocker, V., Schwarte-Waldhoff, I., Henne-Bruns, D., Kloppel, G., Schmiegel, W., and Hahn, S. A. (2001). Allelic loss is often the first hit in the biallelic inactivation of the p53 and DPC4 genes during pancreatic carcinogenesis. Am J Pathol *158*, 1677-1683.

Maitra, A., Fukushima, N., Takaori, K., and Hruban, R. H. (2005). Precursors to invasive pancreatic cancer. Adv Anat Pathol *12*, 81-91.

Maitra, A., and Hruban, R. H. (2008). Pancreatic cancer. Annu Rev Pathol *3*, 157-188.

Matsubara, K., Kishida, S., Matsuura, Y., Kitayama, H., Noda, M., and Kikuchi, A. (1999). Plasma membrane recruitment of RalGDS is critical for Ras-dependent Ral activation. Oncogene *18*, 1303-1312.

Maurer, M., Su, T., Saal, L. H., Koujak, S., Hopkins, B. D., Barkley, C. R., Wu, J., Nandula, S., Dutta, B., Xie, Y.*, et al.* (2009). 3-Phosphoinositide-dependent kinase 1 potentiates upstream lesions on the phosphatidylinositol 3-kinase pathway in breast carcinoma. Cancer Res *69*, 6299-6306.

Mazur, P. K., Gruner, B. M., Nakhai, H., Sipos, B., Zimber-Strobl, U., Strobl, L. J., Radtke, F., Schmid, R. M., and Siveke, J. T. (2010). Identification of epidermal Pdx1 expression discloses different roles of Notch1 and Notch2 in murine Kras(G12D)-induced skin carcinogenesis in vivo. PLoS One *5*, e13578.

Means, A. L., Meszoely, I. M., Suzuki, K., Miyamoto, Y., Rustgi, A. K., Coffey, R. J., Jr., Wright, C. V., Stoffers, D. A., and Leach, S. D. (2005). Pancreatic epithelial plasticity mediated by acinar cell transdifferentiation and generation of nestin-positive intermediates. Development *132*, 3767-3776.

Metzger, D., Clifford, J., Chiba, H., and Chambon, P. (1995). Conditional site-specific recombination in mammalian cells using a ligand-dependent chimeric Cre recombinase. Proc Natl Acad Sci U S A *92*, 6991-6995.

Miyamoto, Y., Maitra, A., Ghosh, B., Zechner, U., Argani, P., Iacobuzio-Donahue, C. A., Sriuranpong, V., Iso, T., Meszoely, I. M., Wolfe, M. S.*, et al.* (2003). Notch mediates TGF alpha-induced changes in epithelial differentiation during pancreatic tumorigenesis. Cancer Cell *3*, 565-576.

Moore, M. J., Goldstein, D., Hamm, J., Figer, A., Hecht, J. R., Gallinger, S., Au, H. J., Murawa, P., Walde, D., Wolff, R. A.*, et al.* (2007). Erlotinib plus gemcitabine compared with gemcitabine alone in patients with advanced pancreatic cancer: a phase III trial of the National Cancer Institute of Canada Clinical Trials Group. J Clin Oncol *25*, 1960-1966.

Morris, J. P. t., Wang, S. C., and Hebrok, M. (2010). KRAS, Hedgehog, Wnt and the twisted developmental biology of pancreatic ductal adenocarcinoma. Nat Rev Cancer *10*, 683-695.

Morrison, D. K., and Cutler, R. E. (1997). The complexity of Raf-1 regulation. Curr Opin Cell Biol *9*, 174-179.

Muzumdar, M. D., Tasic, B., Miyamichi, K., Li, L., and Luo, L. (2007). A global double-fluorescent Cre reporter mouse. Genesis *45*, 593-605.

Nakhai, H., Sel, S., Favor, J., Mendoza-Torres, L., Paulsen, F., Duncker, G. I., and Schmid, R. M. (2007). Ptf1a is essential for the differentiation of GABAergic and glycinergic amacrine cells and horizontal cells in the mouse retina. Development *134*, 1151-1160.

Obata, J., Yano, M., Mimura, H., Goto, T., Nakayama, R., Mibu, Y., Oka, C., and Kawaichi, M. (2001). p48 subunit of mouse PTF1 binds to RBP-Jkappa/CBF-1, the intracellular mediator of Notch signalling, and is expressed in the neural tube of early stage embryos. Genes Cells *6*, 345-360.

Oda, K., Stokoe, D., Taketani, Y., and McCormick, F. (2005). High frequency of coexistent mutations of PIK3CA and PTEN genes in endometrial carcinoma. Cancer Res *65*, 10669-10673.

Offield, M. F., Jetton, T. L., Labosky, P. A., Ray, M., Stein, R. W., Magnuson, M. A., Hogan, B. L., and Wright, C. V. (1996). PDX-1 is required for pancreatic outgrowth and differentiation of the rostral duodenum. Development *122*, 983-995.

Ohlsson, H., Karlsson, K., and Edlund, T. (1993). IPF1, a homeodomain-containing transactivator of the insulin gene. Embo J *12*, 4251-4259.

Olive, K. P., Jacobetz, M. A., Davidson, C. J., Gopinathan, A., McIntyre, D., Honess, D., Madhu, B., Goldgraben, M. A., Caldwell, M. E., Allard, D.*, et al.* (2009). Inhibition of Hedgehog signaling enhances delivery of chemotherapy in a mouse model of pancreatic cancer. Science *324*, 1457-1461.

Olive, K. P., Tuveson, D. A., Ruhe, Z. C., Yin, B., Willis, N. A., Bronson, R. T., Crowley, D., and Jacks, T. (2004). Mutant p53 gain of function in two mouse models of Li-Fraumeni syndrome. Cell *119*, 847-860.

Orban, P. C., Chui, D., and Marth, J. D. (1992). Tissue- and site-specific DNA recombination in transgenic mice. Proc Natl Acad Sci U S A *89*, 6861-6865.

Ornitz, D. M., Hammer, R. E., Messing, A., Palmiter, R. D., and Brinster, R. L. (1987). Pancreatic neoplasia induced by SV40 T-antigen expression in acinar cells of transgenic mice. Science *238*, 188-193.

Osborn, M., van Lessen, G., Weber, K., Kloppel, G., and Altmannsberger, M. (1986). Differential diagnosis of gastrointestinal carcinomas by using monoclonal antibodies specific for individual keratin polypeptides. Lab Invest *55*, 497-504.

Perez-Mancera, P. A., Guerra, C., Barbacid, M., and Tuveson, D. A. (2012). What we have learned about pancreatic cancer from mouse models. Gastroenterology *142*, 1079-1092.

Provenzano, P. P., Cuevas, C., Chang, A. E., Goel, V. K., Von Hoff, D. D., and Hingorani, S. R. (2012). Enzymatic targeting of the stroma ablates physical barriers to treatment of pancreatic ductal adenocarcinoma. Cancer Cell *21*, 418-429.

Pylayeva-Gupta, Y., Grabocka, E., and Bar-Sagi, D. (2011). RAS oncogenes: weaving a tumorigenic web. Nat Rev Cancer *11*, 761-774.

Quaife, C. J., Pinkert, C. A., Ornitz, D. M., Palmiter, R. D., and Brinster, R. L. (1987). Pancreatic neoplasia induced by ras expression in acinar cells of transgenic mice. Cell *48*, 1023-1034.

Rangarajan, A., and Weinberg, R. A. (2003). Opinion: Comparative biology of mouse versus human cells: modelling human cancer in mice. Nat Rev Cancer *3*, 952-959.

Reichert, M., and Rustgi, A. K. (2011). Pancreatic ductal cells in development, regeneration, and neoplasia. J Clin Invest *121*, 4572-4578.

Reichert, M., Saur, D., Hamacher, R., Schmid, R. M., and Schneider, G. (2007). Phosphoinositide-3-kinase signaling controls S-phase kinase-associated protein 2 transcription via E2F1 in pancreatic ductal adenocarcinoma cells. Cancer Res *67*, 4149-4156.

Rozenblum, E., Schutte, M., Goggins, M., Hahn, S. A., Panzer, S., Zahurak, M., Goodman, S. N., Sohn, T. A., Hruban, R. H., Yeo, C. J., and Kern, S. E. (1997). Tumor-suppressive pathways in pancreatic carcinoma. Cancer Res *57*, 1731-1734.

Sandgren, E. P., Luetteke, N. C., Palmiter, R. D., Brinster, R. L., and Lee, D. C. (1990). Overexpression of TGF alpha in transgenic mice: induction of epithelial hyperplasia, pancreatic metaplasia, and carcinoma of the breast. Cell *61*, 1121-1135.

Sandgren, E. P., Quaife, C. J., Paulovich, A. G., Palmiter, R. D., and Brinster, R. L. (1991). Pancreatic tumor pathogenesis reflects the causative genetic lesion. Proc Natl Acad Sci U S A *88*, 93-97.

Schneider, G., Siveke, J. T., Eckel, F., and Schmid, R. M. (2005). Pancreatic cancer: basic and clinical aspects. Gastroenterology *128*, 1606-1625.

Schönhuber, N., Seidler, B., Schuck, K., Veltkamp, C., Schachtler, C., Zukowska, M., Eser, S., Feyerabend, T. B., Paul, M. C., Eser, P.*, et al.* (2014). A next-generation dual-recombinase system for time- and host-specific targeting of pancreatic cancer. Nat Med.

Scortegagna, M., Ruller, C., Feng, Y., Lazova, R., Kluger, H., Li, J. L., De, S. K., Rickert, R., Pellecchia, M., Bosenberg, M., and Ronai, Z. A. (2013). Genetic inactivation or pharmacological inhibition of Pdk1 delays development and inhibits metastasis of Braf(V600E)::Pten(-/-) melanoma. Oncogene *33*, 4330-4339.

Shi, C., Klein, A. P., Goggins, M., Maitra, A., Canto, M., Ali, S., Schulick, R., Palmisano, E., and Hruban, R. H. (2009). Increased Prevalence of Precursor Lesions in Familial Pancreatic Cancer Patients. Clin Cancer Res *15*, 7737-7743.

Shields, J. M., Pruitt, K., McFall, A., Shaub, A., and Der, C. J. (2000). Understanding Ras: 'it ain't over 'til it's over'. Trends Cell Biol *10*, 147-154.

Siegel, P. M., and Massague, J. (2003). Cytostatic and apoptotic actions of TGF-beta in homeostasis and cancer. Nat Rev Cancer *3*, 807-821.

Siegel, R., Ma, J., Zou, Z., and Jemal, A. (2014). Cancer statistics, 2014. CA Cancer J Clin *64*, 9-29.

Song, M. S., Salmena, L., and Pandolfi, P. P. (2012). The functions and regulation of the PTEN tumour suppressor. Nat Rev Mol Cell Biol *13*, 283-296.

Southern, E. M. (1975). Detection of specific sequences among DNA fragments separated by gel electrophoresis. J Mol Biol *98*, 503-517.

Stanger, B. Z., Stiles, B., Lauwers, G. Y., Bardeesy, N., Mendoza, M., Wang, Y., Greenwood, A., Cheng, K. H., McLaughlin, M., Brown, D.*, et al.* (2005). Pten constrains centroacinar cell expansion and malignant transformation in the pancreas. Cancer Cell *8*, 185-195.

Stolzenberg-Solomon, R. Z., Graubard, B. I., Chari, S., Limburg, P., Taylor, P. R., Virtamo, J., and Albanes, D. (2005). Insulin, glucose, insulin resistance, and pancreatic cancer in male smokers. Jama *294*, 2872-2878.

Tan, J., Lee, P. L., Li, Z., Jiang, X., Lim, Y. C., Hooi, S. C., and Yu, Q. (2010). B55beta-associated PP2A complex controls PDK1-directed myc signaling and modulates rapamycin sensitivity in colorectal cancer. Cancer Cell *18*, 459-471.

Thayer, S. P., di Magliano, M. P., Heiser, P. W., Nielsen, C. M., Roberts, D. J., Lauwers, G. Y., Qi, Y. P., Gysin, S., Fernandez-del Castillo, C., Yajnik, V.*, et al.* (2003). Hedgehog is an early and late mediator of pancreatic cancer tumorigenesis. Nature *425*, 851-856.

Vanhaesebroeck, B., Ali, K., Bilancio, A., Geering, B., and Foukas, L. C. (2005). Signalling by PI3K isoforms: insights from gene-targeted mice. Trends Biochem Sci *30*, 194-204.

Vasudevan, K. M., Barbie, D. A., Davies, M. A., Rabinovsky, R., McNear, C. J., Kim, J. J., Hennessy, B. T., Tseng, H., Pochanard, P., Kim, S. Y.*, et al.* (2009). AKT-independent

signaling downstream of oncogenic PIK3CA mutations in human cancer. Cancer Cell *16*, 21-32.

Vincent, A., Herman, J., Schulick, R., Hruban, R. H., and Goggins, M. (2011). Pancreatic cancer. Lancet *378*, 607-620.

Vivanco, I., Palaskas, N., Tran, C., Finn, S. P., Getz, G., Kennedy, N. J., Jiao, J., Rose, J., Xie, W., Loda, M.*, et al.* (2007). Identification of the JNK signaling pathway as a functional target of the tumor suppressor PTEN. Cancer Cell *11*, 555-569.

Von Hoff, D. D., Ervin, T., Arena, F. P., Chiorean, E. G., Infante, J., Moore, M., Seay, T., Tjulandin, S. A., Ma, W. W., Saleh, M. N.*, et al.* (2013). Increased survival in pancreatic cancer with nab-paclitaxel plus gemcitabine. N Engl J Med *369*, 1691-1703.

Wagner, M., Luhrs, H., Kloppel, G., Adler, G., and Schmid, R. M. (1998). Malignant transformation of duct-like cells originating from acini in transforming growth factor transgenic mice. Gastroenterology *115*, 1254-1262.

Wolpin, B. M., Chan, A. T., Hartge, P., Chanock, S. J., Kraft, P., Hunter, D. J., Giovannucci, E. L., and Fuchs, C. S. (2009). ABO blood group and the risk of pancreatic cancer. J Natl Cancer Inst *101*, 424-431.

Wu, C. Y., Carpenter, E. S., Takeuchi, K. K., Halbrook, C. J., Peverley, L. V., Bien, H., Hall, J. C., DelGiorno, K. E., Pal, D., Song, Y.*, et al.* (2014). PI3K Regulation of RAC1 Is Required for Kras-Induced Pancreatic Tumorigenesis in Mice. Gastroenterology.

Ying, H., Elpek, K. G., Vinjamoori, A., Zimmerman, S. M., Chu, G. C., Yan, H., Fletcher-Sananikone, E., Zhang, H., Liu, Y., Wang, W.*, et al.* (2011). Pten is a major tumor suppressor in pancreatic ductal adenocarcinoma and regulates an NF-kappaB-cytokine network. Cancer Discov *1*, 158-169.

9. Acknowledgements

I want to sincerely thank everybody who supported me during the time of my PhD research in any possible way

First of all, I thank Prof. Roland M. Schmid for giving me the opportunity to do my PhD research in his department at Klinikum rechts der Isar.
Especially, I am very grateful to Prof. Angelika Schnieke for being my second advisor.
Furthermore, I thank Dr. Günter Schneider for being my mentor.

Above all, I want to thank Prof. Dieter Saur for giving me the opportunity to work on my PhD research in his group. By offering such an interesting topic and always supporting me, he contributed a large part to this dissertation.

I further thank Juliana Götzfried, Miriam Schiller, Ursula Götz, Marco Göbel and Magdalena Zukowska for excellent technical support. For scientific input and discussions I want to thank Barbara Seidler.

Many thanks to all the members of the Saur and Schneider group for the great working atmosphere throughout all the years.

Finally and most importantly, I want to thank my husband and my parents for their constant help. Without their support this dissertation would not have been possible.